TECHNISCHE UNIVERSITÄT MÜNCHEN
Fakultät für Informatik
Lehrstuhl III – Datenbanksysteme

Query Processing and Optimization in Modern Database Systems

Viktor Leis

Vollständiger Abdruck der von der Fakultät für Informatik der Technischen Universität München zur Erlangung des akademischen Grades eines

Doktors der Naturwissenschaften (Dr. rer. nat.)

genehmigten Dissertation.

Vorsitzender: Univ.-Prof. Dr. Hans-Joachim Bungartz

Prüfer der Dissertation: Univ.-Prof. Dr. Thomas Neumann,
Prof. Michael Stonebraker, Ph.D. (MIT, Cambridge, USA)
Univ.-Prof. Alfons Kemper, Ph.D.

Die Dissertation wurde am 25.05.2016 bei der Technischen Universität München eingereicht und durch die Fakultät für Informatik am 30.09.2016 angenommen.

Abstract

Relational database management systems, which were designed decades ago, are still the dominant data processing platform. Large DRAM capacities and servers with many cores have fundamentally changed the hardware landscape. Traditional database systems were designed with very different hardware in mind and cannot exploit modern hardware effectively. This thesis focuses on the challenges posed by modern hardware for transaction processing, query processing, and query optimization. We present a concurrent transaction processing system based on hardware transactional memory and show how to synchronize data structures efficiently. We further design a parallel query engine for many-core CPUs that supports the important relational operators including join, aggregation, window functions, etc. Finally, we dissect the query optimization process in the main memory setting and show the contribution of each query optimizer component to the overall query performance.

Zusammenfassung

Relationale Datenbankmanagementsysteme, deren ursprüngliche Entwicklung bereits Jahrzehnte zurückliegt, sind auch heute noch die dominierende Datenverarbeitungsplattform. Rechner mit großen DRAM-Kapazitäten und vielen Kernen haben die Hardwarelandschaft jedoch fundamental verändert. Traditionelle Datenbanksysteme wurden für Systeme entwickelt, die sich sehr von aktuellen unterscheiden, und können deshalb moderne Hardware nicht effektiv nutzen. Die vorliegende Arbeit befasst sich mit den Herausforderungen moderner Hardware für die Transaktionsverarbeitung, Anfrageverarbeitung und Anfrageoptimierung. Zunächst präsentieren wir ein Transaktionsverarbeitungssystem basierend auf Hardware Transactional Memory und zeigen wie Datenstrukturen effizient synchronisiert werden können. Darüber hinaus entwickeln wir eine parallele Anfrageverarbeitungkomponente für Rechner mit vielen Kernen, welche unter anderem die wichtigen relationalen Operatoren Verbund, Aggregation und Windowfunktionen unterstützt. Schließlich untersuchen wir den Anfrageoptimierungsprozess in Haupspeicherdatenbanken und zeigen den Beitrag der einzelnen Optimererkomponenten zu der Gesamtanfragegeschwindigkeit.

Contents

List of Figures

List of Tables

1 Introduction

Relational database management systems have stood the test of time and are still the dominant data processing platform. The basic design of these systems stems from the 1980s and was largely unchanged for decades. The core ideas include row-wise storage as well as B-trees on fixed-sized pages backed by a buffer pool, ARIES-style logging, and Two Phase Locking. Recent years, however, have seen many of the design decisions become obsolete due to fundamental changes in the hardware landscape. In the rest of the chapter we give a brief outline of modern database systems and discuss some of the challenges posed by modern hardware for these systems. This discussion forms the background and motivation for this thesis. We close by giving an outline of the following chapters.

1.1 Column Stores

After decades of only minor, incremental changes to the basic database architecture, a radically new design, column stores, started to gain traction in the years after 2005. C-store [167] (commercialized as Vertica) and MonetDB/X100 [20] (commercialized as Vectorwise) are two influential systems that gained significant mind share during that time frame. The idea of organizing relations by column is, of course, much older [21]. Sybase IQ [125] and MonetDB [22] are two pioneering column stores that originated in the 1990s.

Column stores are read-optimized and often used as data warehouses, i.e., non-operational databases that ingest changes periodically (e.g., every night). In comparison with row stores, column stores have the obvious advantage that scans only need to read those attributes accessed by a particular query resulting in less I/O operations. A second advantage is that the query engine of a column store can be implemented in a much more CPU-efficient way: Column stores can amortize the interpretation overhead of the iterator model by processing batches of rows ("vector-at-a-time"), instead of working only on individual rows ("tuple-at-a-time").

The major database vendors have reacted to the changing landscape by combining multiple storage and query engines in their products. In Microsoft SQL Server, for example, users now can choose between the

- traditional general-purpose row store,

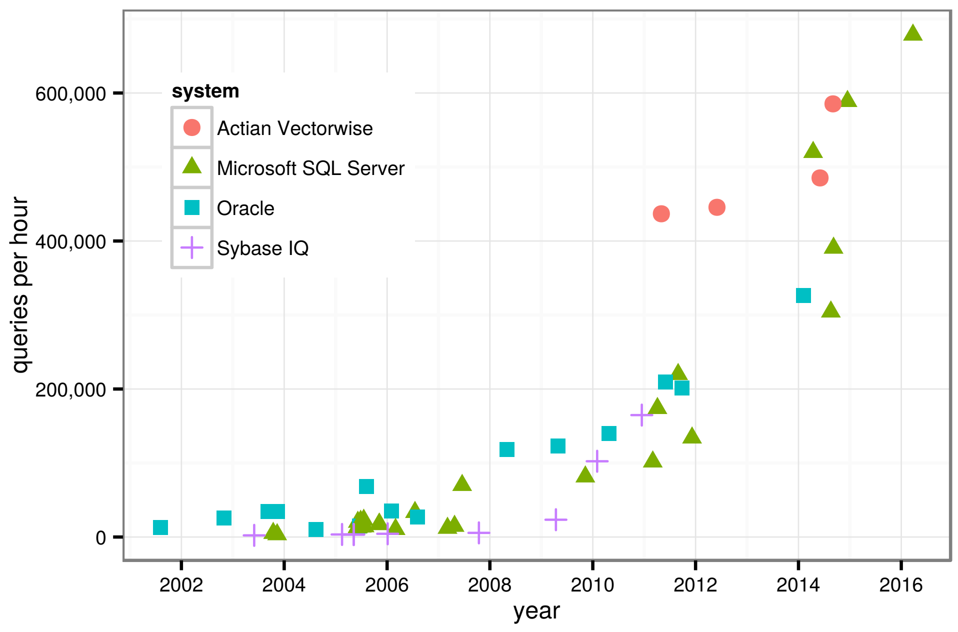

Figure 1.1: TPC-H single-machine performance for scale factor 1000 (1 TB)

- a column store [100] for OnLine Analytical Processing (OLAP), and
- in-memory storage optimized for Online transaction processing (OLTP) [37].

Each of these options comes with its own query processing model and specific performance characteristics, which must be carefully considered by the database administrator.

The impact of column stores can be seen in Figure 1.1, which shows the performance on TPC-H, a widely used OLAP benchmark. Before 2011, multiple vendors competed for the TPC-H crown, with the lead changing from time to time between Oracle, Microsoft, and Sybase[1]. This changed with the arrival of Actian Vectorwise in 2011, which disrupted the incremental “rat race” between the traditional vendors. The dominance of Vectorwise as official TPC-H leader lasted until 2014, when Microsoft submitted new results with their column store engine Apollo [100], which is currently the leading system.

1.2 Main-Memory Database Systems

The lower CPU overhead of column store query engines was of only minor importance as long as data was mainly stored on disk (or even SSD). In 2000 one had to pay over

[1]IBM submitted results for other scale factors, but not for scale factor 1000.

1000$ for 1 GB of DRAM[2]. At these prices, any non-trivial database workload resulted in a significant number of disk I/O operations, and main-memory DBMSs—which were a research topic as early as the 1980s [50]—were still niche products. In 2008, with the same 1000$ one could already buy 100 GB of RAM[3]. This rapid decrease in DRAM prices had consequences for the architecture of database management systems.

Harizopoulos et al.'s paper from 2008 [63] showed that on the—suddenly very common—memory-resident OLTP workloads virtually all time was wasted on overhead like

- buffer management,
- locking,
- latching,
- heavy-weight logging, and
- an inefficient implementation.

The goal of any database system's designer thus gradually shifted from minimizing the number of disk I/O operations to reducing CPU overhead and cache misses. This lead to a resurgence of research into main-memory database systems. The main idea behind main-memory DBMSs is to assume that all data fits into RAM and to optimize for CPU and cache efficiency. Using careful engineering and by making the right architectural decisions that take modern hardware into account, database systems can achieve orders of magnitude higher performance. Well-known main-memory database systems include H-Store/VoltDB [83, 168], SAP HANA [43], Microsoft Hekaton [102], solidDB [118], Oracle TimesTen [95], Calvin [171], Silo [172], MemSQL, and HyPer [87].

The work described in this thesis has been done in the context of the HyPer project, which started in 2010 [86]. HyPer follows some of the design decisions of other main-memory systems (e.g., no buffer manager, no locks, no latches, and (originally) command logging). To avoid fine-grained latches, HyPer also initially followed H-Store's approach of relying on user-controlled, physical partitioning of the database to enable multi-threading.

HyPer has, however, a number of features that distinguish it from many other main-memory systems: From the very beginning, HyPer supported both OLTP and OLAP in the same database in order to make the physical separation between the transactional and data warehouse databases obsolete. Initially, HyPer used OS-supported snapshots [87], which were later replaced with a software-controlled Multi-Version

[2]DRAM prices are taken from `http://www.jcmit.com/memoryprice.htm`.

[3]The cost continues to decline. At the time of writing, in 2016, the cost was around 4$ per GB.

Concurrency Control (MVCC) approach [143]. The second unique feature of HyPer is that, via the LLVM [104] compiler infrastructure, it compiles SQL queries and stored procedures to machine code [139]. Compilation avoids the interpretation overhead inherent in the iterator model and thereby enables extremely high performance. LLVM is a widely used open source compiler backend that can generate efficient machine code for many different target platforms, which makes this approach portable. In contrast to previous compilation approaches (e.g., [94]), HyPer compiles multiple relational operators from the same query pipeline into a single intertwined code fragment, which allows it to keep values in CPU registers for as long as possible.

In terms of architecture, most column stores have converged to a similar design [1], which was pioneered by systems like Vectorwise [20] and Vertica [167]. In-memory OLTP systems, in contrast, show more architectural variety. Compilation is, however, becoming a common building block for OLTP systems, as can be observed by the use of compilation by HyPer [139], Hekaton [37], and MemSQL. Other high-performance systems like Silo [172] also implicitly assume (but do not yet implement) compilation, as the stored procedures are hand-written in C or C++ in these systems. In other areas like concurrency control (e.g., [172] vs. [98] vs. [143]), indexing (e.g., [108] vs. [129] vs. [114]), and logging (e.g., [127] vs. physiological) there is much more variety between the systems.

1.3 The Challenges of Modern Hardware

Besides increasing main-memory sizes, a second important trend in the hardware landscape is the ever increasing number of cores. Figure 1.2 shows the number of cores for server CPUs[4]. Over the entire time frame, the clock rate stayed between 2 GHz and 3 GHz and, as a result, single-threaded performance increased only very slowly (by single-digit percentages per year). Note that the graph only shows "real" cores for a single socket. Many servers have 2, 4, or even 8 sockets in a single system and each Intel core nowadays has 2-way HyperThreading. As a result, the affordable and commonly used 2-socket configurations will soon routinely have over 100 hardware threads in a single system. Memory bandwidth has largely kept up with the increasing number of cores and will reach over 100 GB/s per socket with Skylake EP. However, it is important to note that a single core can only utilize a small fraction of the available bandwidth, making effective parallelization essential.

Long before the many-core revolution, high-end database servers often combined a handful of processors—connected by a shared memory bus—in a Symmetric Multi-Processing (SMP) system. Furthermore, database systems have, for a long time, been

[4]The data is from `https://en.wikipedia.org/wiki/List_of_Intel_Xeon_microprocessors`. For Broadwell EX and Skylake EP server CPUs we show estimates from the press as they were not yet released at the time of writing.

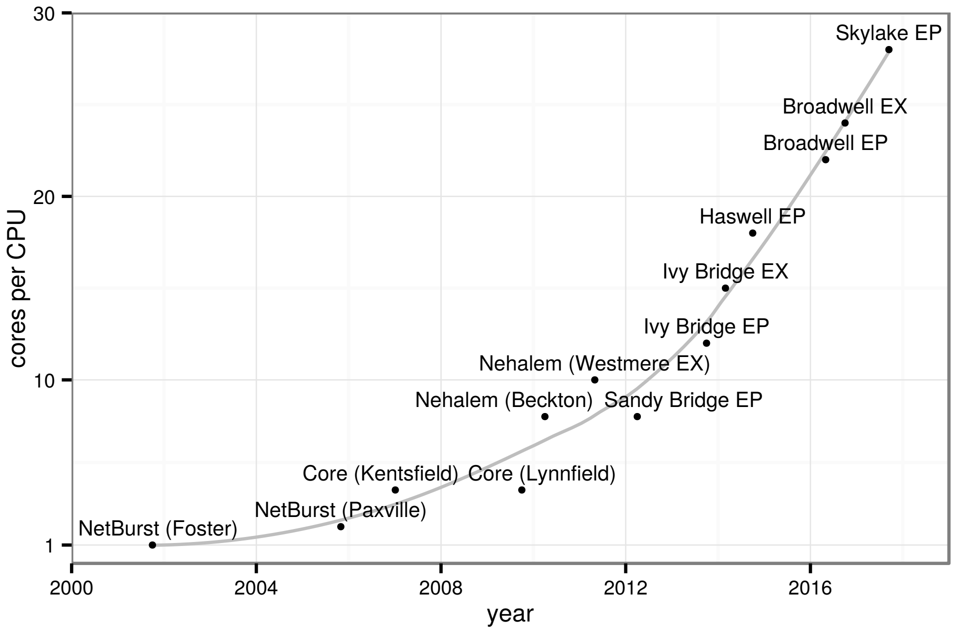

Figure 1.2: Number of cores in Intel Xeon server processors (for the largest configuration in each microarchitecture)

capable of executing queries concurrently by using appropriate locking and latching techniques. So one might reasonably ask if any fundamental changes to the database architecture are required at all. Modern hardware, however, has unique challenges not encountered in the past:

Latches are expensive and prevent scaling. Traditional database systems use latches extensively to access shared data structures from concurrent threads. As long as disk I/O operations were frequent, the overhead of short-term latching was negligible. On modern hardware, however, even short-term, uncontested latches can be expensive and prevent scalability. The reason is that each latch acquisition causes cache line invalidations for *all other cores*. As we show experimentally, this effect often prevents scalability on multi-core CPUs.

Intra-query parallelism is not optional any more. For a long time, many systems relied on parallelism from the "outside", i.e., inter-query parallelism. With dozens or hundreds of cores, intra-query parallelism is not an optional optimization because many workloads simply do not have enough parallel query sessions. Without intra-query parallelism, the computational resources of modern servers lie dormant. The widely used PostgreSQL system, for example, will finally introduce (limited) intra-query parallelism in the upcoming version 9.6—20 years after the project started.

Query engines should be designed with multi-core parallelism in mind. Some commercial systems added support for intra-query parallelism a decade ago. This was often done by introducing “exchange” operators [52] that encapsulate parallelism without redesigning the actual operators. This pragmatic approach was sufficient at a time when the degree of parallelism in database servers was low (e.g., 10 threads). To get good scalability on systems with dozens of cores, the query processing algorithms should be redesigned from scratch with parallelism in mind.

Database systems should take Non-Uniform Memory Architecture (NUMA) into account. In contrast to earlier SMP systems, where all processors shared a common memory bus, current systems are generally based on the Non-Uniform Memory Architecture (NUMA). In this architecture each processor has its own memory, but can transparently and cache-coherently access remote memory through an interconnect. Because remote memory accesses are more expensive than local accesses, NUMA-aware data placement can improve performance considerably. Thus, database systems must optimize for NUMA to obtain optimal performance.

Together, these changes explain why traditional systems (e.g., as described in [66]) cannot fully exploit the resources provided today’s commodity servers. To utilize modern hardware well, fundamental changes to core database components including storage, concurrency control, low-level synchronization, query processing, logging, etc. are necessary. Database systems specifically designed for modern hardware can be orders of magnitude faster than their predecessors.

1.4 Outline

This thesis addresses the challenges enumerated above. The solutions were developed within a general-purpose, relational database system (HyPer) and most experiments measure end-to-end performance. Our contributions span the transaction processing, query processing, and query optimization components.

In Chapter 2 we design a low-overhead, *concurrent transaction processing* engine based on Hardware Transactional Memory (HTM). Until recently, transactional memory—although a promising technique—suffered from the absence of an efficient hardware implementation. Since Intel introduced the Haswell microarchitecture hardware transactional memory is available in mainstream CPUs. HTM allows for efficient concurrent, atomic operations, which is also highly desirable in the context of databases. On the other hand, HTM has several limitations that, in general, prevent a one-to-one mapping of database transactions to HTM transactions. We devise several building blocks that can be used to exploit HTM in main-memory databases. We show that HTM allows one to achieve nearly lock-free processing of database transactions by carefully controlling the data layout and the access patterns. The HTM component is used for detecting the (infrequent) conflicts, which allows for an optimistic—and thus very low-overhead execution—of concurrent transactions. We evaluate our approach on a 4-core desktop and a 28-core server system and find that HTM indeed provides a scalable, powerful, and easy to use synchronization primitive.

While Hardware Transactional Memory is easy to use and can offer good performance, it is not yet widespread. Therefore, Chapter 3 studies alternative *low-overhead synchronization* mechanisms for in-memory data structures. The traditional approach, fine-grained locking, does not scale on modern hardware. Lock-free data structures, in contrast, scale very well but are extremely difficult to implement and often require additional indirections. We argue for a middle ground, i.e., synchronization protocols that use locking, but only sparingly. We synchronize the Adaptive Radix Tree (ART) [108] using two such protocols, Optimistic Lock Coupling and Read-Optimized Write EXclusion (ROWEX). Both perform and scale very well while being much easier to implement than lock-free techniques.

Chapter 4 describes the *parallel and NUMA-aware query engine* of HyPer, which scales up to dozens of cores. Our "morsel-driven" query execution framework, where scheduling becomes a fine-grained run-time task that is NUMA-aware. Morsel-driven query processing takes small fragments of input data ("morsels") and schedules these to worker threads that run entire operator pipelines until the next pipeline-breaking operator. The degree of parallelism is not baked into the plan but can elastically change during query execution. The dispatcher can react to the execution speed of different morsels but also adjust resources dynamically in response to newly arriving queries in the workload. Furthermore, the dispatcher is aware of data locality of the NUMA-local morsels and operator state, such that the great majority of executions takes place on NUMA-local memory. Our evaluation on the TPC-H and SSB benchmarks shows extremely high absolute performance and an average speedup of over 30 with 32 cores.

Chapter 5 completes the description of HyPer's query engine by proposing a design for the *SQL:2003 window function* operator. Window functions, also known as analytic OLAP functions, have been neglected in the research literature—despite being part of the SQL standard for more than a decade and being a widely-used feature. Window functions can elegantly express many useful queries about time series, ranking, percentiles, moving averages, and cumulative sums. Formulating such queries in plain SQL-92 is usually both cumbersome and inefficient. Our algorithm is optimized for high-performance main-memory database systems and has excellent performance on modern multi-core CPUs. We show how to fully parallelize all phases of the operator in order to effectively scale for arbitrary input distributions.

The only thing more important for achieving low query response times than a fast and scalable query engine is *query optimization*. In Chapter 6 we shift our focus from the query engine to the query optimizer. Query optimization has been studied for decades, but most experiments were in the context of disk-based systems or were focused on individual query optimization components rather than end-to-end performance. We introduce the Join Order Benchmark (JOB) and experimentally revisit the main components in the classic query optimizer architecture using a complex, real-world data set and realistic multi-join queries. We investigate the quality of industrial-strength cardinality estimators and find that all estimators routinely produce large errors. We further show that while estimates are essential for finding a good join order, query performance is unsatisfactory if the query engine relies too heavily on these estimates. Using another set of experiments that measure the impact of the cost model, we find that it has much less influence on query performance than the cardinality estimates. Finally, we investigate plan enumeration techniques comparing exhaustive dynamic programming with heuristic algorithms and find that exhaustive enumeration improves performance despite the sub-optimal cardinality estimates.

2 Exploiting Hardware Transactional Memory in Main-Memory Databases

Parts of this chapter have previously been published in [109, 110].

2.1 Introduction

The support for hardware transactional memory (HTM) in mainstream processors like Intel's Haswell appears like a perfect fit for main-memory database systems. Transactional memory [69] is a very intriguing concept that allows for automatic atomic and concurrent execution of arbitrary code. Transactional memory allows for code that behaves quite similar to database transactions:

```
transaction {                transaction {
    a = a − 10;                  c = c − 20;
    b = b + 10;                  a = a + 20;
}                            }
Transaction 1                Transaction 2
```

Semantically, the code sections are executed atomically and in isolation from each other. In the case of runtime conflicts (i.e., read/write conflicts or write/write conflicts) a transaction might get aborted, undoing all changes performed so far. The transaction model is a very elegant and well understood idea that is much simpler than the classical alternative, namely fine-grained locking. Locking is much more difficult to formulate correctly. Fine-grained locking is error prone and can lead to deadlocks due to differences in locking order. Coarse-grained locking is simpler, but greatly reduces concurrency. Transactional memory avoids this problem by keeping track of read and write sets and thus by detecting conflicts on the memory access level. Starting with the Intel's Haswell microarchitecture this is supported by hardware, which offers excellent performance.

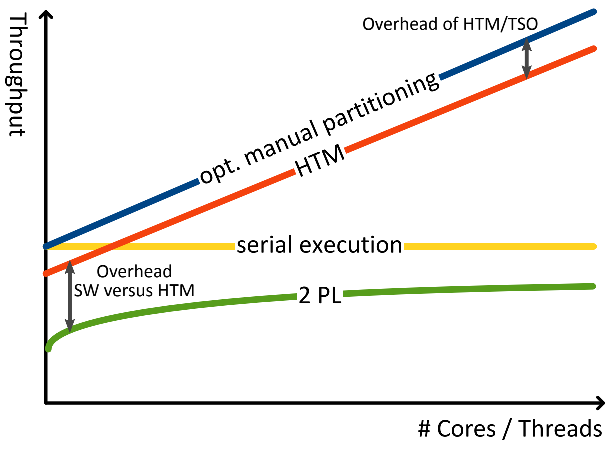

Figure 2.1: HTM versus 2PL, sequential, partitioned

Figure 2.1 sketches the performance benefits of our HTM-based transaction manager in comparison to other concurrency control mechanisms that we investigated. For main-memory database applications the well-known Two Phase Locking scheme was shown to be inferior to serial execution [63]! However, serial execution cannot exploit the parallel compute power of modern multi-core CPUs. Under serial execution, scaling the throughput in proportion to the number of cores would require an optimal partitioning of the database such that transactions do not cross these boundaries. This allows for "embarrassingly" parallel execution—one thread within each partition. Unfortunately, this is often not possible in practice; therefore, the upper throughput curve "opt. manual partitioning" of Figure 2.1 is only of theoretical nature. HTM, however, comes very close to an optimal static partitioning scheme as its transaction processing can be viewed as an adaptive dynamic partitioning of the database according to the transactional access pattern.

However, transactional memory is no panacea for transaction processing. First, database transactions also require properties like durability, which are beyond the scope of transactional memory. Second, all current hardware implementations of transactional memory are limited. For the Haswell microarchitecture, for example, the scope of a transaction is limited, because the read/write set, i.e., every cache line a transaction accesses, has to fit into the L1 cache with a capacity of 32KB. Furthermore, HTM transactions may fail due to a number of unexpected circumstances like collisions caused by cache associativity, hardware interrupts, etc. Therefore, it is, in general, not viable to map an entire database transaction to a single monolithic HTM transaction. In addition, one always needs a "slow path" to handle the pathological cases (e.g., associativity collisions).

We therefore propose an architecture where transactional memory is used as a build-

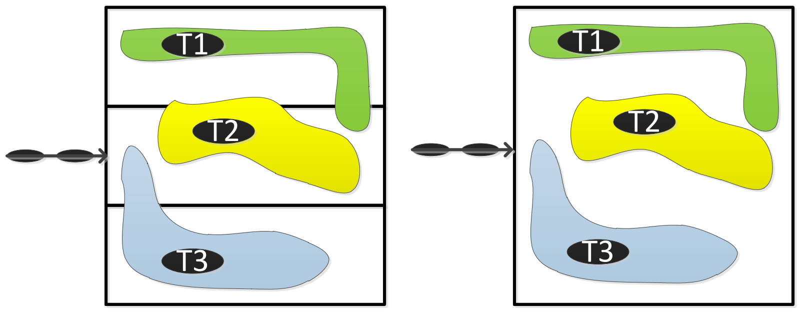

Figure 2.2: Schematic illustration of static partitioning (left) and concurrency control via HTM resulting in dynamic partitioning (right)

ing block for assembling complex database transactions. Along the lines of the general philosophy of transactional memory we start executing transactions optimistically, using (nearly) no synchronization and thus running at full clock speed. By exploiting HTM we get many of the required checks for free, without complicating the database code, and can thus reach a much higher degree of parallelism than with classical locking or latching. In order to minimize the number of conflicts in the transactional memory component, we carefully control the data layout and the access patterns of the involved operations, which allows us to avoid explicit synchronization most of the time.

Note that we explicitly do not assume that the database is partitioned in any way. In some cases, and in particular for the well-known TPC-C benchmark, the degree of parallelism can be improved greatly by partitioning the database at the schema level (using the *warehouse* attribute in the case of TPC-C). Such a static partitioning scheme is exemplified on the left-hand side of Figure 2.2. VoltDB for example makes use of static partitioning for parallelism [168]. But such a partitioning is hard to find in general, and users usually cannot be trusted to find perfect partitioning schemes [98]. In addition, there can always be transactions that cross partition boundaries, as illustrated by Figure 2.2. In the figure the horizontal axis represents time and the colored areas represent the read/write sets of transactions T1, T2, and T3. The read/write sets do not overlap, but nevertheless there is no static partitioning scheme (horizontal line) that isolates the transactions. These transactions have to be isolated with a serial (or locking-based) approach as the static partitioning scheme cannot guarantee their isolation. If available, we could still exploit partitioning information in our HTM approach, of course, as then conflicts would be even more unlikely. But we explicitly do not assume the presence of such a static partitioning scheme and rely on the implicit adaptive partitioning of the transactions as sketched on the right-hand side of Figure 2.2.

The rest of this chapter is structured as follows: First, we discuss the different alternatives for concurrency control within database systems in Section 2.2. Then, we

synchronization method	1 thread	4 threads
2PL	50,541	108,756
serial execution	129,937	-
manually partitioned, serial	119,232	369,549

Table 2.1: Transaction rates for various synchronization methods in HyPer

discuss the advantages and limitations of hardware transactional memory in Section 2.3 and Section 2.4. In Section 2.5, we present our transaction manager, which uses hardware transactional memory as a building block for highly concurrent transaction execution. After that, we explain in Section 2.6 an HTM-friendly data layout which minimizes false conflicts. Experimental results are explained in Section 2.7. Finally, after presenting related work in Section 2.8, we summarize this chapter in Section 2.9.

2.2 Background and Motivation

As databases are expected to offer ACID transactions, they have to implement a mechanism to synchronize concurrent transactions. The traditional concurrency control method used in most database systems is some variant of two-phase locking (2PL) [178]. Before accessing a database item (tuple, page, etc.), the transaction acquires a lock in the appropriate lock mode (shared, exclusive, etc.). Conflicting operations, i.e., conflicting lock requests, implicitly order transactions relative to each other and thus ensure serializability.

In the past this model worked very well. Concurrent transaction execution was necessary to hide I/O latency, and the costs for checking locks was negligible compared to the processing costs in disk-based systems. However, this has changed in modern systems, where large parts of the data are kept in main memory, and where query processing is increasingly CPU bound. In such a setup, lock-based synchronization constitutes a significant fraction of the total execution time, in some cases even dominates the processing [63, 134].

This observation has motivated some main-memory based systems to adopt a serial execution model [63]: Instead of expensive synchronization, all transactions are executed serially, eliminating any need for synchronization. And as a main-memory based system does not have to hide I/O latency, such a model works very well for short, OLTP-style transactions.

Table 2.1 shows TPC-C transaction rates under these two models. We used HyPer [87] as the basis for the experiments. The serial execution mode easily outperforms 2PL. Due to the inherent overhead of maintaining a synchronized lock manager in 2PL, serial execution achieves 2.6 times the transaction rate of 2PL. This is a strong argument in favor of the serial execution mode proposed by [63]. On the other hand, the figure also shows the weakness of serial execution: Increasing the degree of parallelism in 2PL increases the transaction rate. Admittedly the effect is relatively minor in the TPC-C setting, using 4 threads results in a speedup of only 2, but there still is an effect. Serial execution cannot make use of additional threads, and thus the transaction rate remains constant. As the number of cores in modern systems grows while single-threaded performance stagnates, this becomes more and more of a problem.

Systems like H-Store/VoltDB [168] or HyPer [87] tried to solve this problem by partitioning the data. Both systems would partition the TPC-C workload along the *warehouse* attribute, and would then execute all transactions concurrently that operate on separate warehouses. If transactions access more than one warehouse, the system falls back to the serial execution model. In the TPC-C benchmark this occurs for about 11% of the transactions. Nevertheless, this model works relatively well for TPC-C, as shown in Figure 2.1, where it is about 3 times faster than serial execution for 4 threads. But it is not very satisfying to depend on static partitioning.

First of all, it needs human intervention. The database administrator has to specify how the data should be partitioned; HyPer has no automatic mechanism for this, whereas in H-Store there were attempts to derive such partitioning schemes automatically, e.g., Schism [34]. But, as mentioned by Larson et al. [98], a good partitioning scheme is often hard to find, in particular when workloads may shift over time. For TPC-C the partitioning schema is obvious—as it was (artificially) specified as a schema tree—but for other schemata it is not. Second, the partitioning scheme breaks if transactions frequently cross their partition boundaries. For TPC-C this is not much of a problem, as only relatively few transactions cross partition boundaries and the workload does not change, but in general it is hard to find a partitioning scheme that fits a complex workload well. And it is important to note that a partition-crossing transaction does not necessarily conflict with any other transaction! In the static partitioning execution model two transactions will be serialized if they access the same partition, even if the data items they access are completely distinct. This is highlighted in Figure 2.2 where all three transactions on the left-hand side are viewed as potentially conflicting as they (occasionally) cross their partition boundaries.

As this state of the art is not very satisfying, we will in the following develop a synchronization mechanism that is as fine-grained as 2PL and, in terms of overhead, nearly as cheap as serial execution. With our HTM-supported, dynamically-partitioned execution model the transactions shown on the right-hand side of Figure 2.2 are executed in parallel without conflicts as their read/write-sets do not overlap.

Note that in this chapter we concentrate on relatively short, non-interactive transactions. The methods we propose are not designed for transactions that touch millions of tuples or that wait minutes for user interaction. In HyPer such long-running transactions are moved into a snapshot with snapshot-isolation semantics [87, 134, 143]. As these snapshots are maintained automatically by the OS, there is no interaction between these long-running transactions and the shorter transactions we consider here. In general, any system that adopts our techniques will benefit from a separate snapshotting mechanism to avoid the conflicts with long-running transactions, such as OLAP queries and interactive transactions.

2.3 Transactional Memory

Traditional synchronization mechanisms are usually implemented using some form of mutual exclusion (mutex). For 2PL, the DBMS maintains a lock structure that keeps track of all currently held locks. As this lock structure is continuously updated by concurrent transactions, the structure itself is protected by one (or more) mutexes [58]. On top of this, the locks themselves provide a kind of mutual exclusion mechanism, and block a transaction if needed.

The problem with locks is that they are difficult to use effectively. In particular, finding the right lock granularity is difficult. Coarse locks are cheap, but limit concurrency. Fine-grained locks allow for more concurrency, but are more expensive and can lead to deadlocks.

For quite some time now, transactional memory has been proposed as an alternative to fine grained locking [69]. The key idea behind transactional memory is that a number of operations can be combined into a transaction, which is then executed atomically. Consider the following small code fragment for transferring money from one account to another account (using GCC syntax):

```
transfer(from,to,amount)
  __transaction_atomic {
    account[from]-=amount;
    account[to]+=amount;
  }
```

The code inside the *atomic* block is guaranteed to be executed atomically, and in isolation. In practice, the transactional memory observes the read set and write set of transactions, and executes transactions concurrently as long as the sets do not conflict. Thus, transfers can be executed concurrently as long as they affect different accounts, they are only serialized if they touch a common account. This behavior is very hard to emulate using locks. Fine-grained locking would allow for high concurrency, too, but would deadlock if accounts are accessed in opposite order. Transactional memory solves this problem elegantly using speculation (and conflict detection).

Transactional memory has been around for a while, but has usually been implemented as Software Transactional Memory (STM), which implements transactions on the programming-language level. Although STM does remove the complexity of lock maintenance, it causes a significant slowdown during execution and thus had limited practical impact [28].

2.3.1 Hardware Support for Transactional Memory

This changed with the Haswell microarchitecture from Intel, which offers Hardware Transactional Memory [73]. Note that Haswell was not the first CPU with hardware support for transactional memory, for example IBM's Blue Gene/Q supercomputers [176] and System z mainframes [76] offered it before, but it is the first mainstream CPU to implement HTM. And in hardware, transactional memory can be implemented much more efficiently than in software: Haswell uses its highly optimized cache coherence protocol, which is needed for all multi-core processors anyway, to track read and write set collisions [155]. Therefore, Haswell offers HTM nearly for free.

Even though HTM is very efficient, there are also some restrictions. First of all, the size of a hardware transaction is limited. For the Haswell microarchitecture it is limited to the size of the L1 cache, which is 32 KB. This implies that, in general, it is not possible to simply execute a database transaction as one monolithic HTM transaction. Even medium-sized database transactions would be too large. Second, in the case of conflicts, the transaction *fails*. In this case the CPU undoes all changes, and then reports an error that the application has to handle. And finally, a transaction might fail due to spurious hardware implementation details like cache associativity limits, interrupts, etc. Some of these failure modes are documented by Intel, while others are not. So, even though in most cases HTM will work fine, there is no guarantee that a transaction will ever succeed (if executed as an HTM transaction).

Therefore, Intel proposes (and explicitly supports by specific instructions) using transactional memory for lock elision [155]. Conceptually, this results in code like the following:

```
transfer(from,to,amount)
  atomic-elide-lock (lock) {
    account[from]-=amount;
    account[to]+=amount;
  }
```

Here, we still have a lock, but ideally the lock is not used at all—it is elided. When the code is executed, the CPU starts an HTM transaction, but does *not* acquire the lock as shown on the left-hand side of Figure 2.3. Only when there is a conflict the transaction rolls back, acquires the lock, and is then executed *non-transactionally*. The right-hand side of Figure 2.3 shows the fallback mechanism to exclusive serial execution, which is controlled via the (previously elided) lock. This lock elision mechanism has two effects. First, ideally, locks are never acquired and transactions are executed

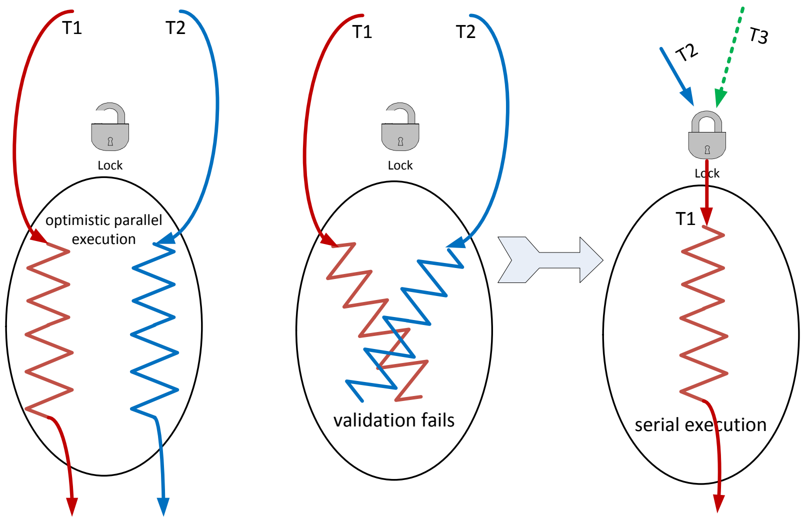

Figure 2.3: Lock elision (left), conflict (middle), and serial execution (right)

concurrently as much as possible. Second, if there is an abort due to a conflict or hardware-limitation, there is a "slow path" available that is guaranteed to succeed.

2.3.2 Caches and Cache Coherency

Even though Intel generally does not publish internal implementation details, Intel did specify two important facts about Haswell's HTM feature [155]:

- The cache coherency protocol is used to detect transactional conflicts.
- The L1 cache serves as a transactional buffer.

Therefore, it is crucial to understand Intel's cache architecture and coherency protocol.

Because of the divergence of DRAM and CPU speed, modern CPUs have multiple caches in order to accelerate memory accesses. Intel's cache architecture is shown in Figure 2.4, and consists of a local L1 cache (32 KB), a local L2 cache (256 KB), and a shared L3 cache (2-45 MB). All caches use 64 byte cache blocks (lines) and all caches are transparent, i.e., programs have the illusion of having only one large main memory. Because on multi-core CPUs each core generally has at least one local cache, a cache coherency protocol is required to maintain this illusion.

Most CPU vendors, including Intel and AMD, use extensions of the well-known MESI protocol [67]. The name of the protocol derives from the four states that each cache line can be in (Modified, Exclusive, Shared, or Invalid). To keep multiple caches coherent, the caches have means of intercepting ("snooping") each other's load and store requests. For example, if a core writes to a cache line which is stored in multiple caches (Shared state), the state must change to Modified in the local cache and all

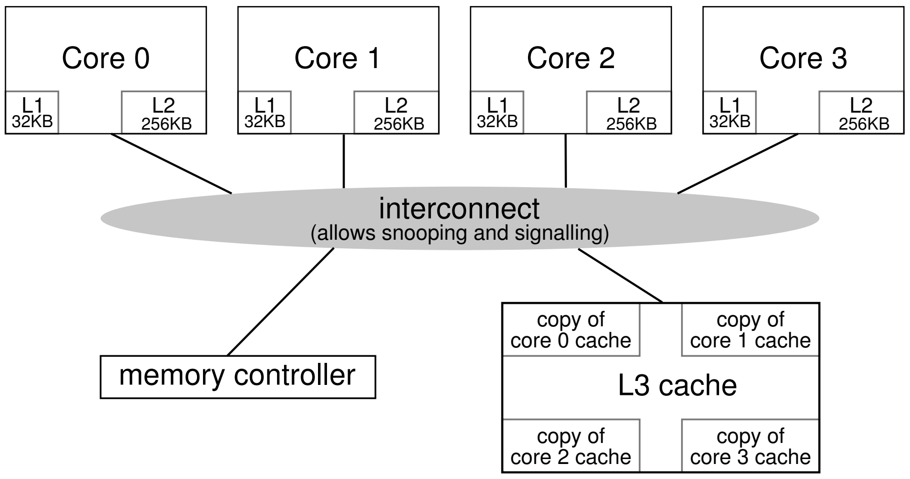

Figure 2.4: Intel cache architecture

copies in remote caches must be invalidated (Invalid state). This logic is implemented in hardware using the cache controller of the shared L3 cache that acts as a central component where all coherency traffic and all DRAM requests pass through.

The key insight that allows for an efficient HTM implementation is that the L1 cache can be used as a local buffer. All transactionally read or written cache lines are marked and the propagation of changes to other caches or main memory is prevented until the transaction commits. Read/write and write/write conflicts are detected by using the same snooping logic that is used to keep the caches coherent. And since the MESI protocol is always active and commits/aborts require no inter-core coordination, transactional execution on Haswell CPUs incurs almost no overhead. The drawback is that the transaction size is limited to the L1 cache. This is fundamentally different from IBM's Blue Gene/Q architecture, which allows for up to 20 MB per transaction using a multi-versioned L2 cache, but has relatively large runtime overhead [176].

Besides the nominal size of the L1 cache, another limiting factor for the maximum transaction size is cache associativity. Caches are segmented into sets of cache lines in order to speed up lookup and to allow for an efficient implementation of the pseudo-LRU replacement strategy (in hardware). Haswell's L1 cache is 8-way associative, i.e., each cache set has 8 entries. This has direct consequences for HTM, because all transactionally read or written cache lines must be marked and kept in the L1 cache until commit or abort. Therefore, when a transaction writes to 9 cache lines that happen to reside in the same cache set, the transaction is aborted. And since the mapping from memory address to cache set is deterministic (bits 7-12 of the address are used), restarting the transaction does not help, and an alternative fallback path is necessary for forward progress.

In practice, bits 7-12 of memory addresses are fairly random, and aborts of very

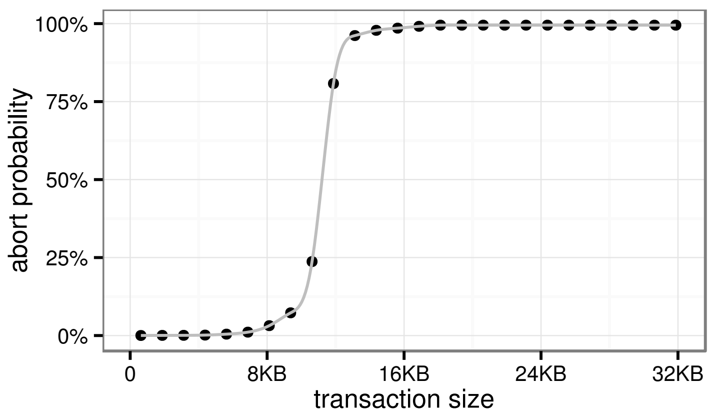

Figure 2.5: Aborts from random memory writes

small transactions are unlikely. Nevertheless, Figure 2.5 shows that the abort probability quickly rises when more than 128 random cache lines (only about one quarter of the L1 cache) are accessed[1]. This surprising fact is caused by a statistical phenomenon related to the birthday paradox: For example with a transaction size of 16 KB, *for any one* cache set it is quite unlikely that it contains more than 8 entries. However, at the same time, it is likely that *at least one* cache set exceeds this limit. The hardware ensures that the eviction of a cache line that has been accessed in an uncommitted transaction leads to a failure of this transaction, as it would otherwise become impossible to detect conflicting writes to this cache line.

The previous experiment was performed with accesses to memory addresses fully covered by the translation lookaside buffer (TLB). TLB misses do *not* immediately cause transactions to abort, because, on x86 CPUs, the page table lookup is performed by the hardware (and not the operating system). However, TLB misses do increase the abort probability, as they cause additional memory accesses during page table walks.

Besides memory accesses, another important reason for transactional aborts is interrupts. Such events are unavoidable in practice and limit the maximum duration of transactions. Figure 2.6 shows that transactions that take more than 1 million CPU cycles (about 0.3 ms) will likely be aborted. This happens due to interrupts and even if these transaction do not execute any memory operations. These results clearly show that Haswell's HTM implementation cannot be used for long-running transactions but is designed for short critical sections. Despite these limitations we found that Haswell's HTM implementation offers excellent scalability as long as transactions are short and free of conflicts with other transactions.

[1]The experiments in this section were performed on an Intel i5 4670T.

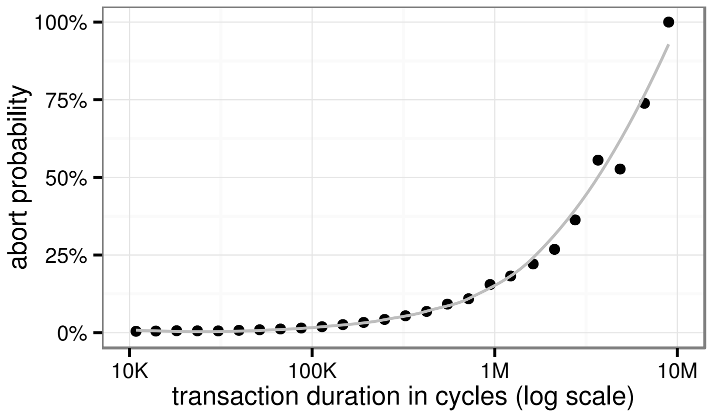

Figure 2.6: Aborts from transaction duration

2.4 Synchronization on Many-Core CPUs

To execute transactional workloads, a DBMS must provide (1) high-level concurrency control to logically isolate transactions, and (2) a low-level synchronization mechanism to prevent concurrent threads from corrupting internal data structures. Both aspects are very important, as each of them may prevent scalability. In this section we focus on the low-level synchronization aspect, before describing our concurrency control scheme in Section 2.5. We experimentally evaluate HTM on a Haswell system with 28 cores and compare it with common synchronization alternatives like latching.

The experiments in this section use a Haswell EP system with *two* Intel E5-2697 v3 processors that are connected through an internal CPU interconnect, which Intel calls QuickPath Interconnect (QPI). The processor is depicted in Figure 2.7 and has 14 cores, i.e., in total, the system has 28 cores (56 HyperThreads). The figure also shows that the CPU has two internal communication rings that connect cores and 2.5 MB slices of the L3 cache. An internal link connects these two rings, but is not to be confused with the QPI interconnect that connects the two sockets of the system. The system supports two modes, which can be selected in the systems' BIOS:

- The hardware can hide the internal ring internal structure, i.e., our two-socket system would expose two NUMA nodes with 14 cores each.
- In the "cluster on die" configuration each internal ring is exposed as a separate NUMA node, i.e., our two-socket system has four NUMA nodes with 7 cores each.

Using the first setting, each socket has 35 MB of L3 cache but higher latency, because an L3 access often needs to use the internal link. The cluster-on-die configuration,

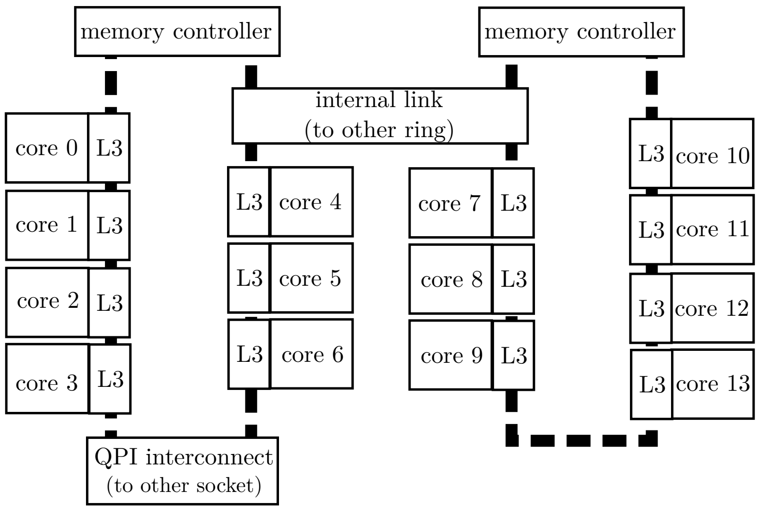

Figure 2.7: Intel E5-2697 v3

which we use for all experiments, has lower latency and 17.5 MB of cache per "cluster", each of which consists of 7 threads.

As has been widely reported, all Haswell systems shipped so far, including our system, contain a hardware bug in the Transactional Synchronization Extensions (TSX). According to Intel, this bug occurs "under a complex set of internal timing conditions and system events". We have not encountered this bug during our tests. It seems to be very rare, as evidenced by the fact that it took Intel over a year to even find it. Furthermore, Intel has announced that the bug will be fixed in upcoming CPU generations.

2.4.1 The Perils of Latching

Traditionally, database systems synchronize concurrent access to internal data structures (e.g., index structures) with latches. Internally, a latch is implemented using atomic operations like compare-and-swap, which allow one to exclude other threads from entering a critical section. To increase concurrency, read/write latches are often used, which, at any time, allow multiple concurrent readers but only a single writer. Unfortunately, latches do not scale on modern hardware as Figure 2.8, which performs lookups in an Adaptive Radix Tree [108], shows. The curve labeled as "rw_spin_lock" shows the performance when we add a single read/write latch at the root node of the tree[2]. With many cores, using no synchronization is faster by an order of magnitude! Note that this happens on a read-only workload without any logical contention, and is not caused by a bad latch implementation[3]: When we replace the latch with a sin-

[2]In reality, one would use lock-coupling and one latch at each node, so the performance would be even worse.

[3]We used `spin_rw_mutex` from the Intel Thread Building Blocks library.

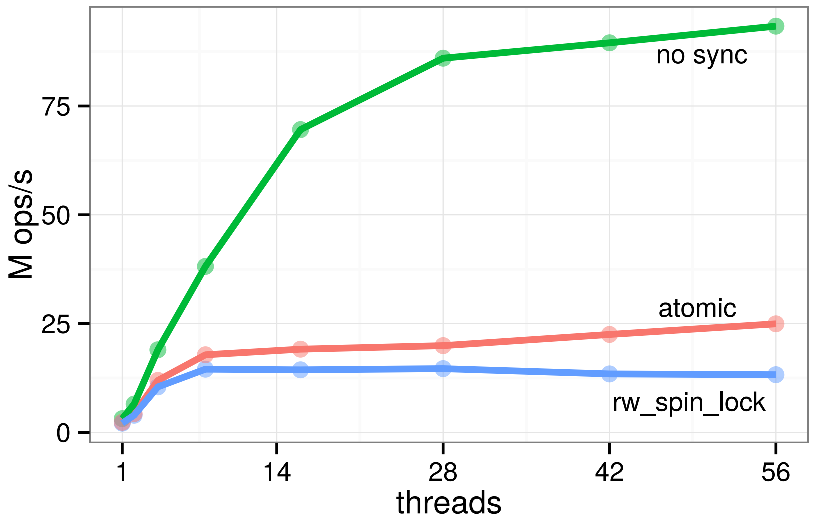

Figure 2.8: Lookups in a search tree with 64M entries

gle atomic integer increment operation, which is the cheapest possible atomic write operation, the scalability is almost as bad as with the latch.

The reason for this behavior is that to acquire a latch, CPUs must acquire exclusive access to the cache line where the latch is stored. As a result, threads compete for this cache line, and every time the latch is acquired, all copies of this cache line are invalidated in all other cores ("cache line ping-pong"). This happens even with atomic operations like atomic increment, although this operation never fails in contrast to compare-and-swap, which is usually used to implement latches. Note that latches also result in some overhead during single-threaded execution, but this overhead is much lower as the latch cache line is not continuously invalidated. Cache line ping-pong is often the underlying problem that prevents systems from scaling on modern multi-core CPUs.

2.4.2 Latch-Free Data Structures

As a reaction to the bad scalability of latching some systems use latch-free data structures. Microsoft's in-memory transaction engine Hekaton, for example, uses a lock-free hash table and the latch-free Bw-Tree [114] as index structures. In the latch-free approach read accesses can proceed in a non-blocking fashion without acquiring any latches and without waiting. Writes must make sure that any modification is performed using a sequence of atomic operations while ensuring that simultaneous reads are not disturbed. Since readers do not perform writes to global memory locations, this approach generally results in very good scalability for workloads that mostly consist of reads. However, latch-free data structure have a number of disadvantages:

- The main difficulty is that, until the availability of Hardware Transactional Memory, CPUs provided only very primitive atomic operations like compare-and-swap, and a handful of integer operations. Synchronizing any non-trivial data structure with this limited tool set is very difficult and bug-prone, and for many efficient data structures, including the Adaptive Radix Tree, so far, no latch-free synchronization protocol exists. In practice, data structures must be designed with latch-freedom in mind, and the available atomic operations restrict the design space considerably.

- And even if one succeeds in designing a latch-free data structure, this may not guarantee optimal performance. The reason is that, usually, additional indirections must be introduced, which often add significant overhead in comparison with an unsynchronized variant of the data structure. The Bw-Tree [114], for example, requires a page table indirection, which must be used on each node access and incurs additional cache misses.

- Finally, memory reclamation is an additional problem. Without latches, a thread can never be sure when it is safe to reclaim memory, because concurrent readers might still be active. An additional mechanism (e.g., epoch-based reclamation), which again adds some overhead, is required to allow for safe memory reclamation.

For these reasons, we believe that it is neither realistic nor desirable to replace all the custom data structures used by database systems with latch-free variants. Hardware Transactional Memory offers an easy to use, and, as we will show, efficient alternative. In particular, HTM has no memory reclamation issues and one can simply wrap each data structure access in a hardware transaction. This means that data structures can be designed without spending too much thought on how to synchronize them—though some understanding of how HTM works and its limitations is certainly beneficial.

2.4.3 Hardware Transactional Memory on Many-Core Systems

Figure 2.9 shows the performance of HTM on the same read-only workload as Figure 2.8. We compare different lock elision approaches (with a single global, elided latch), and we again show the performance without synchronization as a theoretical upper bound. Surprisingly, the built-in hardware lock elision (HLE) instructions do not scale well when more than 4 cores are used. The internal implementation of HLE is not disclosed, but the reason for its bad performance is likely an insufficient number of restarts. As we have mentioned previously, a transaction can abort spuriously for many reasons. A transaction should therefore retry a number of times instead of giving up immediately and acquiring the fallback latch. The graph shows that for a read-only

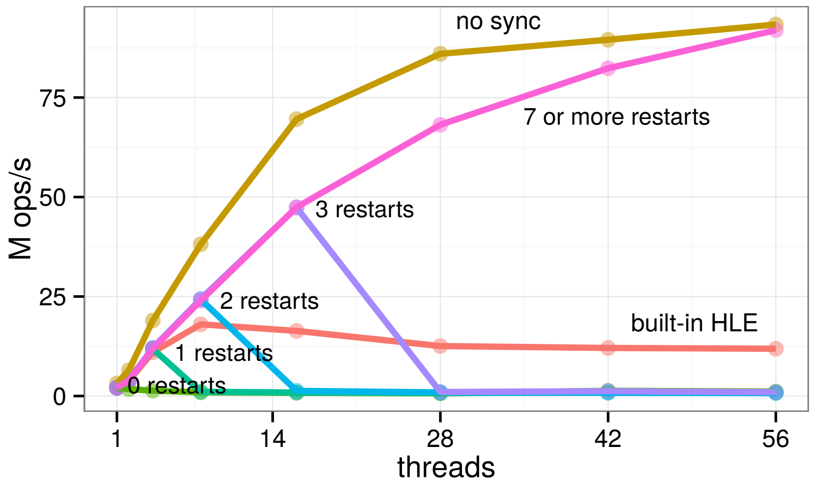

Figure 2.9: Lookups in an ART index with 64M integer entries under a varying number of HTM restarts

workload, restarting at least 7 times is necessary, though a higher number of restarts also works fine.

Therefore, we implemented lock elision manually using the restricted transactional memory (RTM) primitives `xbegin`, `xend`, `xabort`, but with a configurable number of restarts. Figure 2.10 shows the state diagram of our implementation. Initially the optimistic path (left-hand side of the diagram) is taken, i.e., the critical section is simply wrapped by `xbegin` and `xend` instructions. If an abort happens in the critical section (e.g., due to a read/write conflict), the transaction is restarted a number of times before falling back to actual latch acquisition (right-hand side of the diagram). Furthermore, transactions add the latch to their read set and only proceed into the critical section optimistically when the latch is free. When it is not free, this means that another thread is in the critical section exclusively (e.g., due to code that cannot succeed transactionally). In this case, the transaction has to wait for the latch to become free, but can then continue to proceed optimistically using RTM. Note that all this logic is completely hidden behind a typical acquire/release latch interface, and—once it has been implemented—it can be used just as easily as ordinary latches or Itel's Hardware Lock Elision instructions. Furthermore, as Diegues and Romano [39] have shown, the configuration parameters of the restart strategy can be determined dynamically.

When sufficient restarts are used, the overhead of HTM in comparison to unsynchronized access is quite low. Furthermore, we found that HyperThreading improves performance for many workloads, though one has to keep in mind that because each pair of HyperThreads shares one L1 cache, the effective maximum working set size is halved, so there might be workloads where it is beneficial to avoid this feature.

Good scalability on read-only workloads should be expected, because only infre-

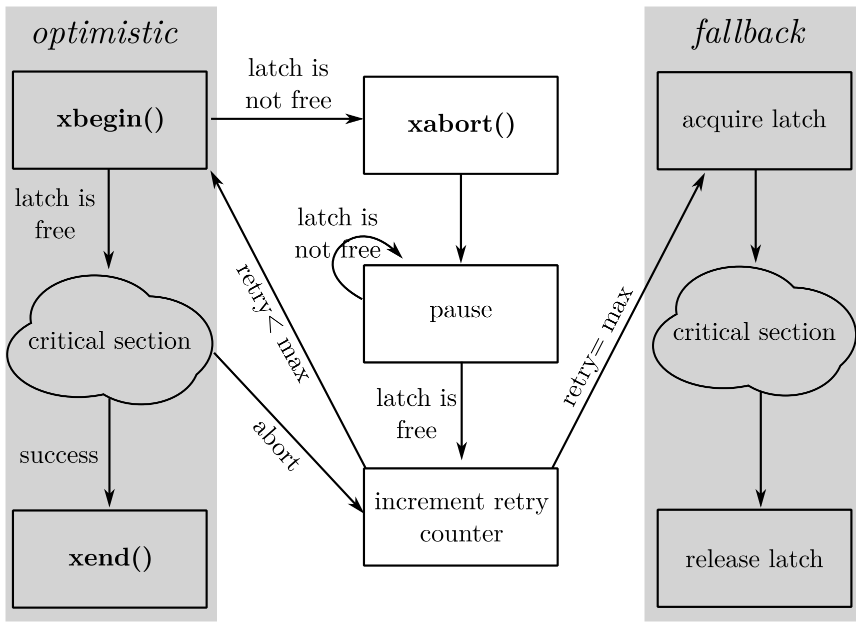

Figure 2.10: Implementation of lock elision with restarts using RTM operations

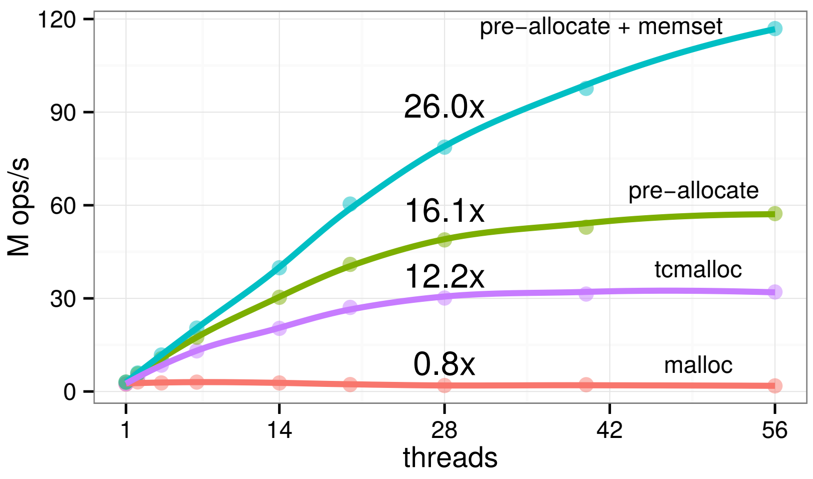

Figure 2.11: 64M random inserts into an ART index using different memory allocators and 30 restarts

quent, transient failures occur, thus we now turn our attention to more challenging workloads. Figure 2.11 reports the results for a random insert workload with 30 restarts and different memory allocators. With the default memory allocator on Linux (labeled as "malloc"), the insert workload does not scale at all. The tcmalloc[4] (Thread-Caching Malloc) allocator improves scalability considerably, but the speedup with 28 threads is still only 12.2×. Optimal scalability is only achieved with pre-allocated and pre-initialized[5] memory, which results in a speedup of 26.0× with 28 cores. Initialization is important, because the first write to a freshly-allocated memory page *always* causes the transaction to abort as an operating system trap that initializes the page happens. Although these page initialization operations are quite infrequent (less than 5% of the single-threaded execution time), they cause the elided latch to be acquired and therefore full serialization of all threads occurs.

So far, in all experiments the memory was interleaved between the four memory nodes. In order to investigate the NUMA effects on HTM, we repeated the insert and lookup experiments with 1 and 7 threads, but forced the threads and memory allocations to one cluster, one socket, or two sockets:

	1 cluster	1 socket	2 sockets
insert (1 thread)	5.3	4.3	3.0
insert (7 threads)	30.6	26.8	20.2
lookup (1 thread)	9.2	5.4	3.6
lookup (7 threads)	53.0	36.0	24.5

The results are in M ops/s and show that there are significant NUMA effects: remote accesses are up to a factor 2.5 more expensive than local accesses. At the same time, HTM scales very well even across clusters or sockets. To some extent, this is not very surprising, because NUMA systems have an effective cache coherency protocol implementation, which is also used for efficient transactional conflict detection.

Finally, let us close this section with an experiment that shows that modern CPUs do not scale under very high contention regardless of which synchronization primitives are used. Figure 2.12 shows the performance for an extreme workload where there is a single atomic counter that is incremented by all threads. We implemented a number of synchronization primitives:

- Intel's Hardware Lock Elision feature ("HLE")
- hardware transactional memory as described in Figure 2.10 ("RTM")

[4]`http://goog-perftools.sourceforge.net/doc/tcmalloc.html`

[5]Modern operating systems by default do not provide physical memory pages on allocation. Instead, the first write a to page will cause a context switch into the kernel that will provide the page. Scalability with HTM is affected because a context switch always aborts the transaction. It is therefore beneficial to allocate and initialize memory outside of HTM transactions.

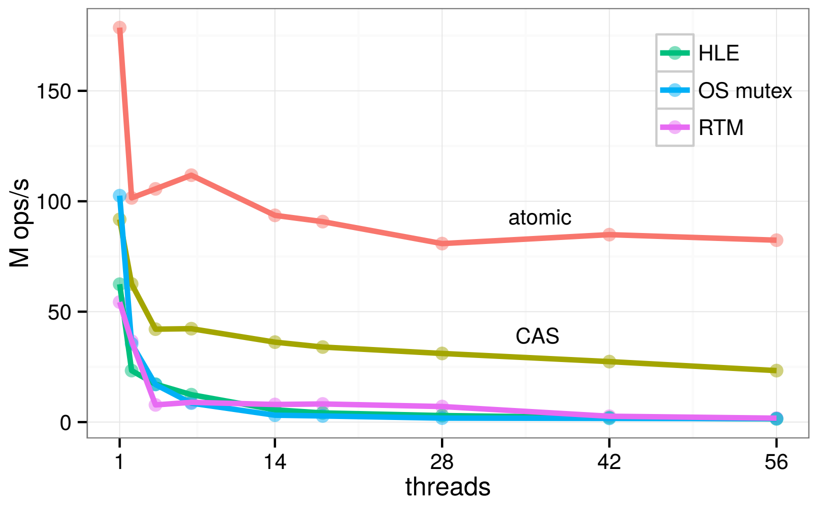

Figure 2.12: Incrementing a single, global counter (extreme contention)

- operating system mutex ("OS mutex")
- atomic increment instruction ("atomic")
- atomic compare-and-swap instruction ("CAS")

In all cases performance degrades with more cores due to cache line ping-pong. For workloads with high contention one needs an approach that solves the root cause, physical contention, e.g., by duplicating the contended item [137].

2.4.4 Discussion

The great advantage of HTM is that it is the only synchronization approach that offers good performance and scalability while being very easy to use. Our experiments with hardware transactional memory on a 28-core system with Non-Uniform Memory Access (NUMA) have shown that HTM can indeed scale to large systems. However, we have also seen that to get good performance a number of important points must be considered:

- The built-in Hardware Lock Elision feature does not scale when many cores are used.
- Instead, one should implement lock elision using the Restricted Transactional Memory primitives, and set the number of retries to 20 or more.
- Additionally, one has to make sure that the percentage of transactions that cannot be executed transactionally, e.g., due to kernel traps, is very low. Otherwise

failed lock elision will cause serialization, and Amdahl's Law severely limits scalability.

- HTM, just like latching or atomic operations, does not scale under very high contention workloads.

Nevertheless, HTM is a powerful and efficient new synchronization primitive for many-core systems.

2.5 HTM-Supported Transaction Management

Writing scalable *and* efficient multithreaded programs is widely considered a very difficult problem. In particular, it is very hard to decide at which granularity latching/locking should be performed: if very fine-grained latching is used, the additional overhead will annihilate any speedup from parallelism; with coarse-grained latches, parallelism is, limited. For non-trivial programs, this is a very difficult problem, and the most efficient choice can often only be decided empirically. The granularity problem is even more difficult for a database system because it must efficiently support arbitrary workloads. With hardware support, transactional memory offers an elegant solution: As long as conflicts are infrequent, HTM offers the parallelism of fine-grained latching, but without its overhead; if hotspots occur frequently, the best method in main-memory databases is serial execution, which is exactly the fallback path for HTM conflicts. Therefore, HTM is a highly promising building block for high performance database systems.

2.5.1 Mapping Database Transactions to HTM Transactions

As the maximum size of hardware transactions is limited, only a database transaction that is small can directly be mapped to a single hardware transaction. Therefore, we assemble complex database transactions by using hardware transactions as building blocks, as shown in Figure 2.13. The key idea here is to use a customized variant of timestamp ordering (TSO) to "glue" together these small hardware transactions. TSO is a classic concurrency control technique, which was extensively studied in the context of disk-based and distributed database systems [27, 16]. For disk-based systems, TSO is not competitive to locking because most read accesses result in an update of the read timestamp, and thus a write to disk. These timestamp updates are obviously much cheaper in RAM. Fine-grained locking, in contrast, is much more expensive than maintaining timestamps in main memory, as we will show in Section 2.7.

Timestamp ordering uses read and write timestamps to identify read/write and write/write conflicts. Each transaction is associated with a monotonically increasing timestamp, and whenever a data item is read or updated its associated timestamp is updated, too.

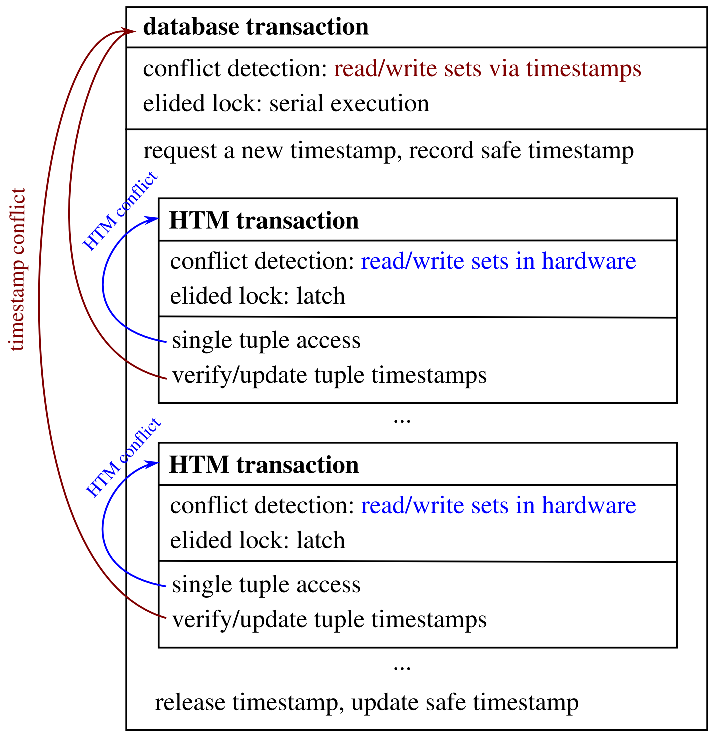
database transaction
conflict detection: read/write sets via timestamps
elided lock: serial execution
request a new timestamp, record safe timestamp
HTM transaction
conflict detection: read/write sets in hardware
elided lock: latch
single tuple access
verify/update tuple timestamps
...
HTM transaction
conflict detection: read/write sets in hardware
elided lock: latch
single tuple access
verify/update tuple timestamps
...
release timestamp, update safe timestamp
timestamp conflict
HTM conflict
HTM conflict

Figure 2.13: Transforming database transactions into HTM transactions

The *read timestamp* of a data item records the youngest reader of this particular item, and the *write timestamp* records the last writer. This way, a transaction recognizes if its operation collides with an operation of a “younger” transactions (i.e., a transaction with a larger timestamp), which would be a violation of transaction isolation. In particular, an operation fails if a transaction tries to read data from a younger transaction, or if a transaction tries to update a data item that has already been read by a younger transaction.

Basic, textbook TSO [27] has two issues: First, by default it does not prevent phantoms. Second, some care is needed to prevent non-recoverable schedules, as by default transactions are allowed to read data from older, but potentially non-committed, transactions. To resolve both issues (phantoms and dirty reads), we deviate from basic TSO by introducing a “safe timestamp”, i.e., a point in time where it is known that all older transactions have already been committed. With classical TSO, when a transaction tries to read a dirty data item (marked by a dirty bit) from another transaction, it must wait for that transaction to finish. In main-memory database systems running at full clock speed, waiting is very undesirable.

We avoid both waiting and phantom problems with the *safe timestamp* concept. The safe timestamp $\mathrm{TS}_{\mathrm{safe}}$ is the youngest timestamp with the following property:

All transactions with an older timestamp TS_{old} with $\text{old} \leq \text{safe}$ have already been committed or aborted. While regular TSO compares transaction timestamps directly, we compare timestamps to the safe timestamp of each transaction: Everything that is older than the safe timestamp can be safely read, and everything that has been read only by transactions up to the safe timestamp can safely be modified. Note that we could also access or modify some tuples with newer timestamps, namely those from transactions that have already committed after this transaction started. But this would require complex and expensive checks during tuple access, in particular if one also wants to prevent phantoms. We therefore use the safe timestamp as a cheap, though somewhat conservative, mechanism to ensure serializability. In the scenario

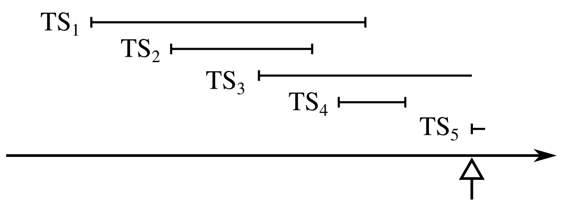

the safe timestamp of TS_5 would be set to TS_2. So transaction TS_5 would validate its read access such that only data items with a write timestamp $\text{TS}_\text{W} \leq \text{TS}_2$ are allowed. Write accesses on behalf of TS_5 must additionally verify that the read timestamp of all items to be written satisfies the condition $\text{TS}_\text{R} \leq \text{TS}_2$. Obviously, a read or write timestamp $\text{TS} = \text{TS}_5$ is permitted as well—in case a transaction accesses the same data item multiple times.

2.5.2 Conflict Detection and Resolution

In our scheme, the read and the write timestamps are stored at each tuple. After looking up a tuple in an index, its timestamp(s) must be verified and updated. Each single tuple access, including index traversal and timestamp update, is executed as a hardware transaction using lock elision. The small granularity ensures that false aborts due to hardware limitations are very unlikely, because Haswell's hardware transactions can access dozens of cache lines (cf. Section 2.3).

Nevertheless, two types of conflicts may occur: If HTM detects a conflict (short blue arrows in Figure 2.13), the hardware transaction is restarted, but this time the latch is acquired. Rolling back a hardware transaction is very cheap, as it only involves invalidating the transactionally modified cache lines, and copies of the original content can still be found in the L2 and/or L3 cache.

For timestamp conflicts, which are detected in software (long red arrows in Figure 2.13), the system must first roll back the database transaction. This rollback utilizes the "normal" logging and recovery infrastructure of the database system, i.e., the undo-log records of the partial database transaction are applied in an ARIES-style

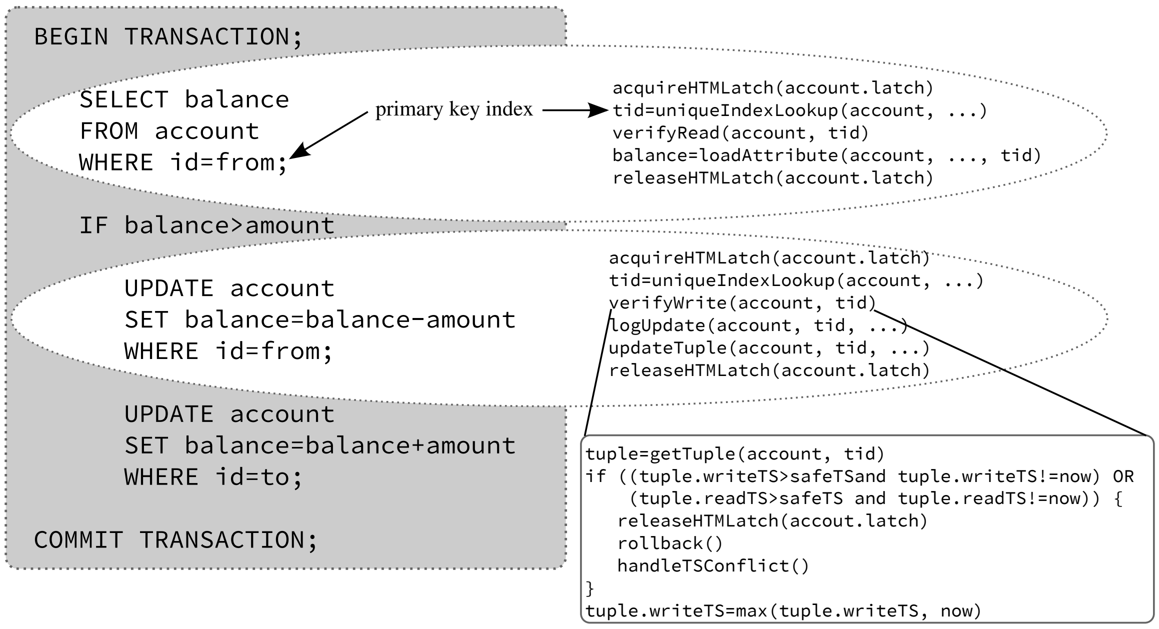

```
BEGIN TRANSACTION;

    SELECT balance
    FROM account
    WHERE id=from;

    IF balance>amount

        UPDATE account
        SET balance=balance-amount
        WHERE id=from;

        UPDATE account
        SET balance=balance+amount
        WHERE id=to;

COMMIT TRANSACTION;
```

```
acquireHTMLatch(account.latch)
tid=uniqueIndexLookup(account, ...)
verifyRead(account, tid)
balance=loadAttribute(account, ..., tid)
releaseHTMLatch(account.latch)
```

```
acquireHTMLatch(account.latch)
tid=uniqueIndexLookup(account, ...)
verifyWrite(account, tid)
logUpdate(account, tid, ...)
updateTuple(account, tid, ...)
releaseHTMLatch(account.latch)
```

```
tuple=getTuple(account, tid)
if ((tuple.writeTS>safeTSand tuple.writeTS!=now) OR
     (tuple.readTS>safeTS and tuple.readTS!=now)) {
   releaseHTMLatch(accout.latch)
   rollback()
   handleTSConflict()
}
tuple.writeTS=max(tuple.writeTS, now)
```

Figure 2.14: Implementing database transactions with timestamps and lock elision

compensation [133]. Then, the transaction is executed serially by using a global lock, rolling the log forward again. This requires logical logging and non-interactive transactions, as we cannot roll a user action backward or forward. We use snapshots to isolate interactive transactions from the rest of the system [134]. The fallback to serial execution ensures forward progress, because in serial execution a transaction will never fail due to conflicts. Note that it is often beneficial to optimistically restart the transaction a number of times instead of resorting to serial execution immediately, as serial execution is very pessimistic and prevents parallelism.

Figure 2.14 details the implementation of a database transaction using lock elision and timestamps. The splitting of stored procedures into smaller HTM transactions is fully automatic (done by our compiler) and transparent for the programmer. As shown in the pseudo code, queries or updates (within a database transaction) that access a single tuple through a unique index are directly translated into a single HTM transaction. Larger statements like range scans should be split into multiple HTM transactions, e.g., one for each accessed tuple. The index lookup and timestamp checks are protected using an elided latch, which avoids latching the index structures themselves. The implementation of the HTM latch is described in Section 2.4.3.

2.5.3 Optimizations

How the transaction manager handles timestamp conflicts is very important for performance. If the conflict is only caused by the conservatism of the safe timestamp (i.e., regular TSO would have no conflict), it is sometimes possible to avoid rolling back the transaction. If the conflicting transaction has a smaller timestamp *and* has already finished, the apparent conflict can be ignored. This optimization is possible because the safe timestamp cannot overtake a currently running transaction's timestamp.

As mentioned before, it is often beneficial to restart an aborted transaction a number of times, instead of immediately falling back to serial execution. In order for the restart to succeed, the safe timestamp must have advanced past the conflict timestamp. Since this timestamp is available (it triggered the abort), the transaction can wait, while periodically recomputing the safe timestamp until it has advanced sufficiently. Then the transaction can be restarted with a new timestamp and safe timestamp. The disadvantage of this approach is that during this waiting period no useful work is performed by the thread.

A more effective strategy is to suspend the aborted transaction and execute other transactions instead. Once the safe timestamp has advanced past the conflicting transaction's timestamp that transaction can be resumed. This strategy avoids wasteful waiting. We found rollback and re-execution to be quite cheap because the accessed data is often in cache. Therefore, our implementation immediately performs an abort after a timestamp conflict, as shown in Figure 2.14, and executes other transactions instead, until the safe timestamp has sufficiently advanced. We additionally limit the number of times a transaction is restarted before falling back to serial execution—thus ensuring forward progress.

While our description here and also our initial implementation uses both read and write timestamps, it is possible to avoid read timestamps. Read timestamps are a bit unfortunate, as they can cause "false" HTM conflicts due to parallel timestamp updates, even though the read operations themselves would not conflict. Semantically the read timestamps are used to detect if a tuple has already been read by a newer transaction, which prohibits updates by older transactions (as they would destroy serializability). However, the read timestamps can be avoided by keeping track of the write timestamps of all data items accessed (read or written) by a certain transaction. Then, at commit time, the transaction re-examines the write timestamps of all data items and aborts if any one of them has changed [45], ensuring serializability. We plan to implement this technique in future work, and expect to get even better performance in the case of read hotspots.

It is illustrative to compare our scheme to software transactional memory (STM) systems. Indeed, our scheme can be considered an HTM-supported implementation of STM. However, we get significantly better performance than pure STM by exploiting DBMS domain knowledge. For example, index structures are protected from concurrent modifications by the HTM transaction, but are not tracked with timestamps, as full transaction isolation would in fact be undesirable there. This is similar to B-tree latching in disk-based systems—however, at minimal cost. The indexed tuples themselves are isolated via timestamps to ensure serializable transaction behavior. Note further that our interpretation of timestamps is different from regular TSO [27]: Instead of deciding about transaction success and failure as in TSO, we use timestamps to detect intersecting read/write sets, just like the hardware itself for the HTM part. In the case of conflicts, we do not abort the transaction or retry with a new timestamp an indefinite number of times, but fall back to the more restrictive sequential execution mode that ensures forward progress and guarantees the eventual success of every transaction.

2.6 HTM-Friendly Data Storage

Transactional memory synchronizes concurrent accesses by tracking read and write sets. This avoids the need for fine-grained locking and greatly improves concurrency as long as objects at different memory addresses are accessed. However, because HTM usually tracks accesses at cache line granularity, false conflicts may occur. For example, if the two data items A and B happen to be stored in a single cache line, a write to A causes a conflict with B. This conflict would not have occurred if each data item had its own dedicated lock. Therefore, HTM presents additional challenges for database systems that must be tackled in order to efficiently utilize this feature.

2.6.1 Data Storage with Zone Segmentation

With a straightforward contiguous main-memory data layout, which is illustrated on the left-hand side of Figure 2.15, an insert into a relation results in appending the tuple to the end of the relation. It is clear that such a layout does not allow concurrent insertions, because each insert writes to the end of the relation. Additionally, all inserts will try to increment some variable N which counts the number of tuples. The memory location at the end of the table and the counter N are hotspots causing concurrent inserts to fail.

In order to allow for concurrent inserts, we use multiple zones per relation, as shown on the right-hand side of Figure 2.15. Each relation has a constant number of these zones, e.g., two times the number of hardware threads. A random zone number is assigned to each transaction, and all inserts of that transaction use this local zone. The same zone number is also used for inserts into other relations. Therefore, with an appropriately chosen number of zones, concurrent inserts can proceed with only a small conflict probability, even if many relations are affected. Besides the relatively small insert zones, each relation has a main zone where, for large relations, most tuples are stored.

The boundary is stored in a counter N. For each zone i, the base B_i and the next insert position N_i are maintained. When a zone becomes full (i.e., when N_i reaches B_{i+1}), it is collapsed into the neighboring zone, and a new zone at the end of the table

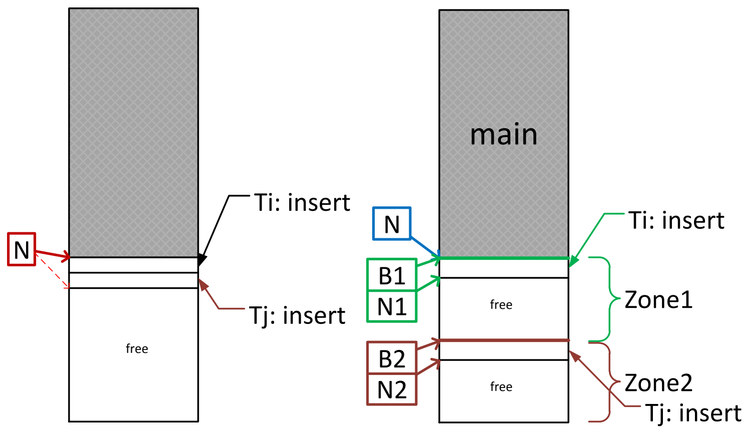

Figure 2.15: Avoiding hotspots by zone segmentation

is created. Note that no tuples are copied and the tuple identifiers do not change, only the sizes of zones need to be adjusted. As a consequence, collapsing zones does not affect concurrent access to the tuples. Eventually, the insert zones are collapsed with the large contiguous main area. For a main-memory databases this guarantees very fast scan performance at clock speed during query processing. The counters N_i and B_i should be stored in separate cache lines for each zone, as otherwise unnecessary conflicts occur while updating these values.

2.6.2 Index Structures

Besides the logical isolation of transactions using 2PL or TSO, database systems must isolate concurrent accesses to index structures. In principle, any data structure can be synchronized using HTM by simply wrapping each access in a transaction. In this section we first discuss how scalability can be improved by avoiding some common types of conflicts, before showing that HTM has much better performance than traditional index synchronization via fine-grained latches.

One common problem is that indexes sometimes have a counter that stores the number of key/value pairs and prevents concurrent modifications. Fortunately, this counter is often not needed and can be removed. For data structures that allocate small memory chunks, another source of HTM conflicts is memory allocation. This problem can be solved by using an allocator that has a thread-local buffer.

Surrogate primary keys are usually implemented as ascending integer sequences. For tree-based index structures, which maintain their data in sorted order, this causes HTM conflicts because all concurrent inserts try to access memory locations in the same vicinity, as illustrated on the left-hand side of Figure 2.16. This problem is very similar to the problem of concurrently inserting values into a table discussed above, and

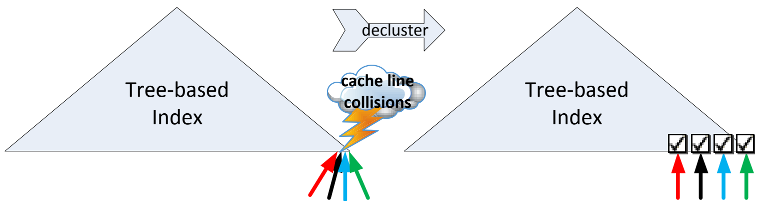

Figure 2.16: Declustering surrogate key generation

indeed the solution is similar: If permitted by the application, the integer sequence is partitioned into multiple constant-sized chunks and values are handed out from one of the chunks depending on the transactions' zone number. This prevents interference of parallel index tree insertions as they are spread across different memory locations—as shown on the right of Figure 2.16. Once all values from a chunk are exhausted, the next set of integers is assigned to it. Note that hash tables are not affected by this problem because the use of a hash function results in a random access pattern which leads to a low conflict probability. But of course, as a direct consequence of this randomization, hash tables do not support range scans.

2.7 Evaluation

For most experiments we used an Intel i5 4670T Haswell processor with 4 cores, 6 MB shared L3 cache, and full HTM support through the Intel Transactional Synchronization Extensions. The maximum clock rate is 3.3 GHz, but can only be achieved when only one core is fully utilized. When utilizing all cores, we measured a sustained clock rate of 2.9 GHz.

By default, HyPer uses serial execution similar to VoltDB [168]; multiple threads are only used if the schema has been partitioned by human intervention. In the following we will call these execution modes *serial* and *partitioned*. Note that the partitioned mode used by HyPer (as in other systems) is somewhat cheating, since the partitioning scheme has to be explicitly provided by a human, and a good partitioning scheme is hard to find in general. In addition to these execution modes we included a *2PL* implementation, described in [134], as baseline for comparisons to standard database systems, and the hardware transactional memory approach (*HTM*) proposed here. We also include TSO with coarse-grained latches (*TSO*) instead of HTM to show that TSO alone is not sufficient for good performance.

For most experiments we used the well-known TPC-C benchmark as basis (without "think times", the only deviation from the benchmark rules). We set the number of warehouses to 32, and for the partitioning experiments the strategy was to partition both the data and the transactions by the main warehouse. We used the Adaptive Radix Tree [108] as index structure, although the scalability is similar with hash tables and

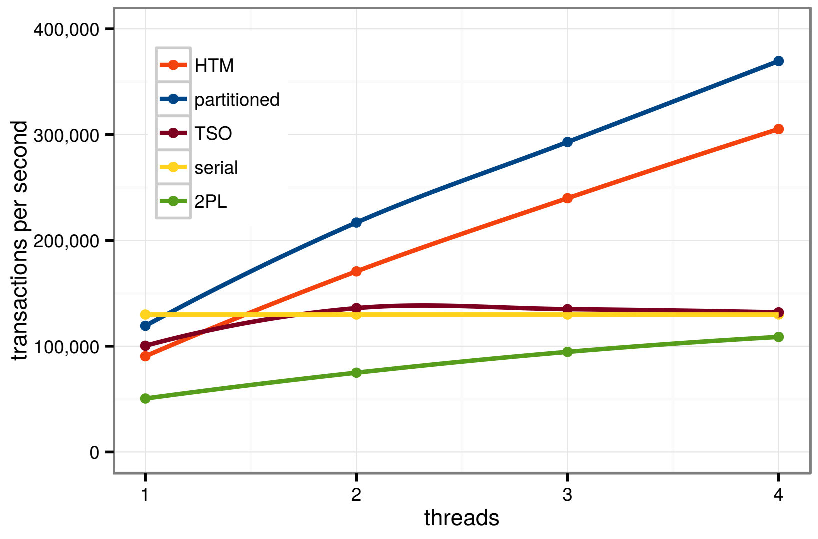

Figure 2.17: Scalability of TPC-C on desktop system

red-black trees. In the following, we first look at scalability results for TPC-C and then study the interaction with HTM in microbenchmarks.

2.7.1 TPC-C Results

In the first experiment, we ran TPC-C and varied the number of threads up to the number of available cores. The results are shown in Figure 2.17 and reveal the following: First, classical 2PL is clearly inferior to all other approaches. Its overhead is too high, and it is even dominated by single-threaded serial execution. The latching-based TSO approach has less overhead than 2PL, but does not scale because the coarse-grained (relation-level) latches severely limit concurrency. Both the partitioned scheme and HTM scale very well, with partitioning being slightly faster. But note that this is a comparison of a human-assisted approach with a fully automatic approach. Furthermore, the partitioning approach works so well only because TPC-C is "embarrassingly partitionable" in this low-thread setup, as we will see in the next experiment.

The reason that partitioning copes well with TPC-C is that most transactions stay within a single partition. By default, about 11% of all transactions cross partition boundaries (and therefore require serial execution to prevent collisions in a lock-free system). The performance depends crucially on the ability of transactions to stay within one partition. As shown in Figure 2.18, varying the percentage of partition-crossing transactions has a very deteriorating effect on the partitioning approach, while the other transaction managers are largely unaffected because, in the case of TPC-C, partition-crossing does not mean conflicting. Therefore, picking the right partitioning

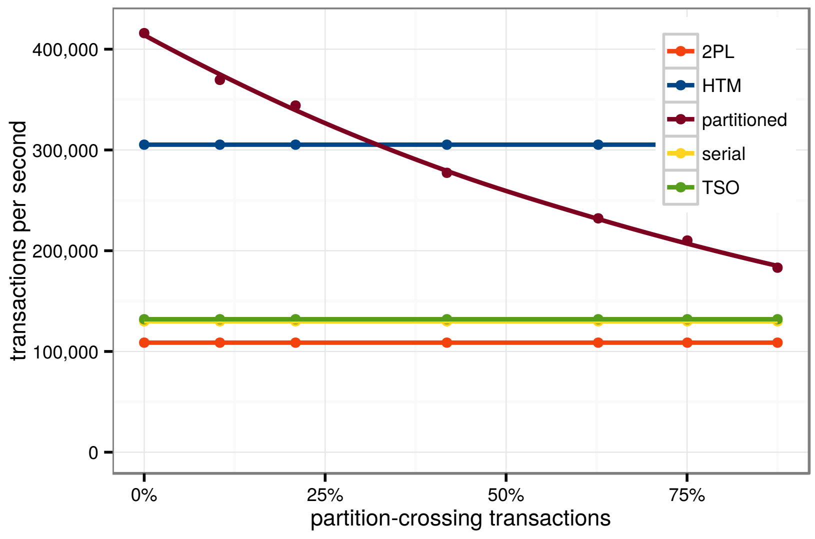

Figure 2.18: TPC-C with modified partition-crossing rates

scheme would be absolutely crucial; however, it is often hard to do—in particular if transactions are added to the workload dynamically.

Figure 2.19 shows results for TPC-C on the 28-core system described in Section 2.4. To reduce the frequent write conflicts, which occur in TPC-C at high thread counts, we set the number of warehouses to 200, the number of insert zones to 64, and the number of restarts to 30. With these settings, our HTM-supported concurrency control scheme achieves a speedup of 15$\times$ and around 1 million TPC-C transactions per second with 28 threads. The other concurrency control schemes show similar performance and scalability characteristics as on the 4-core system. The figure also shows the performance of the Silo system [172] which we measured by using the publicly available source code that includes a hand-coded TPC-C implementation in C++. Silo shows very good scalability, even at high thread counts, but is about 3x slower than HTM-supported HyPer with single-threaded execution.

2.7.2 Microbenchmarks

Our transaction manager was designed to be lightweight. Nevertheless, there is some overhead in comparison with an unsynchronized, purely single-threaded implementation. We determined the overhead by running the TPC-C benchmark using only one thread and enabling each feature separately: The HTM-friendly memory layout, including zone segmentation (with 8 zones), added 5% overhead, mostly because of reduced cache locality. The Hardware Lock Elision spinlocks, which are acquired for each tuple access, added 7% overhead. Checking and updating the timestamps,

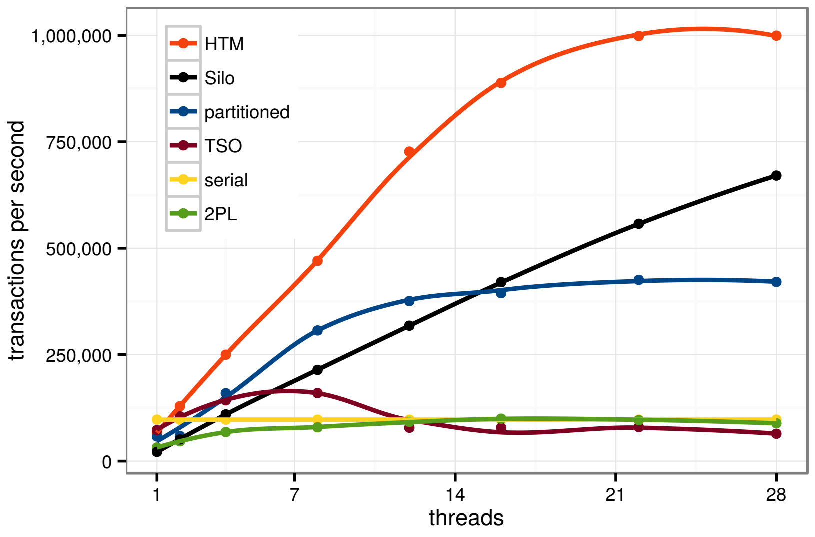

Figure 2.19: Scalability of TPC-C on server system

slowed down execution by 10%. Finally, transaction management, e.g., determining the safe timestamp, the transaction ID, etc. caused 7% overhead. In total, these changes amounted to a slowdown of 29%. HyPer compiles transactions to very efficient machine code, so any additional work will have noticeable impact. However, this is much lower than the overhead of the 2PL implementation, which is 61%! And of course the overhead is completely paid off by the much superior scalability of the HTM approach.

One interesting question is if it would be possible to simply execute a database transaction as one large HTM transaction. To analyze this, we used binary instrumentation of the generated transaction code to record the read and write sets of all TPC-C transactions. We found that only the *delivery* and *order-status* transactions have a cacheline footprint of less than 7 KB and could be executed as HTM transactions. The other transactions access between 18 KB and 61 KB, and would usually exhaust the transactional buffer. Therefore, executing TPC-C transactions as monolithic HTM transactions is not possible. And other workloads will have transactions that are much larger than the relatively simple TPC-C transactions. Therefore, a mechanism like our timestamp scheme is required to cope with large transactions.

As we discussed in Section 2.5, there are two types of conflicts: timestamp conflicts and HTM conflicts. Timestamp conflicts must be handled by the transaction manager and usually result in a rollback of the transaction. We measured that 12% of all TPC-C transactions were aborted due to a timestamp conflict, but only 0.5% required more than 2 restarts. Most aborts occur at the *warehouse* relation, which has only 32 tuples but is updated frequently.

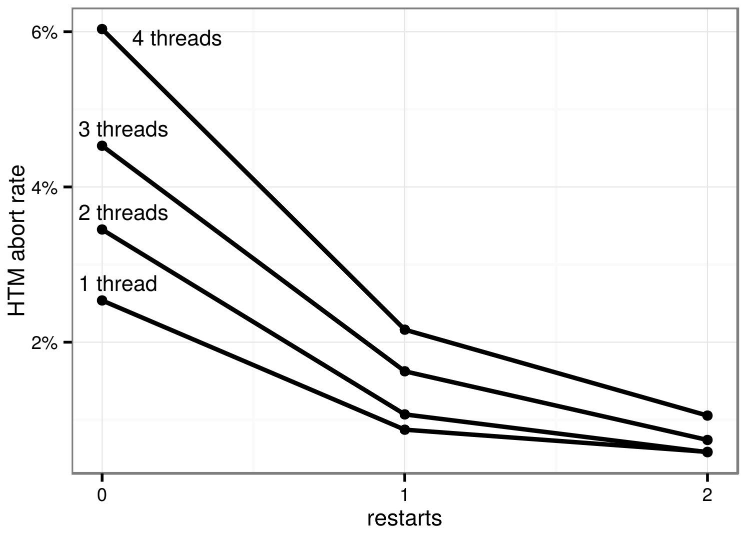

Figure 2.20: HTM abort rate with 8 declustered insert zones

While HTM conflicts do not result in a rollback of the entire transaction, they result in the acquisition of relation-level latches—greatly reducing concurrency. Using hardware counters, we measured the HLE abort rate of TPC-C, and found that 6% of all HLE transactions were aborted. This rate can be reduced by manually restarting transactions after abort by using Restricted Transaction Memory (RTM) instructions instead of HLE. As Figure 2.20 shows, the abort rate can be reduced greatly by restarting aborted transaction, i.e., most aborts are transient. With 4 threads, restarting has only a small positive effect on the overall transaction rate (1.5%), because a 6% abort rate is still "small enough" for 4 threads.

These low abort rates are the outcome of our HTM-friendly storage layout from Section 2.6. Because TPC-C is very insert-heavy, with only one zone, the HLE abort rate rises from 6% to 14%, and the clashes often do not vanish after restarts. Therefore, a careful data layout is absolutely mandatory to benefit from HTM. Note though that we did not decluster surrogate key generation, which makes conflicts even more unlikely, but would have required changes to the benchmark.

2.8 Related Work

Optimizing the transaction processing for modern multi-core and in-memory database systems is a vibrant topic within the database community. In the context of H-Store/VoltDB [63, 80] several approaches for automatically deriving a database partitioning scheme from the pre-defined workload were devised [34, 147] and methods of optimizing partition-crossing transactions were investigated [81]. The partitioning research focused on distributed databases, but is also applicable to shared memory systems. Partitioning the database allows for scalable serial transaction execution as long as the transactions do not cross partition boundaries, which in general is hard to achieve. In [146] a data-oriented transaction processing architecture is devised, where transactions move from one processing queue to another instead of being assigned to a single thread. The locking-based synchronization is optimized via speculative lock inheritance [79]. Ren et al. [157] found that the lock manager is a critical performance bottleneck for main memory database systems. They propose a more lightweight scheme, where, instead of locks in a global lock manager data structure, each tuple has two counters that indicate how many transactions requested read or write access. In an earlier evaluation we showed that timestamp-based concurrency control has become a promising alternative to traditional locking [179].

Tu et al. [172] recently designed an in-memory OLTP system that uses optimistic concurrency control and a novel B-Tree variant [129] optimized for concurrent access. Lomet et al. [122] and Larson et al. [98] devised multi-version concurrency control schemes that, like our approach, use a timestamp-based version control to determine conflicting operations. Unlike our proposal, their concurrency control is fully software-implemented, therefore it bears some similarity to software transactional memory [38].

Herlihy and Moss [69, 68] proposed HTM for lock-free concurrent data structures. Shavit and Touitou [163] are credited for the first STM proposal. A comprehensive account on transactional memory is given in the book by Larus and Rajwar [103]. Due to the entirely software-controlled validation overhead, STM found little resonance in the database systems community—while, fueled by the emergence of the now common many-core processors, it was a vibrant research activity in the parallel computing community [70].

Wang et al. [177] combine Haswell's HTM with optimistic concurrency control to build a scalable in-memory database systems. Their approach similar to ours, but requires a final commit phase that is executed in a single hardware transaction and which encompasses the meta data of the transactions' read and write set. Karnagel et al. [84] performed a careful evaluation of HTM for synchronizing B-Tree access. Litz et al. [119] use multi-versioning, an old idea from the database community, to speed up TM in hardware.

2.9 Summary

There are two developments—one from the hardware vendors, and one from the database software developers—that appear like a perfect match: the emergence of hardware transactional memory (HTM) in modern processors, and main-memory database systems. The data access times of these systems are so short that the concurrency control overhead, in particular for locking/latching, is substantial and can be optimized by carefully designing HTM-supported transaction management. Even though transactions in main-memory databases are often of short duration, the limitations of HTM's read/write set management precludes a one-to-one mapping of DBMS transactions to HTM transactions.

We therefore devised and evaluated a transaction management scheme that transforms a (larger) database transaction into a sequence of more elementary, single tuple access/update HTM transactions. Our approach relies on the well-known timestamp ordering technique to "glue" the sequence of HTM transactions into an atomic and isolated database transaction. Our quantitative evaluation showed that our approach has low overhead and excellent scalability.

3 Efficient Synchronization of In-Memory Index Structures

Parts of this chapter have previously been published in [112].

3.1 Introduction

In traditional database systems, most data structures are protected by fine-grained locks[1]. This approach worked well in the past, since these locks were only acquired for a short time and disk I/O dominated overall execution time. On modern servers with many cores and where most data resides in RAM, synchronization itself often becomes a major scalability bottleneck. And with the increasing number of CPU cores efficient synchronization will become even more important.

Figure 3.1 gives an overview of the synchronization paradigms discussed in this chapter. Besides traditional fine-grained locking, which is known to scale badly on modern CPUs, the figure shows the lock-free paradigm, which offers strong theoretical guarantees, and Hardware Transactional Memory (HTM), which requires special hardware support. When designing a data structure, so far, one had to decide between the extreme difficulty of the lock-free approach, special hardware support of HTM, and poor scalability of locking. In this work, we present two additional points in the design space that fill the void in between. *Optimistic Lock Coupling* and *ROWEX* are much easier to use than lock-free synchronization but offer similar scalability without special hardware support.

We focus on synchronizing the *Adaptive Radix Tree (ART)* [108], a general-purpose, order-preserving index structure for main-memory database systems. ART is an interesting case study, because it is a non-trivial data structure that was *not* designed with concurrency in mind rather with high single-threaded performance. We present a number of synchronization protocols for ART and compare them experimentally.

[1] In this chapter, we always use the term “lock” instead of “latch” since we focus on low-level data structure synchronization, rather than high-level concurrency control.

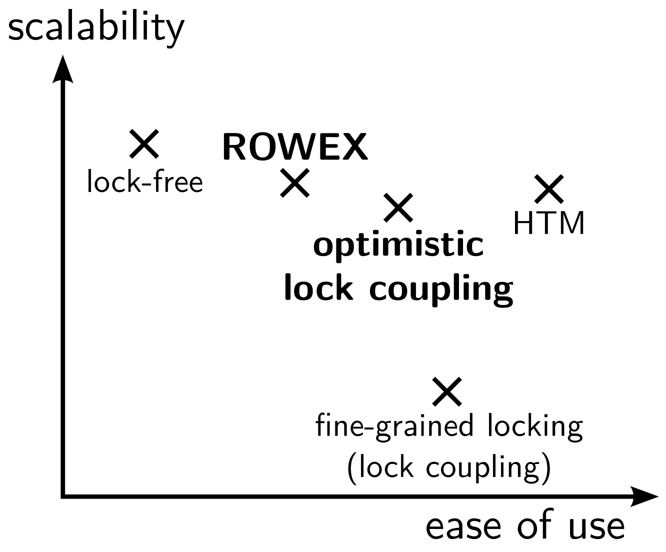

Figure 3.1: Overview of synchronization paradigms

Our main goal in this work, however, is to distill general principles for synchronizing data structures in general. This is important for two reasons. First, besides index structures, database systems also require other data structures that must be concurrently accessible like tuple storage, buffer management data structures, job queues, etc. Second, concurrent programs are very hard to write and even harder to debug. We therefore present our ideas, which, as we discuss in Section 3.6, are not entirely new, as general building blocks that can be applied to other other data structures.

The rest of this work is organized as follows: We first present necessary background about the Adaptive Radix Tree in Section 3.2. The two new synchronization paradigms *Optimistic Lock Coupling* and *Read-Optimized Write EXclusion* are introduced in Section 3.3 and Section 3.4. Section 3.5 evaluates the presented mechanisms. Finally, after discussing related work in Section 3.6, we summarize our results in Section 3.7.

3.2 The Adaptive Radix Tree (ART)

Trie data structures, which are also known as radix trees and prefix trees, have been shown to outperform classical in-memory search trees [108, 92]. At the same time, and in contrast to hash tables, they are order-preserving, making them very attractive indexing structures for main-memory database systems.

What distinguishes ART [108] from most other trie variants is that it uses an **adaptive node structure**. ART dynamically chooses the internal representation of each node from multiple data structures. The four available node types are illustrated in Figure 3.2. Initially, the smallest node type (Node4) is selected, and, as entries are

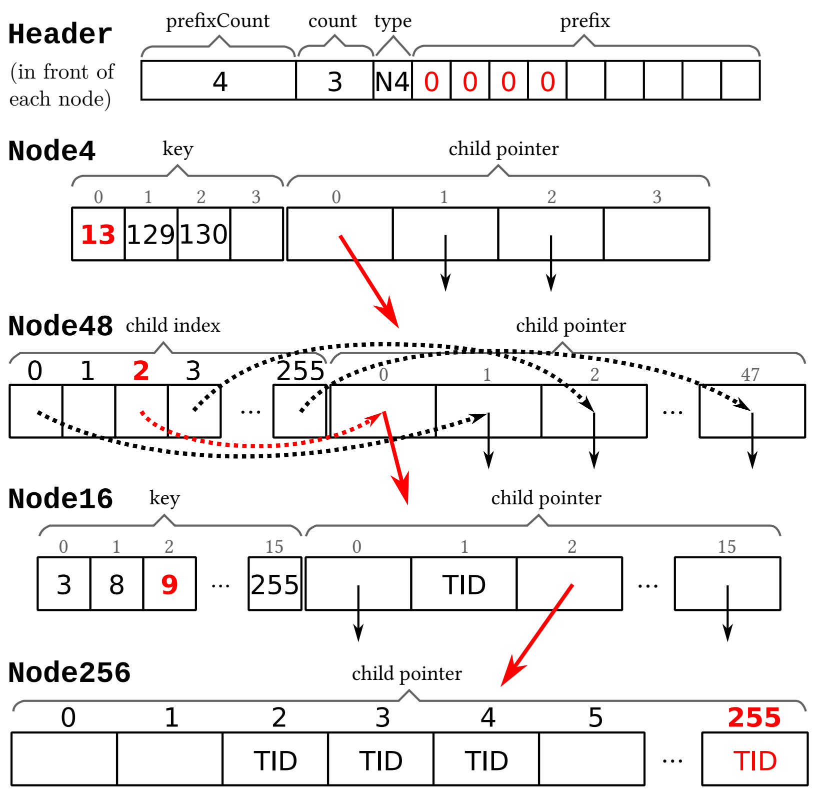

Figure 3.2: The internal data structures of ART

inserted into that node, it is replaced with a larger node type. In the figure, if two more entries would be inserted into the (Node4), which currently holds 3 entries, it would be replaced by a (Node16).

Another important feature of ART is **path compression**, which collapses nodes with only a single child pointer into the first node with more than one child. To implement this, each node stores a *prefix* of key bytes in its header. This allows indexing long keys (e.g., strings) effectively, because the optimization significantly reduces the height of the tree. The example header shown in Figure 3.2 stores a prefix of 4 zero bytes thus reducing the height by 4 levels.

In HyPer, where ART is the default indexing structure [88], ART maps arbitrary keys to **tuple identifiers (TIDs)**. As the figure shows, the TIDs are stored directly inside the pointers. Pointers and TIDs are distinguished using "pointer tagging", i.e., by using one of the pointer's bits.

Adaptive node types and path compression reduce space consumption while allowing for nodes with high fanout and thus ensure high overall performance. At the same time, these features are also the main challenges for synchronizing ART. Tries without these features are easier to synchronize, which makes ART a more interesting case

```
lookup(key, node, level, parent)
   readLock(node)
   if parent != null
      unlock(parent)
   // check if prefix matches, may increment level
   if !prefixMatches(node, key, level)
      unlock(node)
      return null  // key not found
   // find child
   nextNode = node.findChild(key[level])

   if isLeaf(nextNode)
      value = getLeafValue(nextNode)
      unlock(node)
      return value  // key found
   if nextNode == null
      unlock(node)
      return null  // key not found
   // recurse to next level
   return lookup(key, nextNode, level+1, node)
```

```
lookupOpt(key, node, level, parent, versionParent)
   version = readLockOrRestart(node)
   if parent != null
      readUnlockOrRestart(parent, versionParent)
   // check if prefix matches, may increment level
   if !prefixMatches(node, key, level)
      readUnlockOrRestart(node, version)
      return null  // key not found
   // find child
   nextNode = node.findChild(key[level])
   checkOrRestart(node, version)
   if isLeaf(nextNode)
      value = getLeafValue(nextNode)
      readUnlockOrRestart(node, version)
      return value  // key found
   if nextNode == null
      readUnlockOrRestart(node, version)
      return null  // key not found
   // recurse to next level
   return lookupOpt(key, nextNode, level+1, node, version)
```

Figure 3.3: Pseudo code for a lookup operation that is synchronized using lock coupling (left) vs. Optimistic Lock Coupling (right). The necessary changes for synchronization are highlighted

study for synchronizing non-trivial data structures.

3.3 Optimistic Lock Coupling

Lock coupling [12], i.e., holding at most 2 locks at a time during traversal, is the standard method for synchronizing B-trees. One interesting property of ART is that modifications affect at most two nodes: the node where the value is inserted or deleted, and potentially its parent node if the node must grow (during insert) or shrink (during deletion). In contrast to B-trees [11], a modification will never propagate up to more than 1 level. Lock coupling can therefore be applied to ART even more easily than to B-trees.

The left-hand-side of Figure 3.3 shows the necessary changes for synchronizing the lookup operation of ART with lock coupling. The pseudo code uses read-write locks to allow for concurrent readers. Insert and delete operations can also initially acquire read locks before upgrading them to write locks if necessary. This allows one to avoid exclusively locking nodes near the root, which greatly enhances concurrency because most updates only affect nodes far from the root.

Lock coupling is simple and seems to allow for a high degree of parallelism. However, as we show in Section 3.5, it performs very badly on modern multi-core CPUs even if the locks do not logically conflict at all, for example in read-only workloads. The reason is that concurrent locking of tree structures causes many unnecessary cache misses: Each time a core acquires a read lock for a node (by writing to that node), all copies of that cache line are invalidated in the caches of all other cores. Threads, in effect, “fight” for exclusive ownership of the cache line holding the lock. The root node and other nodes close to it become contention points. Therefore, other synchronization mechanisms are necessary to fully utilize modern multi-core CPUs.

Optimistic Lock Coupling is similar to “normal” lock coupling, but offers dramatically better scalability. Instead of preventing concurrent modifications of nodes (as locks do), the basic idea is to optimistically assume that there will be no concurrent modification. Modifications are detected after the fact using version counters, and the operation is restarted if necessary. From a performance standpoint, this optimism makes a huge difference, because it dramatically reduces the number of writes to shared memory locations.

3.3.1 Optimistic Locks

Figure 3.3 compares the pseudo code for lookup in ART using lock coupling and Optimistic Lock Coupling. Clearly, the two versions are very similar. The difference is encapsulated in the `readLockOrRestart` and `readUnlockOrRestart` functions, which mimic a traditional locking interface but are implemented differently. This interface makes it possible for the programmer to reason (almost) as if she was using normal read-write locks.

The pseudo code in Figure 3.4 implements the insert operation using optimistic lock coupling. Initially, the traversal proceed like in the lookup case without acquiring write locks. Once the node that needs to be modified is found, it is locked. In cases where the node must grow the parent is also locked. When two nodes need to be locked, we always lock the parent before its child. This ensures that locks are always acquired in the same, top-down order and therefore avoids deadlocks.

Internally, an *optimistic lock* consists of a lock and a version counter. For writers, optimistic locks work mostly like normal locks, i.e., they provide mutual exclusion by physically acquiring (by writing into) the lock. Additionally, each `writeUnlock` operation causes the version counter associated with the lock to be incremented. Read operations, in contrast, do not actually acquire or release locks. `readLockOrRestart` merely waits until the lock is free, before returning the current version. `readUnlockOrRestart`, which takes a version as an argument, makes sure the lock is still free and that the version (returned by `readLockOrRestart`) did not change. If a change occurred, the lookup operation is restarted from the root of tree. In our implementation we encode the lock and the version counter (and an obsolete flag) in a single 64 bit word that is updated atomically and is stored in the header of each ART node. A full description of the optimistic lock primitives can be found in Figure 3.5.

Let us mention that, for debugging purposes, it is possible to map the optimistic

```
insertOpt(key, value, node, level, parent, parentVersion)
   version = readLockOrRestart(node)
   if !prefixMatches(node, key, level)
      upgradeToWriteLockOrRestart(parent, parentVersion)
      upgradeToWriteLockOrRestart(node, version, parent)
      insertSplitPrefix(key, value, node, level, parent)
      writeUnlock(node)
      writeUnlock(parent)
      return
   nextNode = node.findChild(key[level])
   checkOrRestart(node, version)
   if nextNode == null
      if node.isFull()
         upgradeToWriteLockOrRestart(parent, parentVersion)
         upgradeToWriteLockOrRestart(node, version, parent)
         insertAndGrow(key, value, node, parent)
         writeUnlockObsolete(node)
         writeUnlock(parent)
      else
         upgradeToWriteLockOrRestart(node, version)
         readUnlockOrRestart(parent, parentVersion, node)
         node.insert(key, value)
         writeUnlock(node)
      return
   if parent != null
       readUnlockOrRestart(parent, parentVersion)
   if isLeaf(nextNode)
       upgradeToWriteLockOrRestart(node, version)
       insertExpandLeaf(key, value, nextNode, node, parent)
       writeUnlock(node)
       return
   // recurse to next level
   insertOpt(key, value, nextNode, level+1, node, version)
   return
```

Figure 3.4: Pseudo code for insert using Optimistic Lock Coupling. The necessary changes for synchronization are highlighted

primitives to their pessimistic variants (e.g., pthread_rwlock). This enables thread analysis tools like Helgrind to detect synchronization bugs. Version/lock combinations have been used in the past for synchronizing data structures (e.g., [30, 24, 129]), usually in combination with additional, data structure-specific tricks that reduce the number of restarts. Optimistic Lock Coupling is indeed a very general technique that allows consistent snapshots over multiple nodes (e.g., 2 at a time for lock coupling). The region can even involve more than 2 nodes, but should obviously be as small as possible to reduce conflicts.

3.3.2 Assumptions of Optimistic Lock Coupling

To make Optimistic Lock Coupling work correctly, there are certain properties that an algorithm must fulfill. After readLockOrRestart has been called, a reader may see intermediate, inconsistent states of the data structure. An incorrect state will be detected later by readUnlockOrRestart, but, in some cases, can still cause problems. In particular, care must be taken to avoid (1) infinite loops and (2) invalid pointers. For ART, an infinite loop cannot occur. To protect against invalid pointers, it is necessary to add an additional version check (line 11 in Figure 3.3). Without this check, nextNode might be an invalid pointer, which may cause the program to crash. These additional checks are needed before an optimistically read pointer is dereferenced.

Another aspect that needs some care is deletion of nodes. A node must not be immediately reclaimed after removing it from the tree because readers might still be active. We use epoch-based memory reclamation to defer freeing such nodes. Additionally, when a node has been logically deleted, we mark it as *obsolete* when unlocking the node (cf. writeUnlockObsolete in Figure 3.5). This allows other writers to detect this situation and trigger a restart.

One theoretical problem with Optimistic Lock Coupling is that—in pathological cases—a read operation may be restarted repeatedly. A simple solution for ensuring forward progress is to limit the number of optimistic restarts. After this limit has been reached, the lookup operation can acquire write locks instead.

To summarize, Optimistic Lock Coupling is remarkably simple, requires few changes to the underlying data structure, and, as we show in Section 3.5, performs very well. The technique is also quite general and can be applied to other data structures (e.g., B-trees).

3.3.3 Implementation of Optimistic Locks

The pseudo code in Figure 3.5 implements optimistic locks. Each node header stores a 64 bit version field that is read and written atomically. The two least significant bits

```
struct Node
   atomic<uint64_t> version
   ...

uint64_t readLockOrRestart(Node node)
   uint64_t version = awaitNodeUnlocked(node)
   if isObsolete(version)
      restart()
   return version

void checkOrRestart(Node node, uint64_t version)
   readUnlockOrRestart(node, version)

void readUnlockOrRestart(Node node, uint64_t version)
   if version != node.version.load()
      restart()

void readUnlockOrRestart(Node node, uint64_t version, Node lockedNode)
   if version != node.version.load()
      writeUnlock(lockedNode)
      restart()

void upgradeToWriteLockOrRestart(Node node, uint64_t version)
   if !node.version.CAS(version, setLockedBit(version))
      restart()

void upgradeToWriteLockOrRestart(Node node, uint64_t version, Node lockedNode)
   if !node.version.CAS(version, setLockedBit(version))
      writeUnlock(lockedNode)
      restart()

void writeLockOrRestart(Node node)
   uint64_t version
   do
      version = readLockOrRestart(node)
   while !upgradeToWriteLockOrRestart(node, version)

void writeUnlock(Node node)
   // reset locked bit and overflow into version
   node.version.fetch_add(2)

void writeUnlockObsolete(Node node)
   // set obsolete, reset locked, overflow into version
   node.version.fetch_add(3)

// Helper functions
uint64_t awaitNodeUnlocked(Node node)
   uint64_t version = node.version.load()
   while (version & 2) == 2 // spinlock
      pause()
      version = node.version.load()
   return version

uint64_t setLockedBit(uint64_t version)
   return version + 2

bool isObsolete(uint64_t version)
   return (version & 1) == 1
```

Figure 3.5: Implementation of optimistic locks based on busy waiting

indicate if the node is obsolete or if the node is locked, respectively. The remaining bits store the update counter.

3.4 Read-Optimized Write EXclusion

Like many optimistic concurrency control schemes, Optimistic Lock Coupling performs very well as long as there are few conflicts. The big disadvantage is, however, that all operations may restart. Restarts are particularly undesirable for reads, because they are predominant in many workloads. We therefore present a second synchronization technique that still uses locks for writes, but where reads always succeed and never block or restart. We call this technique *Read-Optimized Write EXclusion (ROWEX)*.

3.4.1 General Idea

ROWEX is a synchronization paradigm that lies between traditional locking and lock-free techniques (cf. Figure 3.1). It provides the guarantee that reads are non-blocking and always succeed. Synchronizing an existing data structure with ROWEX is harder than with (optimistic) lock coupling, but generally still easier (i.e., at least possible) than designing a similar lock-free data structure. The main tool of ROWEX is the write lock, which provides additional leverage in comparison with lock-free approaches that must confine themselves with primitive atomic operations like compare-and-swap. The write locks are acquired only infrequently by writers and never by readers.

The basic idea with ROWEX is that, before modifying a node, the lock for that node is first acquired. This lock only provides exclusion relative to other writers, but not readers, which never acquire any locks (and never check any versions). The consequence is that writers must ensure that reads are always consistent by using atomic operations. As we describe in the following, ROWEX generally requires some modifications to the internal data structures.

Although the name ROWEX indicates that reads are fast, writes are not slow either (despite requiring locks). The reason is that writers only acquire local locks at the nodes that are actually changed, i.e., where physical conflicts are likely. Even lock-free designs will often have cache line invalidations that impair scalability when writing to the same node. ROWEX thus provides very good scalability while still being realistically applicable to many existing data structures.

3.4.2 ROWEX for ART

One important invariant of ART is that every insertion/deletion order results in the same tree[2] because there are no rebalancing operations. Each key, therefore, has a deterministic physical location. In B-link trees [105], in contrast, a key may have been moved to a node on the right (and never to the left due to deliberately omitting underflow handling).

To synchronize ART using ROWEX, we first discuss local modifications within the 4 node types before describing how node replacement and finally path compression are handled.

To allow concurrent **local modifications**, accesses to fields that may be read concurrently must be atomic. These fields include the key bytes (in `Node4` and `Node16`), the child indexes (in `Node48`), and the child pointers (in all node types). In C++ 11 this is done by using the `std::atomic` type, which ensures that appropriate memory barriers are inserted[3]. These changes are already sufficient for the `Node48` and `Node256` types and allow adding (removing) children to (from) these nodes. For the linear node types (`Node4` and `Node16`), which are structurally very similar to each other, some additional conceptual changes are necessary. In the original design, the keys in linear nodes are sorted (cf. Figure 3.2) to simplify range scans. To allow for concurrent modifications while reads are active, we avoid maintaining the sorted order and append new keys at the end of the node instead. Deletions simply set the child pointer to null, and slots are reclaimed lazily by replacing the node with a new one. With this change, lookups must check all keys (i.e., 4 for `Node4` and 16 for `Node16`). However, this is not a problem since SIMD instructions can be used to perform the comparison.

Node replacement can become necessary due to (1) the node becoming too full to encompass another insert or due to (2) the node becoming underfull. In both cases, the required steps for replacing a node are the same:

1. Both the node and its parent are locked.
2. A new node of the appropriate type is created and initialized by copying over all entries from the old node.
3. The location within the parent pointing to the old node is changed to the new node using an atomic store.

[2]Note that ART only supports unique keys. In database systems, uniqueness can be ensured by making the tuple identifier part of the key. As a result, concurrently inserting tuples with equal keys does not cause a problem.

[3] The `std::atomic` type does not change the physical layout. Also note that on x86 an atomic load adds very little overhead, as it does not introduce a memory barrier. Making the fields atomic merely prevents the compiler from reordering instructions but does not introduce additional instructions for readers.

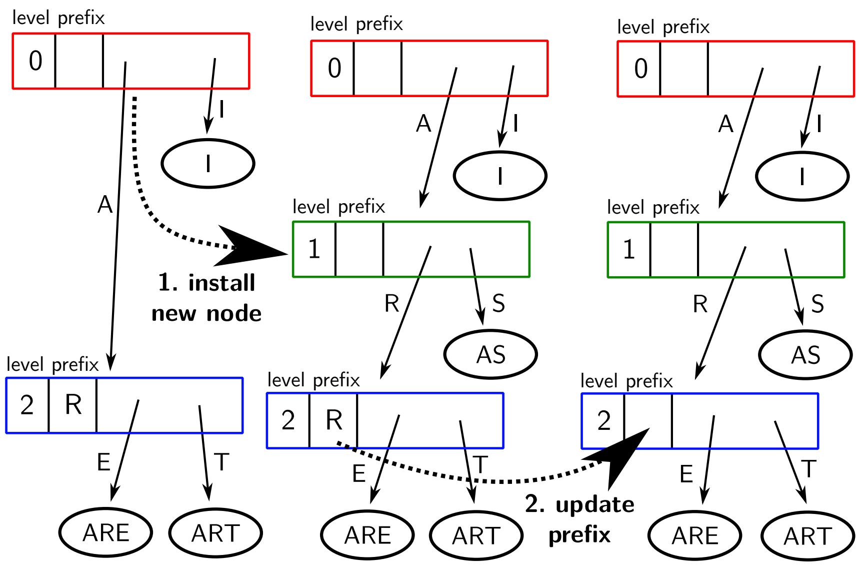

Figure 3.6: Path compression changes for inserting "AS"

4. The old node is unlocked and marked as *obsolete*. The parent node is unlocked.

Like with Optimistic Lock Coupling, once a node is not reachable in the most recent version of the tree (after step 3), the node must be marked as obsolete before being unlocked. Any writer waiting for that lock will detect that the node is obsolete and will restart the entire insert or delete operation. For readers, in contrast, it is safe to read from obsolete nodes.

Path compression is illustrated in Figure 3.6. In the 2-level tree on the left-hand side, the blue node contains the "R" prefix. In order to insert the new key "AS", it is necessary to (1) install a new (green) node and (2) truncate the prefix (at the blue node). Individually, both steps can be performed atomically: Installing the new node can be done by a single (atomic) store. To change the prefix of the node atomically, we store both the prefix and its length in a single 8 byte value, which can be changed atomically[4].

The main difficulty with path compression is that it is not possible to install a new node and truncate the prefix in a single operation. As a consequence, a reader may see the intermediate state in Figure 3.6. To solve this problem, we augment each node with a `level` field, which stores the height of the node including the prefix and which never changes after a node has been created. With this additional information, the intermediate state in Figure 3.6 is safe, because a reader will detect that the prefix at the blue node has to be skipped. Similarly, it is also possible that a reader sees the final

[4]In comparison with the original ART implementation this decision reduces the maximum prefix length from 9 to 4. On x86, 16 byte values can also be accessed atomically, which would also allow storing 12 byte prefixes.

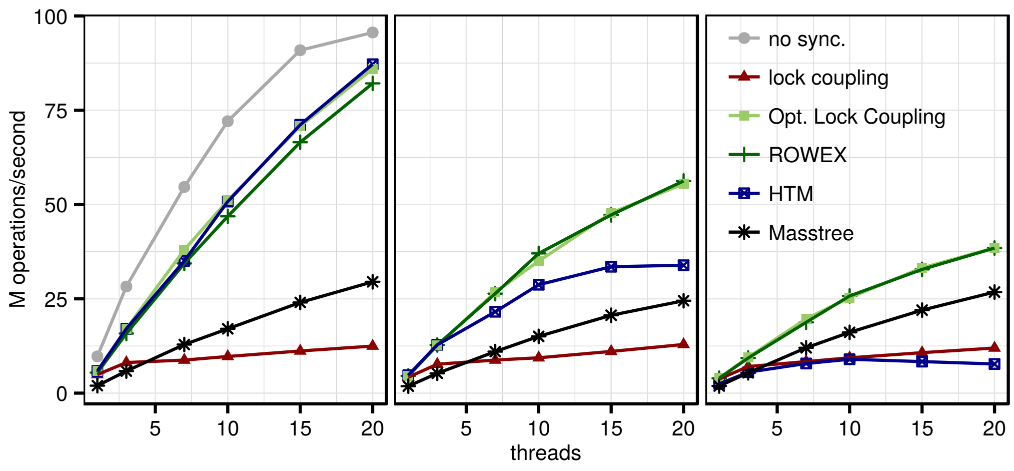

Figure 3.7: Scalability (50M 8 byte integers)

state of the blue node without having seen the green node before. In that situation, the reader can detect the missing prefix using `level` field and retrieve the missing key from the database.

To summarize, whereas in Optimistic Lock Coupling readers detect changes and restart, with ROWEX it is the responsibility of writers to ensure that reads are safe. Thus ROWEX is not a simple recipe that can be applied to any data structure, but must be carefully adapted to it. In some cases, it might even prove impossible without major changes to the underlying data structure. Nevertheless, we believe that ROWEX is an interesting design point between lock-free techniques and locking.

3.5 Evaluation

In this section we experimentally compare a number of ART variants: unmodified ART without support for concurrent modifications, lock coupling with read-write spinlocks, Optimistic Lock Coupling, ROWEX, and hardware transactional memory (HTM) with 20 restarts using a global, elided lock as fallback (as described in [110]). The additional space consumption per node is 4 bytes for lock coupling, 8 bytes for Optimistic Lock Coupling, and 12 bytes for ROWEX. As a competitor we chose Masstree [129], which, to the best of our knowledge, is the fastest publicly available[5], synchronized, order-preserving data structure. Note that the comparison between ART and Masstree is not really "apples-to-apples", as both the synchronization protocol and the data structures themselves differ. All implementations use the `jemalloc` memory allocator and, when required, low-overhead epoch-based memory reclamation. We use a Haswell EP system with an Intel Xeon E5-2687W v3 CPU, which has 10 cores (20 "Hyper-

[5]`https://github.com/kohler/masstree-beta`

Threads”) and 25 MB of L3 cache.

3.5.1 Scalability

In our first experiment we investigate the scalability using 50M random (sparse) 8-byte integers. This is a low contention workload, because conflicts are unlikely with random keys. Figure 3.7 shows the results for individually executing lookup, insert, and remove. As expected, the variant without synchronization, which is only shown for the read-only experiment, performs best. Lock coupling does not scale well, even in the lookup experiment and although we use read-write locks. Optimistic Lock Coupling and ROWEX, in contrast, scale very well and have very similar performance, with Optimistic Lock Coupling being slightly (around 7%) faster for lookup. The HTM variant also performs very well on the lookup experiment, but is slightly slower for insert and significantly slower for remove. We verified that the reason for this is (unnecessary) contention in the memory allocator causing frequent aborts. Masstree scales well but with short keys its overall performance is significantly lower than with ART.

To better understand the lookup results in Figure 3.7, we measured some important CPU statistics:

	1 thread / 20 threads [per lookup]			
	cycles	instruct.	L1 misses	L3 misses
no sync	211 / 381	123 / 124	4.3 / 4.5	1.7 / 1.8
lock coupling	**418 / 2787**	242 / 243	**5.2 / 9.0**	1.8 / 2.0
Opt. Lock Coup.	348 / 418	187 / 187	5.3 / 5.7	1.8 / 2.0
ROWEX	375 / 427	248 / 249	5.6 / 5.8	1.9 / 1.9
HTM	347 / 428	132 / 135	4.3 / 4.5	1.7 / 2.1
Masstree	982 / 1231	897 / 897	20.5 / 21.1	6.5 / 7.1

Single-threaded, the overhead of Optimistic Lock Coupling in comparison with the non-synchronized variant is around 65%, mostly due to additional instructions. With 20 threads, the overhead is reduced to only 10%, likely due to longer delays in the memory controller. With lock coupling, because of cache line invalidations caused by lock acquisitions, the number of L1 misses (highlighted) increases significantly when going from 1 to 20 threads and the CPU cycles increase by a factor of 6.6×. The slowdown would be even larger on multi-socket systems, since such systems do not have a shared cache for inter-thread communication. The CPU statistics also explain why ART is significantly faster than Masstree with integer keys. The Optimistic Lock Coupling variant of ART, for example, requires 4.8× fewer instructions and 3.6× fewer L3 misses than Masstree.

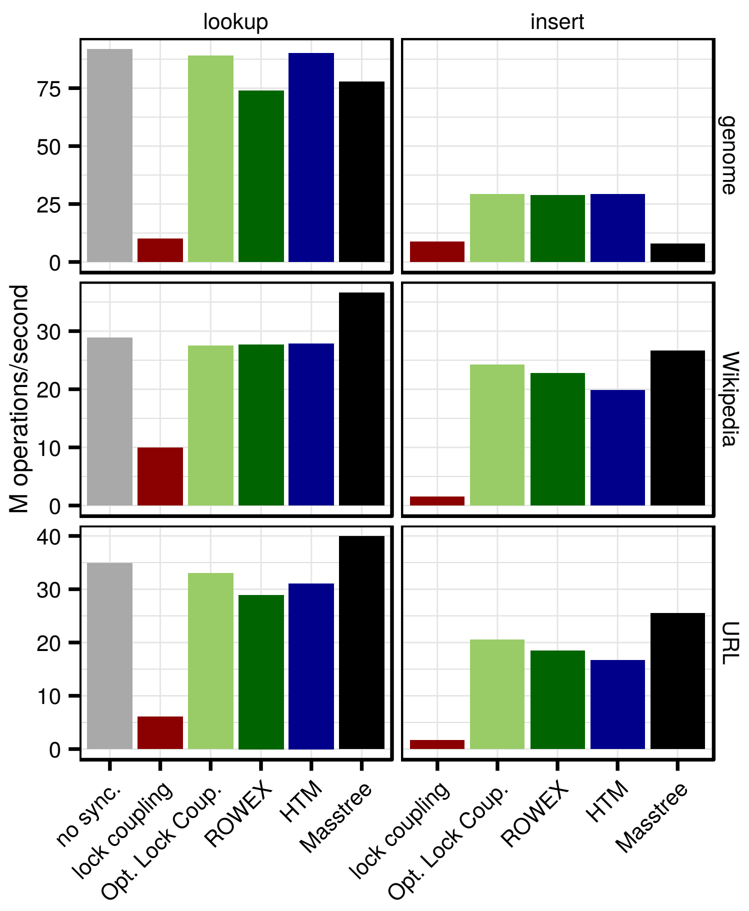

Figure 3.8: Performance for string data with 20 threads

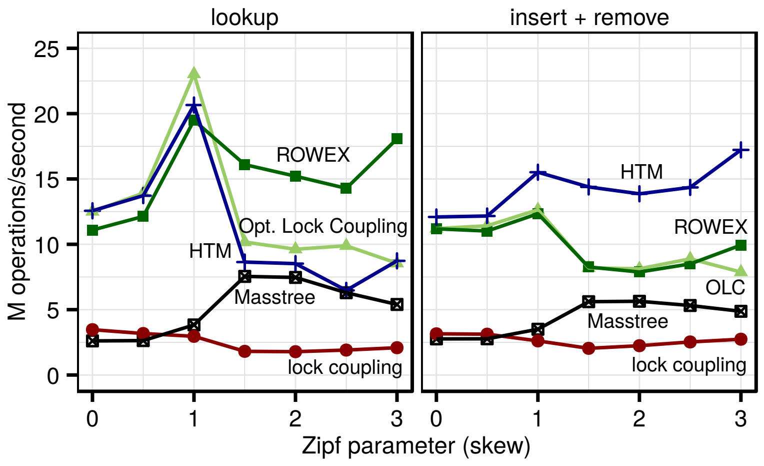

Figure 3.9: Performance under contention (1 lookup thread and 1 insert+remove thread)

3.5.2 Strings

Besides integer keys, we also measured the lookup performance for three real-world string data sets. The "genome" data set has 256K strings of average length 10.0, "Wikipedia" contains 16M article titles of average length 22.4, and "URL" has 6.4M URLs of average length 63.3. The lookup and insert performance with 20 threads is shown in Figure 3.8. Masstree closes its performance gap to ART with longer keys. Again, lock coupling is very slow and the synchronized ART variants are slightly slower than the unsynchronized variant.

3.5.3 Contention

In order to show the effect of contention, we measured simultaneous lookup and update operations (insert+remove) in a tree with 10M dense 8 byte integer keys. We used 1 lookup thread and 1 update thread and varied the skewness of the keys going from uniform to extremely skewed (reading and modifying the same key 83% of the time). The lookup results (left-hand side of Figure 3.9) show that with higher skew most variants initially become faster (due to better cache locality), before eventually slowing down under very high contention. ROWEX is the only exception, as its lookup performance stays very high even under extreme contention due to the non-blocking reads. The performance of the update thread (right-hand side of Figure 3.9) is generally similar to the lookup performance. One exception is HTM, which has higher performance for the update thread than for the lookup thread, because Intel's transactional memory implementation favors writers over reader [126].

3.5.4 Code Complexity

To give a rough indication for the relative complexity of the implementations, we counted the core algorithmic C++ code lines excluding the lock implementations, garbage collection, comments, and empty lines:

	lookup	insert	remove
no synchronization	29	95	87
HTM	30	96	88
lock coupling	41	136	139
Optimistic Lock Coupling	44	148	143
ROWEX	34	200	156

Using HTM is quite trivial, it merely requires wrapping each transaction in a hardware transaction, which we implemented with a `Transaction` object that starts the HTM transaction in the constructor and commits the transaction in the destructor. The two lock coupling variants require more changes, with the optimistic variant being only marginally larger. ROWEX requires most additional code, in particular for the insert and remove operations. The ROWEX numbers actually underestimate the complexity of ROWEX, since its protocol is fairly subtle in comparison with the other variants.

3.6 Related Work

Concurrency control is one of the major areas in the database field. Most prior work, however, focuses on high-level user transactions, and not so much on low-level synchronization of data structures, which is what we study in this work.

Hand-over-hand locking, i.e., the idea underlying Optimistic Lock Coupling, was used to synchronize binary search trees [24]. ROWEX-like ideas have also been used before, for example by the FOEDUS system [91]. The goal of this work has been to consolidate these ideas and to present them as general building blocks as opposed to clever tricks used to synchronize individual data structures.

The traditional method of synchronizing B-trees, lock coupling, was proposed by Bayer and Schkolnick [12]. Graefe's surveys [56, 54] on low-level synchronization of B-trees, which summarize decades of accumulate wisdom in the database community, focus on fine-grained locking. Unfortunately, as was already observed by Cha et al. [30] in 2001, lock coupling simply does not scale on modern multi- and many-core CPUs. Since then, the problem has become even more pronounced and the trend is likely to continue. Like Optimistic Lock Coupling, Cha et al.'s solution (OLFIT) uses versions to detect changes within a node. In contrast to Optimistic Lock Coupling, OLFIT does not keep track of versions across multiple nodes, but uses the B-link tree idea [105] to support concurrent structure modification operations.

Both the *Bw-Tree* [114] and *Masstree* [129] are two B-tree proposals published in 2012, and both eschew traditional lock coupling. The Bw-Tree is latch-free and its nodes can be, due to their relatively large size, moved to disk/SSD [115]. To allow concurrent modifications, delta records are pre-pended to a list of existing changes and the (immutable) B-tree node at the end of the list itself. Nodes do not store physical pointers but offsets into a mapping tables that points to the delta lists and allows one to atomically add new delta records. After a number of updates the deltas and the node are consolidated to a new node. The Bw-Tree has been designed with concurrency in mind and its synchronization protocol is highly sophisticated; structure modification operations (e.g., node splits) are very complex operations involving multiple steps.

Masstree [129] is a hybrid B-tree/trie data structure and, like ART, exclusively focuses on the in-memory case. Like the Bw-Tree, Masstree was designed with concurrency in mind, but the designers took different design decisions. The synchronization protocol of Masstree relies on a mix of local locks, clever use of atomic operations, and hand-over-hand locking (the idea underlying Optimistic Lock Coupling). Like Optimistic Lock Coupling, but unlike ROWEX, Masstree lookups must, in some cases, be restarted when a conflict with a structure-modifying operation is detected.

Previous work has shown that Hardware Transactional Memory can be used to synchronize ART [109, 110] and B-trees [84] with very little effort using elided coarse-grained HTM locks. Makreshanski et al. [126] confirmed these findings in an in-depth experimental study but found that performance with HTM can degrade with large tuples or heavy contention. Cervini et al. [29] found that replacing fine-grained locks with (elided) HTM locks at the same granularity does not improve performance. HTM also has the obvious disadvantage of requiring special hardware support, which is not yet widespread.

3.7 Summary

We presented two synchronization protocols for ART that have good scalability despite relying on locks. The first protocol, *Optimistic Lock Coupling* is very simple, requires few changes to the underlying data structure, and performs very well as long as conflicts are not too frequent. The *Read-Optimized Write EXclusion (ROWEX)* protocol is more complex, but has the advantage that reads never block. ROWEX generally requires changes to the data structure itself, as opposed to simply adding a lock at each node. However, in our experience, while synchronizing an existing, non-trivial data structure using ROWEX may be non-trivial, it is, at least, realistic. Truly lock-free algorithms, in contrast, are much more complicated. They also generally require radical changes and additional indirections to the underlying data structure. The Bw-Tree, for example, requires an indirection table that causes additional cache misses whenever a node is accessed. Similarly, the state-of-the-art lock-free hash table, the split-ordered list [162], requires "dummy" nodes—again at the price of more cache misses.

It is an open question how a lock-free variant of ART would look like and how well it would perform. We speculate that it would likely be significantly slower than the Optimistic Lock Coupling and ROWEX implementations. We therefore argue that one should not discount the use of locks as long as these locks are infrequently acquired like in our two protocols. Optimistic Lock Coupling and ROWEX are two pragmatic paradigms that result in very good overall performance. We believe both to be highly practical and generally applicable.

4 Parallel NUMA-Aware Query Processing

Parts of this chapter have previously been published in [106].

4.1 Introduction

The main impetus of hardware performance improvement nowadays comes from increasing multi-core parallelism rather than from speeding up single-threaded performance [5]. As we discussed in Section 1.3, mainstream servers with 100 and more hardware threads will soon be very common. We use the term *many-core* for such architectures with tens or hundreds of cores.

At the same time, increasing main memory capacities of up to several TB per server have led to the development of main-memory database systems. In these systems query processing is no longer I/O bound, and the huge parallel compute resources of many-cores can be truly exploited. Unfortunately, the trend to move memory controllers into the chip and hence the decentralization of memory access, which was needed to scale throughput to huge memories, leads to non-uniform memory access (NUMA). In essence, the computer has become a network in itself as the access costs of data items varies depending on which chip the data and the accessing thread are located. Therefore, many-core parallelization needs to take RAM and cache hierarchies into account. In particular, the NUMA division of the RAM has to be considered carefully to ensure that threads work (as much as possible) on NUMA-local data.

Abundant research in the 1990s into parallel processing led the majority of database systems to adopt a form of parallelism inspired by the Volcano [52] model, where operators are kept largely unaware of parallelism. Parallelism is encapsulated by so-called "exchange" operators that route tuple streams between multiple threads each executing identical pipelined segments of the query plan. Such implementations of the Volcano model can be called *plan-driven*: the optimizer statically determines at query compile-time how many threads should run, instantiates one query operator plan for

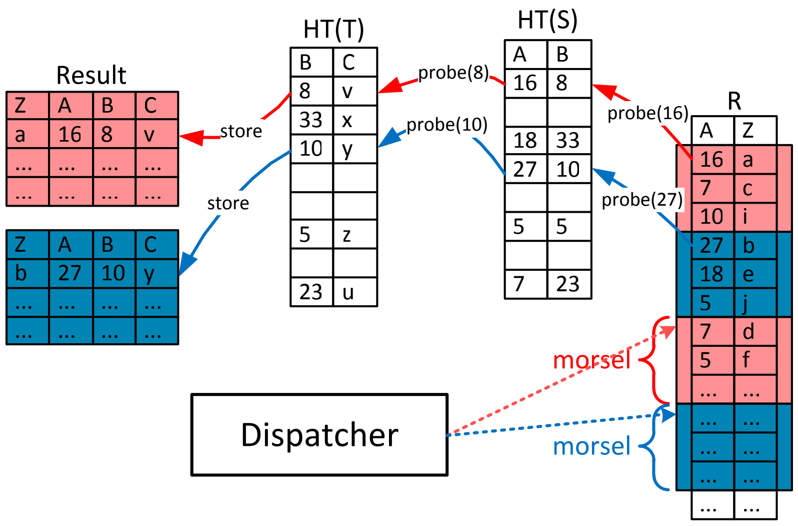

Figure 4.1: Idea of morsel-driven parallelism: $R \Join_A S \Join_B T$

each thread, and connects these with exchange operators.

In this chapter we present the adaptive *morsel-driven* query execution framework, which we designed for HyPer. Our approach is sketched in Figure 4.1 for the three-way-join query $R \Join_A S \Join_B T$. In HyPer, this query consists of three "pipelines", which are fragments of the query that are processed without materializing the data. The first two pipelines consist of building hash tables for S and T. The third (probe) pipeline scans R and probes in both hash tables without materializing in between.

Parallelism is achieved by processing each pipeline on different cores in parallel, as indicated by the two (upper/red and lower/blue) pipelines in the figure. The core idea is a *scheduling* mechanism (the "dispatcher") that allows flexible parallel execution of an operator pipeline, that can change the parallelism degree even during query execution. A query is divided into segments, and each executing segment takes a morsel (e.g, 100,000) of input tuples and executes these, materializing results in the next pipeline breaker. The morsel framework enables NUMA local processing as indicated by the color coding in the figure: A thread operates on NUMA-local input and writes its result into a NUMA-local storage area[1]. Our dispatcher runs a fixed, machine-dependent number of threads, such that even if new queries arrive there is no resource over-subscription, and these threads are pinned to the cores, such that no unexpected loss of NUMA locality can occur due to the OS moving a thread to a different core.

The crucial feature of morsel-driven scheduling is that task distribution is done at run-time and is thus *fully elastic*. This achieves perfect load balancing, even in the face of uncertain size distributions of intermediate results, as well as the hard-to-predict

[1]NUMA locality is achieved by pinning worker threads to cores (and thereby a specific NUMA node) and allocating memory on specific memory nodes.

performance of modern CPU cores that varies even if the amount of work they get is the same. It is elastic in the sense that it can handle workloads that change at run-time (by reducing or increasing the parallelism of already executing queries in-flight) and can easily integrate a mechanism to run queries at different priorities.

The morsel-driven idea extends from just scheduling into a complete query execution framework because all physical query operators must be able to execute morsel-wise in parallel in all their execution stages (e.g., both hash-build and probe). This is a crucial need for achieving many-core scalability in the light of Amdahl's law. An important part of the morsel-wise framework is awareness of data locality. This starts from the locality of the input morsels and materialized output buffers, but extends to the state (data structures, such as hash tables) possibly created and accessed by the operators. This state is shared data that can potentially be accessed by any core, but does have a high degree of NUMA locality. Thus morsel-wise scheduling is flexible, but strongly favors scheduling choices that maximize NUMA-local execution. This means that remote NUMA access only happens when processing a few morsels per query, in order to achieve load balance. By mainly accessing local RAM, memory latency is optimized and cross-socket memory traffic, which can slow other threads down, is minimized.

In a pure Volcano-based parallel framework, parallelism is hidden from operators and shared state is avoided, which leads to plans doing on-the-fly data partitioning in the exchange operators. We argue that this does not always lead to the optimal plan (as partitioning effort does not always pay off), while the locality achieved by on-the-fly partitioning can be achieved by our locality-aware dispatcher. Other systems have advocated per-operator parallelization [99] to achieve flexibility in execution, but this leads to needless synchronization between operators in one pipeline segment. Nevertheless, we are convinced that the morsel-wise framework can be integrated in many existing systems, e.g., by changing the implementation of exchange operators to encapsulate morsel-wise scheduling, and introduce, e.g., hash-table sharing. Our framework also fits systems using Just-In-Time (JIT) code compilation [94, 139] as the generated code for each pipeline occurring in the plan, can subsequently be scheduled morsel-wise. In fact, HyPer uses this JIT compilation approach [139].

In this chapter, we present a number of related ideas that enable efficient, scalable, and elastic parallel processing. The main contribution is an architectural blueprint for a query engine incorporating the following:

- **Morsel-driven query execution** is a new parallel query evaluation framework that fundamentally differs from the traditional Volcano model in that it distributes work between threads dynamically using work-stealing. This prevents unused CPU resources due to load imbalances, and allows for *elasticity*, i.e., CPU resources can be reassigned between different queries at any time.

- A set of fast **parallel algorithms** for the most important relational operators.
- A systematic approach to integrating **NUMA-awareness** into database systems.

The remainder of this chapter is organized as follows: We start by discussing the many-core challenges in Section 4.2. Section 4.3 is devoted to a detailed discussion of pipeline parallelization and the fragmentation of the data into morsels. In Section 4.4 we discuss the dispatcher, which assigns tasks (pipeline jobs) and morsels (data fragments) to the worker threads. The dispatcher enables the full elasticity which allows to vary the number of parallel threads working on a particular query at any time. Section 4.5 discusses algorithmic and synchronization details of the parallel join, aggregation, and sort operators. The virtues of the query engine are evaluated in Section 4.6 by way of the entire TPC-H query suite. After discussing related work in order to point out the novelty of our parallel query engine architecture in Section 4.7 Finally, Section 4.8 summarizes our results.

4.2 Many-Core Challenges

In recent years, the importance of parallel query processing has greatly increased, since computer architects have shifted attention for investing their ever-increasing transistor budgets away from increasing single-threaded performance towards embedding more independent CPU cores on the same chip. Mainstream servers with dozens of cores are now a reality and the trend is continuing unabated; thus we are transitioning from multi-CPU processing into the “many-core” era.

In this work, we focus on this many-core trend, showing what is required to deal with truly large amounts of cores. For example, techniques that used to work for 4-8 threads simply do not scale to machines with 64 hardware threads. One observation is that parallelism needs to be literally *everywhere* in a query plan to achieve good scalability with many cores [78]. In the TPC-H Benchmark, for example, 97.4% of the tuples in joins arrive from the probe side. Thus, on a system with 64 threads, parallelizing *only* the probe side limits the theoretical overall speedup to 24.3 instead of 64, which wastes more than half of the aggregate compute power. While we use the number 64 as an example, we note that the many-core trend is in full swing and the number of cores continues to grow.

Another challenge in the many-core era is load balancing. Each of the 64 cores needs to get exactly the same amount of work. Approaches that divide the work at query optimization time like Volcano [52] must take into account skew, because intermediate operators such as selections, aggregations and joins, even if they receive exactly the same amount of input data may produce (somewhat) differing amounts of result tuples due to, e.g., data distributions and (slight) correlations with query predicates. Query

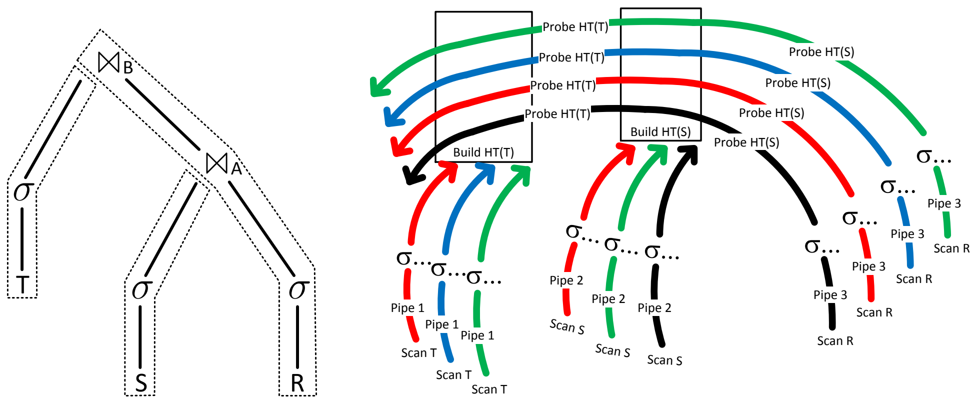

Figure 4.2: Parallellizing the three pipelines of the sample query plan: (left) algebraic evaluation plan; (right) three- respectively four-way parallel processing of each pipeline

optimizers could try to use statistics to help divide the work evenly. However, small errors are still bound to occur and propagate. Thus, operators higher up in the pipeline may not get the same amount of work.

Moreover, in 64-way parallel plans even variations that are small in the absolute sense will have strongly detrimental consequences for overall speed-up. Load-balancing is further complicated by the problem that even if parallel pipelines would get exactly equally sized amounts of work they are likely to take different time to execute it. This is caused by the high complexity of modern out-of-order cores. Slight variations in data distributions among the data given to different threads will cause operators to have different cache locality, different branch prediction rates, and different levels of data dependencies. Finally, concurrent scheduling on nearby cores may cause the clock rate experienced by a thread to get throttled down, and in case of HyperThreading (Simultaneous MultiThreading) the instruction mix run by the thread with whom one shares instruction units may cause unexpected slowdowns.

Another difficulty stems from Non-Uniform Memory Access. Modern database servers have multiple multi-core CPUs, which are connected through fast interconnects. Though these links are very fast in comparison with normal networks, accesses to local memory have a lower latency and higher bandwidth than remote accesses to a different NUMA node [117]. Therefore, in order to fully utilize the compute power and memory bandwidth of these systems, NUMA must be taken into account.

4.3 Morsel-Driven Execution

Adapted from the motivating query of Section 4.1, we will demonstrate our parallel pipeline query execution on the following example query plan:

$$\sigma_{\ldots}(R) \bowtie_A \sigma_{\ldots}(S) \bowtie_B \sigma_{\ldots}(T)$$

Assuming that R is the largest table (after filtering) the optimizer would choose R as probe input and build hash tables for the other two, S and T. The resulting algebraic query plan (as obtained by a cost-based optimizer) consists of the three pipelines illustrated on the left-hand side of Figure 4.2:

1. Scanning, filtering and building the hash table $HT(T)$ of base relation T,
2. Scanning, filtering and building the hash table $HT(S)$ of argument S,
3. Scanning, filtering R and probing the hash table $HT(S)$ of S and probing the hash table $HT(T)$ of T and storing the result tuples.

HyPer uses Just-In-Time (JIT) compilation to generate highly efficient machine code. Each pipeline segment, including all operators, is compiled into one code fragment. This achieves very high raw performance, since interpretation overhead as experienced by traditional query evaluators, is eliminated. Further, in HyPer the operators in the pipelines do not even materialize their intermediate results, as done by modern column-store query engines [187, 167].

The morsel-driven execution of the algebraic plan is controlled by a so called *QEPobject* which transfers executable pipelines to a dispatcher—cf. Section 4.4. It is the *QEPobject*'s responsibility to keep track of data dependencies. In our example query, the third (probe) pipeline can only be executed after the two hash tables have been built, i.e., after the first two pipelines have been fully executed. For each pipeline the *QEPobject* allocates the temporary storage areas into which the parallel threads executing the pipeline write their results. Note that morsels are a logical concept: After completion of the entire pipeline the temporary storage areas are logically re-fragmented into equally sized morsels; this way the succeeding pipelines start with new homogeneously sized morsels instead of retaining morsel boundaries across pipelines which could easily result in skewed morsel sizes. The number of parallel threads working on any pipeline at any time is bounded by the number of hardware threads of the processor. In order to write NUMA-locally and to avoid synchronization while writing intermediate results the *QEPobject* allocates a storage area for each such thread/core for each executable pipeline.

The **parallel** processing of the pipeline for filtering T and building the hash table $HT(T)$ is shown in Figure 4.3. Let us concentrate on the processing of the first phase of the pipeline that filters input T and stores the "surviving" tuples in temporary storage

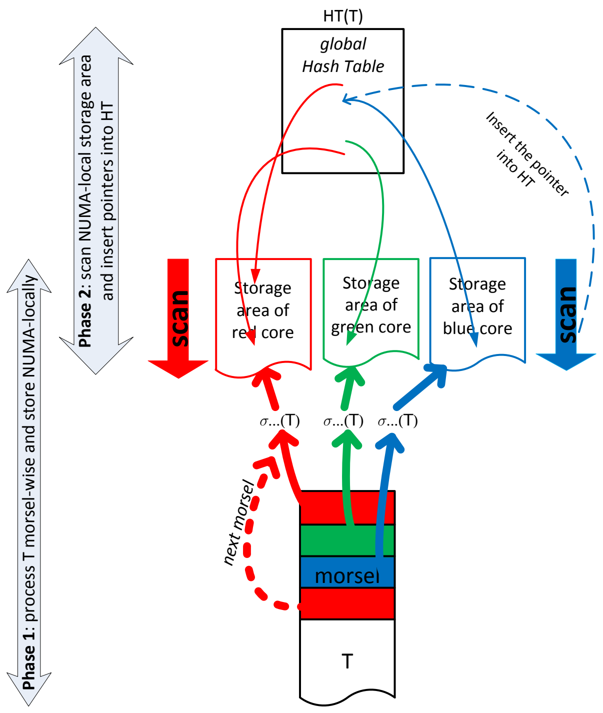
HT(T)
global Hash Table
Insert the pointer into HT
Phase 2: scan NUMA-local storage area and insert pointers into HT
Phase 1: process T morsel-wise and store NUMA-locally
scan
Storage area of red core
Storage area of green core
Storage area of blue core
scan
σ...(T)
σ...(T)
σ...(T)
next morsel
morsel
T

Figure 4.3: NUMA-aware processing of the build-phase

areas. In our figure three parallel threads are shown, each of which operates on one *morsel* at a time. As our base relation T is stored "morsel-wise" across a NUMA-organized memory, the scheduler assigns, whenever possible, a morsel located on the same socket where the thread is executed. This is indicated by the coloring in the figure: The red thread that runs on a core of the red socket is assigned the task to process a red-colored morsel, i.e., a small fragment of the base relation T that is located on the red socket. Once, the thread has finished processing the assigned morsel it can either be delegated (dispatched) to a different task or it obtains another morsel (of the same color) as its next task. As the threads process one morsel at a time the system is fully elastic. The degree of parallelism can be reduced or increased at any point (more precisely, at morsel boundaries) while processing a query.

The logical algebraic pipeline of (1) scanning/filtering the input T and (2) building the hash table is actually broken up into two physical processing pipelines marked as phases on the left-hand side of the figure. In the first phase the filtered tuples are inserted into NUMA-local storage areas, i.e., for each core there is a separate storage area in order to avoid synchronization. To preserve NUMA-locality in further processing stages, the storage area of a particular core is locally allocated on the same socket.

After all base table morsels have been scanned and filtered, in the second phase these storage areas are scanned—again by threads located on the corresponding cores—and

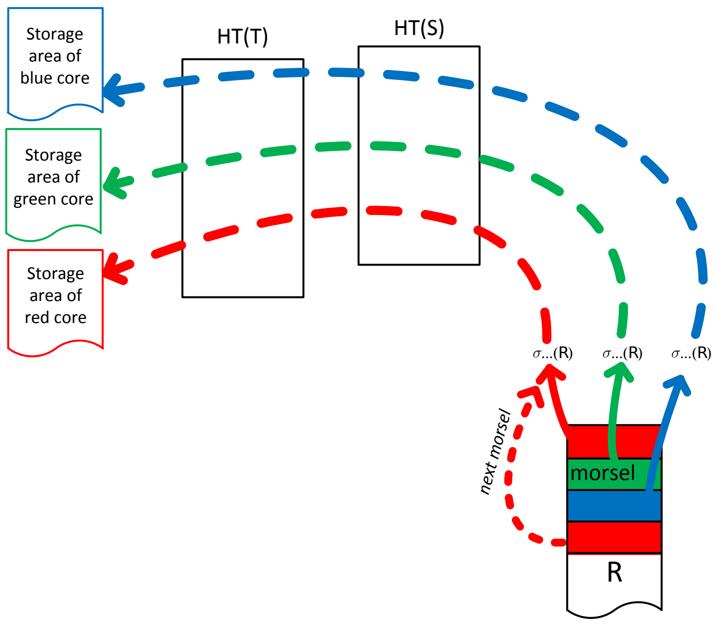

Figure 4.4: Morsel-wise processing of the probe phase

pointers are inserted into the hash table. Segmenting the logical hash table building pipeline into two phases enables perfect sizing of the global hash table because after the first phase is complete, the exact number of "surviving" objects is known. This (perfectly sized) global hash table will be probed by threads located on various sockets of a NUMA system; thus, to avoid contention, it should not reside in a particular NUMA-area and is therefore is interleaved (spread) across all sockets. As many parallel threads compete to insert data into this hash table, a lock-free implementation is essential. The implementation details of the hash table are described in Section 4.5.2.

After both hash tables have been constructed, the probing pipeline can be scheduled. The detailed processing of the probe pipeline is shown in Figure 4.4. Again, a thread requests work from the dispatcher which assigns a morsel in the corresponding NUMA partition. That is, a thread located on a core in the red NUMA partition is assigned a morsel of the base relation R that is located on the corresponding "red" NUMA socket. The result of the probe pipeline is again stored in NUMA local storage areas in order to preserve NUMA locality for further processing (not present in our sample query plan).

In all, morsel-driven parallelism executes multiple pipelines in parallel, which is similar to typical implementations of the Volcano model. Different from Volcano, however, is the fact that the pipelines are not independent. That is, they share data structures and the operators are aware of parallel execution and must perform synchronization, which is done in a lock-free fashion. A further difference is that the number of threads executing the plan is fully elastic. That is, the number may differ not only between different pipeline segments, as shown in Figure 4.2, but also inside the same pipeline segment *during* query execution—as described in the following.

4.4 Dispatcher: Scheduling Parallel Pipeline Tasks

The *dispatcher* is controlling and assigning the compute resources to the parallel pipelines. This is done by assigning tasks to worker threads. We (pre-)create one worker thread for each hardware thread that the machine provides and permanently bind each worker to it. Thus, the level of parallelism of a particular query is not controlled by creating or terminating threads, but rather by assigning them particular tasks of possibly different queries. A task that is assigned to such a worker thread consists of a pipeline job and a particular morsel on which the pipeline has to be executed. Preemption of a task occurs at morsel boundaries—thereby eliminating potentially costly interrupt mechanisms. We experimentally determined that for OLAP queries a morsel size of about 100,000 tuples yields good tradeoff between instant elasticity adjustment, load balancing and low maintenance overhead.

There are three main goals for assigning tasks to threads that run on particular cores:

1. Preserving (NUMA-)locality by assigning data morsels to cores on which the morsels are allocated

2. Full elasticity concerning the level of parallelism of a particular query

3. Load balancing requires that all cores participating in a query pipeline finish their work at the same time in order to prevent (fast) cores from waiting for other (slow) cores[2].

In Figure 4.5 the architecture of the *dispatcher* is sketched. It maintains a list of pending pipeline jobs. This list only contains pipeline jobs whose prerequisites have already been processed. E.g., for our running example query the build input pipelines are first inserted into the list of pending jobs. The probe pipeline is only inserted after these two build pipelines have been finished. As described before, each of the active queries is controlled by a *QEPobject* which is responsible for transferring executable pipelines to the dispatcher. Thus, the dispatcher maintains only lists of pipeline jobs for which all dependent pipelines were already processed. In general, the dispatcher queue will contain pending pipeline jobs of different queries that are executed in parallel to accommodate inter-query parallelism.

[2]This assumes that the goal is to minimize the response time of a particular query. Of course, an idle thread could start working on another query otherwise.

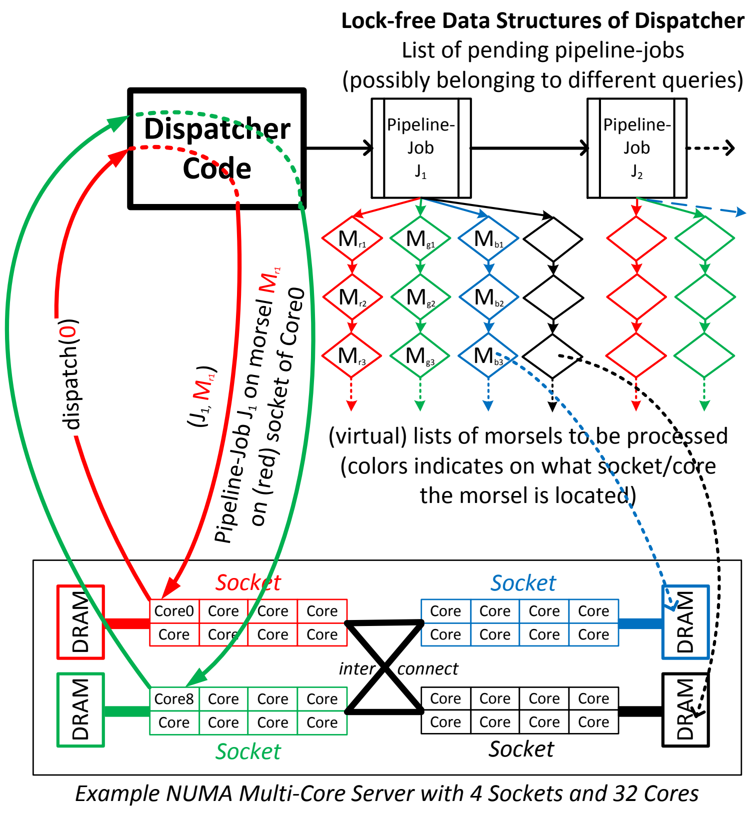
Lock-free Data Structures of Dispatcher
List of pending pipeline-jobs
(possibly belonging to different queries)
Dispatcher Code
Pipeline-Job J1
Pipeline-Job J2
dispatch(0)
(J1, Mr1)
Pipeline-Job J1 on morsel Mr1 on (red) socket of Core0
(virtual) lists of morsels to be processed (colors indicates on what socket/core the morsel is located)
Socket
DRAM
Core0
Core8
Core
inter connect
Example NUMA Multi-Core Server with 4 Sockets and 32 Cores

Figure 4.5: Dispatcher assigns pipeline-jobs on morsels to threads depending on the core

4.4.1 Elasticity

The fully elastic parallelism, which is achieved by dispatching jobs "a morsel at a time", allows for intelligent scheduling of these inter-query parallel pipeline jobs depending on a quality of service model. It enables the scheduler to gracefully decrease the degree of parallelism of, say a long-running query Q_l at any stage of processing in order to prioritize a possibly more important interactive query Q_+. Once the higher prioritized query Q_+ is finished, the pendulum swings back to the long running query by dispatching all or most cores to tasks of the long running query Q_l. In Section 4.6.4 we demonstrate this dynamic elasticity experimentally. In our current implementation all queries have the same priority, so threads are distributed equally over all active queries. A priority-based scheduling component can be based on these ideas but is beyond the scope of this work.

For each pipeline job the dispatcher maintains lists of pending morsels on which the pipeline job has still to be executed. For each core a separate list exists to ensure that a work request of, say, Core 0 returns a morsel that is allocated on the same socket as Core 0. This is indicated by different colors in our architectural sketch. As soon as Core 0 finishes processing the assigned morsel, it requests a new task, which may or may not stem from the same pipeline job. This depends on the prioritization of the different pipeline jobs that originate from different queries being executed. If a high-priority query enters the system it may lead to a decreased parallelism degree for the current query. Morsel-wise processing allows one to re-assign cores to different pipeline jobs without any drastic interrupt mechanism.

4.4.2 Implementation Overview

For illustration purposes we showed a (long) linked list of morsels for each core in Figure 4.5. In reality (i.e., in our implementation) we maintain storage area boundaries for each core/socket and segment these large storage areas into morsels on demand; that is, when a core requests a task from the dispatcher the next morsel of the pipeline argument's storage area on the particular socket is "cut out". Furthermore, in Figure 4.5 the *Dispatcher* appears like a separate thread. This, however, would incur two disadvantages: (1) the dispatcher itself would need a core to run on or might preempt query evaluation threads and (2) it could become a source of contention, in particular if the morsel size was configured quite small. Therefore, the dispatcher is implemented as a lock-free data structure only. The dispatcher's code is then executed by the work-requesting query evaluation thread itself. Thus, the dispatcher is automatically executed on the (otherwise unused) core of this worker thread. Relying on lock-free data structures (i.e., the pipeline job queue as well as the associated morsel queues) reduces contention even if multiple query evaluation threads request new tasks at the same time. Analogously, the *QEPobject* that triggers the progress of a particular query by observing data dependencies (e.g., building hash tables before executing the probe pipeline) is implemented as a passive state machine. The code is invoked by the dispatcher whenever a pipeline job is fully executed as observed by not being able to find a new morsel upon a work request. Again, this state machine is executed on the otherwise unused core of the worker thread that originally requested a new task from the dispatcher.

Besides the ability to assign a core to a different query at any time—called elasticity—the morsel-wise processing also guarantees load balancing and skew resistance. All threads working on the same pipeline job run to completion in a "photo finish": they are guaranteed to reach the finish line within the time period it takes to process a single morsel. If, for some reason, a core finishes processing all morsels on its particular socket, the dispatcher will "steal work" from another core, i.e., it will assign morsels on a different socket. On some NUMA systems, not all sockets are directly connected with each other; here it pays off to steal from closer sockets first. Under normal circumstances, work-stealing from remote sockets happens very infrequently;

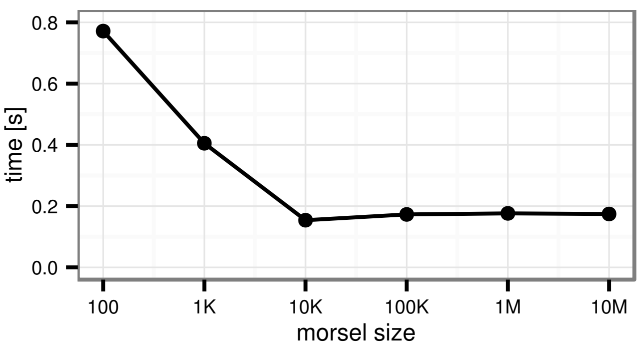

Figure 4.6: Effect of morsel size on query execution

nevertheless it is necessary to avoid idle threads. And the writing into temporary storage will be done into NUMA local storage areas anyway (that is, a red morsel turns blue if it was processed by a blue core in the process of stealing work from the core(s) on the red socket).

So far, we have discussed intra-pipeline parallelism. Our parallelization scheme can also support *bushy parallelism*, e.g., the pipelines "filtering and building the hash table of T" and "filtering and building the hash table of S" of our example are independent and could therefore be executed in parallel. However, the usefulness of this form of parallelism is limited. The number of independent pipelines is usually much smaller than the number of cores, and the amount of work in each pipeline generally differs. Furthermore, bushy parallelism can decrease performance by reducing cache locality. Therefore, we currently avoid to execute multiple pipelines from one query in parallel; in our example, we first execute pipeline T, and only after T is finished, the job for pipeline S is added to the list of pipeline jobs.

Besides elasticity, morsel-driven processing also enables an elegant implementation of query canceling. A user may have aborted her query request or a runtime exception (e.g., a numeric overflow, out-of-memory condition) may have happened. If any of these events happen, the involved query is marked in the dispatcher. The marker is checked whenever a morsel of that query is finished, therefore, very soon all worker threads will stop working on this query. In contrast to forcing the operating system to kill threads, this approach allows each thread to clean up (e.g., free allocated memory).

4.4.3 Morsel Size

In contrast to systems like Vectorwise [20] and IBM's BLU [156], which use vectors/strides to pass data between operators, there is no performance penalty if a morsel does not fit into cache. Morsels are used to break a large task into small, constant-sized work units to facilitate work-stealing and preemption. Consequently, the morsel size is not very critical for performance, it only needs to be large enough to amortize scheduling overhead while providing good response times. To show the effect of morsel size on query performance we measured the performance for the query

```
select min(a) from R.
```

We used 64 threads on a Nehalem EX system, which is described in Section 4.6. This query is very simple, so it stresses the work-stealing data structure as much as possible. Figure 4.6 shows that the morsel size should be set to the smallest possible value where the overhead is negligible, in this case to a value above 10,000. The optimal setting depends on the hardware, but can easily be determined experimentally.

On many-core systems, any shared data structure, even if lock-free, can eventually become a bottleneck. In the case of our work-stealing data structure, however, there are a number of aspects that prevent it from becoming a scalability problem. In our implementation the total work is initially split between all threads, such that each thread temporarily owns a local range. Each local range is stored in a separate cache line to ensure that conflicts are unlikely. Only when this local range is exhausted, a thread will try to steal work from another range. Finally, it is always possible to increase the morsel size. This results in fewer accesses to the work-stealing data structure. In the worst case, a too large morsel size results in underutilized threads but does not affect throughput of the system if enough concurrent queries are being executed.

4.5 Parallel Operator Details

In order to be able to completely parallelize each pipeline, each operator must be capable of accepting tuples in parallel (e.g., by synchronizing shared data structures) and, for operators that start a new pipeline, of producing tuples in parallel. In this section we discuss the implementation of the most important parallel operators.

4.5.1 Hash Join

As discussed in Section 4.3 and shown in Figure 4.3, the hash table construction of our hash join consists of two phases. In the first phase, the build input tuples are materialized into a thread-local storage area[3]; this requires no synchronization. Once all input tuples have been consumed that way, an empty hash table is created with the perfect size, because the input size is now known precisely. This is much more efficient than dynamically growing hash tables, which incur a high overhead in a parallel setting. In the second phase of the parallel build phase each thread scans its storage area and inserts pointers to its tuples using the atomic compare-and-swap instruction. The details are explained in Section 4.5.2.

[3]We also reserve space for a next pointer within each tuple for handling hash collisions.

Outer join is a minor variation of the described algorithm. In each tuple a marker is additionally allocated that indicates if this tuple had a match. In the probe phase the marker is set indicating that a match occurred. Before setting the marker it is advantageous to first check that the marker is not yet set, to avoid unnecessary contention. Semi and anti joins are implemented similarly.

Using a number of single-operation benchmarks, Balkesen et al. showed that a highly-optimized radix join can achieve higher performance than a single-table join [10]. However, in comparison with radix join our single-table hash join

- is fully pipelined for the larger input relation, thus uses less space as the probe input can be processed *in place*,
- is a "good team player" meaning that multiple small (dimension) tables can be joined as a team by a probe pipeline of the large (fact) table through all these dimension hash tables,
- is very efficient if the two input cardinalities differ strongly, as is very often the case in practice,
- can benefit from skewed key distributions[4] [17],
- is insensitive to tuple size, and
- has no hardware-specific parameters.

Because of these practical advantages, a single-table hash join is often preferable to radix join in complex query processing. For example, in the TPC-H benchmark, 97.4% of all joined tuples arrive at the probe side, and therefore the hash table often fits into cache. This effect is even more pronounced with the Star Schema Benchmark where 99.5% of the joined tuples arrive at the probe side. Therefore, we concentrated on a single-table hash join which has the advantage of not relying on query optimizer estimates while providing very good (if the table fits into cache) or at least decent (if the table is larger than cache) performance. We left the radix join implementation, which is beneficial in some scenarios due to higher locality, for future enhancement of our query engine.

4.5.2 Lock-Free Tagged Hash Table

The hash table that we use for the hash join operator has an early-filtering optimization, which improves performance of selective joins, which are quite common. The key idea is to tag a hash bucket list with a small filter into which all elements of that particular

[4]One example that occurs in TPC-H is positional skew, i.e., in a 1:n join all join partners occur in close proximity which improves cache locality.

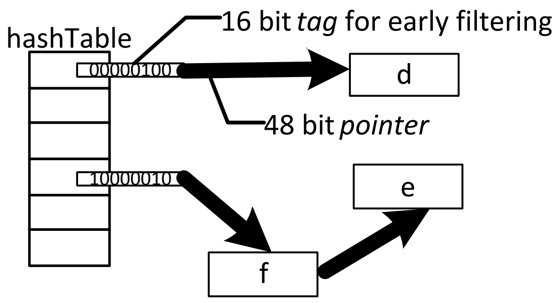

Figure 4.7: Hash table with tagging

```
1  insert(entry) {
2    // determine slot in hash table
3    slot = entry->hash >> hashTableShift
4    do {
5      old = hashTable[slot]
6      // set next to old entry without tag
7      entry->next = removeTag(old)
8      // add old and new tag
9      new = entry | (old&tagMask) | tag(entry->hash)
10     // try to set new value, repeat on failure
11   } while (!CAS(hashTable[slot], old, new))
12 }
```

Figure 4.8: Lock-free insertion into tagged hash table

list are "hashed" to set their 1-bit. For selective probes, i.e., probes that would not find a match by traversing the list, the filter usually reduces the number of cache misses to 1 by replacing a list traversal with a tag check. As shown in Figure 4.7, we encode a tag directly into 16 bits of each pointer in the hash table. This saves space and, more importantly, allows updating both the pointer and the tag using a single atomic compare-and-swap operation when building the hash table.

For low-cost synchronization we exploit the fact that in a join the hash table is insert-only and lookups occur only after all inserts are completed. Figure 4.8 shows the pseudo code for inserting a new entry into the hash table. In line 11, the pointer to the new element (e.g, "f" in the picture) is set using compare-and-swap (CAS). This pointer is augmented by the new tag, which is computed from the old and the new tag (line 9). If the CAS failed (because another insert occurred simultaneously), the process is repeated.

Our tagging technique has a number of advantages in comparison to Bloom filters, which can be used similarly and are, for example, used in Vectorwise [19], SQL Server [99], and BLU [156]. First, a Bloom filter is an additional data structure that incurs multiple reads. And for large tables, the Bloom filter may not fit into cache (or only relatively slow last-level cache), as the Bloom filter size must be proportional to the hash table size to be effective. Therefore, the overhead can be quite high, although Bloom filters can certainly be a very good optimization in some cases. In our approach no unnecessary memory accesses are performed. The only additional work is a small number of cheap bitwise operations. Therefore, hash tagging has very low overhead and can always be used, without relying on the query optimizer to estimate selectivities. Besides being useful for joins, tagging is also very beneficial during aggregation of mostly unique attributes.

The hash table array only stores pointers, and not the tuples themselves, i.e., we do not use open addressing. There are a number of reasons for this: Since the tuples are usually much larger than pointers, the hash table can be sized quite generously to at least twice the size of the input. This reduces the number of collisions without wasting too much space. Furthermore, chaining allows for tuples of variable size, which is not possible with open addressing. Finally, probe misses are typically faster with chaining than with open addressing, because only a single filter needs to be checked rather than (potentially) multiple open addressing entries.

We use large virtual memory pages (2 MB) both for the hash table and the tuple storage areas. This has several positive effects: The number of TLB misses is reduced, the page table is guaranteed to fit into L1 cache, and scalability problems from too many kernel page faults during the build phase are avoided. We allocate the hash table using the Unix *mmap* system call, if available. Modern operating systems do not eagerly allocate the memory immediately, but only when a particular page is first written to. This has two positive effects. First, there is no need to manually initialize the hash table to zero in an additional phase. Second, the table is adaptively distributed over the NUMA nodes, because the pages will be located on the same NUMA node as the thread that has first written to that page. If many threads build the hash table, it will be pseudo-randomly interleaved over all nodes. In case only threads from a single NUMA node construct the hash table, it will be located on that node—which is exactly as desired.

4.5.3 NUMA-Aware Table Partitioning

In order to implement NUMA-local table scans, relations have to be distributed over the memory nodes. The most obvious way to do this is round-robin assignment. A better alternative is to partition relations using the hash value of some "important" attribute. The benefit is that in a join between two tables that are both partitioned on the join key (e.g., by the primary key of one and by the foreign key of the other relation), matching tuples usually reside on the same socket. A typical example (from TPC-H) would be to partition *orders* and *lineitem* on the *orderkey* attribute. Note that this is more a performance hint than a hard partitioning: Work stealing or data imbalance can

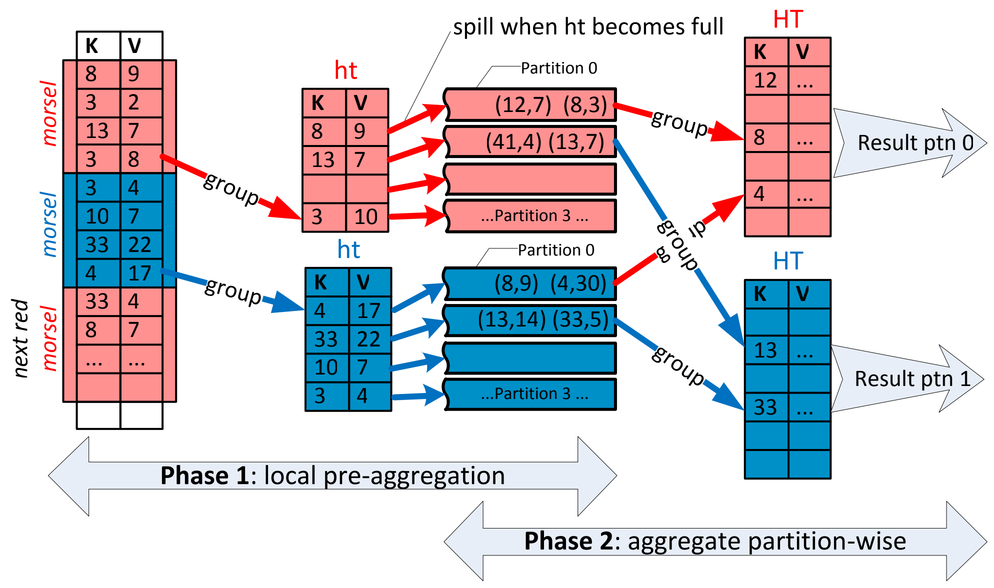

Figure 4.9: Parallel aggregation

still lead to joins between tuples from different sockets, but most join pairs will come from the same socket. The result is that there is less cross-socket communication, because the relations are co-located for this frequent join. This also affects the hash table array, because the same hash function used for determining the hash partition is also used for the highest bits of the hash buckets in a hash join. Except for the choice of the partitioning key, this scheme is completely transparent, and each partition contains approximately the same number of tuples due to the use of hash-based fragmentation.

4.5.4 Grouping/Aggregation

The performance characteristics of the aggregation operator differs very much depending on the number of groups (distinct keys). If there are few groups, aggregation is very fast because all groups fit into cache. If, however, there are many groups, many cache misses happen. Contention from parallel accesses can be a problem in both cases (if the key distribution is skewed). To achieve good performance and scalability in all these cases, without relying on query optimizer estimates, we use an approach similar to IBM BLU's aggregation [156].

As indicated by Figure 4.9, our algorithm has two phases. In the first phase, thread-local pre-aggregation efficiently aggregates heavy hitters using a thread-local, fixed-sized hash table. When this small pre-aggregation table becomes full, it is flushed to overflow partitions. After all input data has been partitioned, the partitions are exchanged between the threads.

The second phase consists of each thread scanning a partition and aggregating it into a thread-local hash table. As there are more partitions than worker threads, this process is repeated until all partitions are finished. Whenever a partition has been fully aggregated, its tuples are immediately pushed into the following operator before processing any other partitions. As a result, the aggregated tuples are likely still in cache and can be processed more efficiently.

Note that the aggregation operator is fundamentally different from join in that the results are only produced after all the input has been read. Since pipelining is not possible anyway, we use partitioning instead of a single hash table as in our join operator.

4.5.5 Set Operators

In contrast to aggregation, which is a unary operator (one input), and join, which is a binary operator (two inputs), HyPer models the SQL (multi-)set operators `UNION`, `INTERSECT`, `EXCEPT`, `INTERSECT ALL`, and `EXCEPT ALL` as n-ary operators (2 or more inputs). This is more efficient than implementing set operators as binary operators, as it allows one to reuse data structures (e.g., hash tables) already built. Furthermore, our implementation is based on hashing and uses pre-aggregation similar to the aggregation operator.

`UNION` treats all inputs symmetrically, i.e., the tuple streams of all inputs are, in effect, appended. After pre-aggregated (using a fixed-sized hash table as in the aggregation), all tuples are hash partitioned, and finally unique, per-partition hash tables are built.

The other variants are executed as follows:

1. *process first input:* Pre-aggregate and then build hash tables for each hash partition from the first input.

2. *merge each additional input:* First the input is partitioned (again after pre-aggregation), then each partition is "merged" into the corresponding, existing hash table from step 1.

3. *output result:* The hash tables are scanned and the tuples in it are the final result.

Step 1 is very similar for all variants. The merge in step 2 differs depending on the variant. `EXCEPT` simply removes entries from the hash table if it encounters a match. `INTERSECT` first removes the key from the hash table and moves it into a new hash table. This new hash table replaces the original one after all tuples have been consumed.

Another difference between the variants is duplicate handling. `UNION`, `INTERSECT`, and `EXCEPT` can simply discard any duplicates. `INTERSECT ALL` and `EXCEPT ALL`, in contrast, count the number of occurrences for each value in the hash table (during step 1). During the merge for `EXCEPT ALL` the count is decremented and

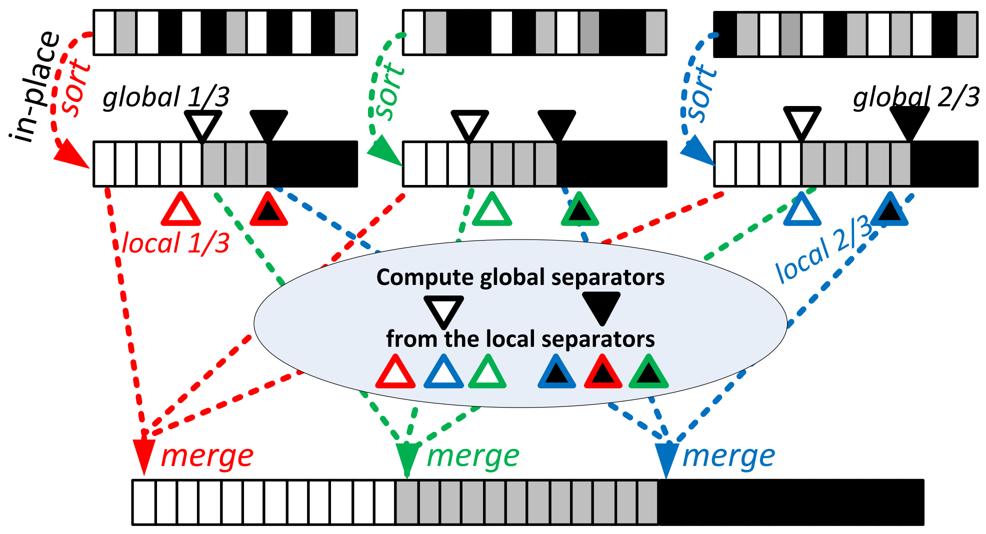

Figure 4.10: Parallel merge sort

the entry is only removed from the hash table if its count reaches zero. `INTERSECT ALL` maintains a second counter in the hash table, which is incremented during the merge. For `INTERSECT ALL`, step 3 produces the minimum of the two counters as the number of output tuples.

4.5.6 Sorting

In main memory, hash-based algorithms are usually faster than sorting [9]. Therefore, we currently do not use sort-based join or aggregation, and only sort to implement the *order by* or *top-k* clause. In our parallel sort operator each thread first materializes and sorts its input locally and in place. In the case of top-k queries, each thread directly maintains a heap of k tuples.

After local sort, the parallel merge phase begins, as shown in Figure 4.10. The difficulty lies in computing separators, so that merges are independent and can be executed in parallel without synchronization. To do this, each thread first computes local separators by picking equidistant keys from its sorted run. Then, to handle skewed distribution and similar to the median-of-medians algorithm, the local separators of all threads are combined, sorted, and the eventual, global separator keys are computed. After determining the global separator keys, binary (or interpolation) search finds the indexes of them in the data arrays. Using these indexes, the exact layout of the output array can be computed. Finally, the runs can be merged into the output array without any synchronization.

Note that while this merge sort algorithm scales very well, it is not morsel-driven. Finding an efficient and scalable morsel-driven sorting algorithm is left for future

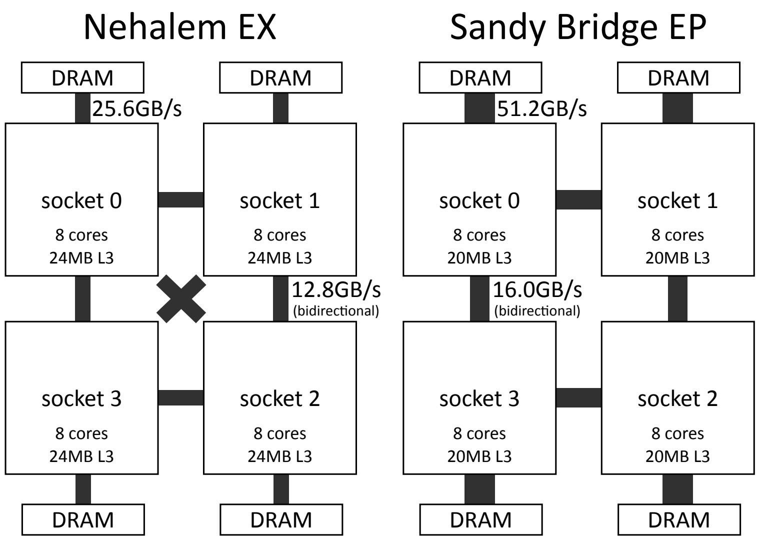

Figure 4.11: NUMA topologies, theoretical bandwidth

work.

4.6 Evaluation

In this evaluation we focus on ad hoc decision support queries, and, except for declaring primary keys, do not enable any additional index structures. Therefore, our results mainly measure the performance and scalability of the table scan, aggregation, and join (including outer, semi, anti join) operators. HyPer supports both row and column-wise storage; we used the column format in all experiments. All data was stored in RAM.

4.6.1 Experimental Setup

We used two different hardware platforms—both running Linux. Unless indicated otherwise we use a 4-socket Nehalem EX (Intel Xeon X7560 at 2.3GHz). Additionally, some experiments are performed on a 4-socket Sandy Bridge EP (Intel Xeon E5-4650L at 2.6GHz-3.1GHz). Such systems are particularly suitable for main-memory database systems, as they support terabytes of RAM at reasonable cost. Although both systems have 32 cores, 64 hardware threads, and almost the same amount of cache, their NUMA topology is quite different. As Figure 4.11 shows, each of the Sandy Bridge CPUs has twice the theoretical per-node memory bandwidth but is only connected to two other sockets. Consequently, some memory accesses (e.g., from socket 0 to socket 2) require two hops instead of one; this increases latency and reduces memory bandwidth because of cross traffic [117]. Note that the upcoming 4-socket Ivy Bridge platform will come in two versions, Ivy Bridge EX which is fully connected like Nehalem EX, and Ivy Bridge EP with only a single interconnect per node like Sandy Bridge EP.

As our main competitor we chose Vectorwise, which was the official single-server TPC-H leader when the experiments were performed. We also measured the performance of the open source row store PostgreSQL and a column store that is integrated into one of the major commercial database systems. On TPC-H, in comparison with HyPer, PostgreSQL was slower by a factor of 30 on average, the commercial column store by a factor of 10. We therefore concentrate on Vectorwise (version 2.5) in further experiments, as it was much faster than the other systems.

In this evaluation we used a classical ad-hoc TPC-H situation. This means that no hand-tuning of physical storage was used, as this way the plans used are similar (hash joins everywhere). The Vectorwise results from the TPC web site include this additional tuning, mainly clustered indexes, which allows executing some of the larger joins with merge-join algorithms. Additionally, these indexes allow the query optimizer to propagate range restrictions from one join side to the other [19], which greatly improves performance for a small number of queries, but does not affect the query processing itself very much. This tuning also does not improve the scalability of query execution; on average the speedup is below 10× both with and without tuning. For completeness, we also provide results for Vectorwise on Nehalem EX with the settings from the TPC-H full disclosure report:

system	geo. mean	sum	scal.
HyPer	0.45s	15.3s	28.1×
Vectorwise	2.84s	93.4s	9.3×
Vectorwise, full-disclosure settings	1.19s	41.2s	8.4×

In HyPer the data can be updated cheaply in-place, since the column format used in our experiments does not use compression. Thus, the two TPC-H refresh streams on scale factor 100 execute in less than 1 second. This is in contrast to heavily read-optimized systems (e.g., [36]), where updates are expensive due to heavy indexing and reordering. Our system transparently distributes the input relations over all available NUMA sockets by partitioning each relation using the first attribute of the primary key into 64 partitions. The execution times include memory allocation and deallocation (from the operating system) for intermediate results, hash tables, etc.

4.6.2 TPC-H

Figure 4.12 compares the scalability of HyPer with Vectorwise on the Nehalem system; both DBMSs are normalized by the single-threaded execution time of HyPer. Note that up to 32 threads, "real" cores are used, the rest are HyperThreads. For most queries, HyPer reaches a speedup close to 30. In some cases a speedup close to or

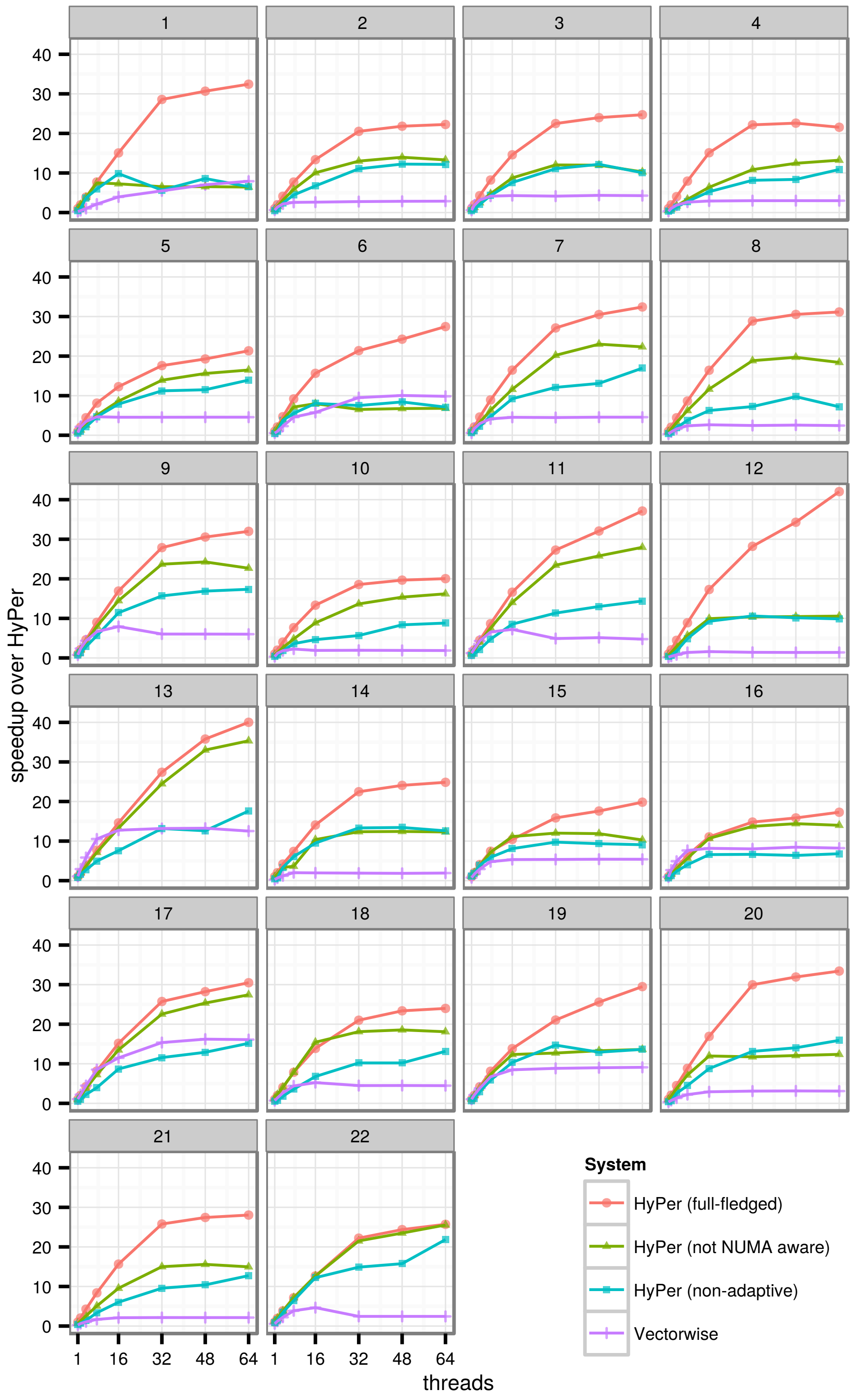

Figure 4.12: TPC-H scalability on Nehalem EX (32 cores, 64 hardware threads)

above 40 is reached due to HyperThreading. Although Vectorwise has similar single-threaded performance as HyPer, its overall performance is severely limited by its low speedup, which is often less than 10. One problem is load balancing: in the—trivially parallelizable—scan-only query 6 the slowest thread often finishes work 50% before the last. While in real-world scenarios it is usually data skew that challenges load balancing, this is not the case in the fully uniform TPC-H. These issues are related to the use of the Volcano model for parallelizing queries in Vectorwise [6]. This approach, which is commonly followed (e.g., in Oracle and SQL Server), as it allows implementing parallelism without affecting existing query operators, bakes the parallelism into the plan at planning time by instantiating a set of query plans on separate plans and connecting then using "exchange" operators [52]. We point out that fixed work division combined with lack of NUMA-awareness can lead to significant performance differences between threads (Vectorwise up to version 3 is not NUMA-aware, as confirmed by our experiments in Section 4.6.3).

Figure 4.12 also shows scalability results where we disabled some important features of our query engine. Performance is significantly lower when we disable explicit NUMA-awareness and rely on the operating system instead (cf. "HyPer (not NUMA aware)"). A further performance penalty can be observed, if we additionally disable adaptive morsel-wise processing and the performance enhancements introduced in this work like hash tagging. This gives an impression of the effects of the individual techniques. But note that we still use JIT compilation and highly tuned operator implementations that try to maximize locality.

Table 4.1 and Table 4.2 allow one to compare the TPC-H performance of the Nehalem and Sandy Bridge systems. The overall performance is similar on both systems, because the missing interconnect links on Sandy Bridge EP, which result in slightly lower scalability, are compensated by its higher clock rate. Notice that all queries complete within 3 seconds—on a 100 GB data set using ad hoc hash joins and without using any index structures.

4.6.3 NUMA Awareness

Table 4.1 shows memory bandwidth and QPI statistics[5] for each of the 22 TPC-H queries. Query 1, which aggregates the largest relation, for example, reads 82.6 GB/s getting close to the theoretical bandwidth maximum of 100 GB/s. The "remote" column in the table shows the percentage of data being accessed though the interconnects (remotely), and therefore measures the locality of each query. Because of NUMA-

[5]These statistics were obtained using the Open Source tool "Intel Performance Counter Monitor" (`www.intel.com/software/pcm`). The "rd." (read), "wr." (write), and "remote" values are aggregated over all sockets. The "QPI" column shows the utilization of the most-utilized QPI link (though with NUMA-awareness the utilization of the links is very similar). Unfortunately, these statistics are not exposed on Sandy Bridge EP.

TPC-H	**HyPer**				[%]		**Vectorwise**				[%]	
	time	scal.	rd.	wr.	remote		time	scal.	rd.	wr.	remote	
#	[s]	[×]	[GB/s]			QPI	[s]	[×]	[GB/s]			QPI
1	0.28	32.4	82.6	0.2	1	40	1.13	30.2	12.5	0.5	74	7
2	0.08	22.3	25.1	0.5	15	17	0.63	4.6	8.7	3.6	55	6
3	0.66	24.7	48.1	4.4	25	34	3.83	7.3	13.5	4.6	76	9
4	0.38	21.6	45.8	2.5	15	32	2.73	9.1	17.5	6.5	68	11
5	0.97	21.3	36.8	5.0	29	30	4.52	7.0	27.8	13.1	80	24
6	0.17	27.5	80.0	0.1	4	43	0.48	17.8	21.5	0.5	75	10
7	0.53	32.4	43.2	4.2	39	38	3.75	8.1	19.5	7.9	70	14
8	0.35	31.2	34.9	2.4	15	24	4.46	7.7	10.9	6.7	39	7
9	2.14	32.0	34.3	5.5	48	32	11.42	7.9	18.4	7.7	63	10
10	0.60	20.0	26.7	5.2	37	24	6.46	5.7	12.1	5.7	55	10
11	0.09	37.1	21.8	2.5	25	16	0.67	3.9	6.0	2.1	57	3
12	0.22	42.0	64.5	1.7	5	34	6.65	6.9	12.3	4.7	61	9
13	1.95	40.0	21.8	10.3	54	25	6.23	11.4	46.6	13.3	74	37
14	0.19	24.8	43.0	6.6	29	34	2.42	7.3	13.7	4.7	60	8
15	0.44	19.8	23.5	3.5	34	21	1.63	7.2	16.8	6.0	62	10
16	0.78	17.3	14.3	2.7	62	16	1.64	8.8	24.9	8.4	53	12
17	0.44	30.5	19.1	0.5	13	13	0.84	15.0	16.2	2.9	69	7
18	2.78	24.0	24.5	12.5	40	25	14.94	6.5	26.3	8.7	66	13
19	0.88	29.5	42.5	3.9	17	27	2.87	8.8	7.4	1.4	79	5
20	0.18	33.4	45.1	0.9	5	23	1.94	9.2	12.6	1.2	74	6
21	0.91	28.0	40.7	4.1	16	29	12.00	9.1	18.2	6.1	67	9
22	0.30	25.7	35.5	1.3	75	38	3.14	4.3	7.0	2.4	66	4

Table 4.1: TPC-H (scale factor 100) statistics on Nehalem EX

	1	2	3	4	5	6	7	8	9	10	11
time [s]	0.21	0.10	0.63	0.30	0.84	0.14	0.56	0.29	2.44	0.61	0.10
scal. [×]	39.4	17.8	18.6	26.9	28.0	42.8	25.3	33.3	21.5	21.0	27.4
	12	13	14	15	16	17	18	19	20	21	22
time [s]	0.33	2.32	0.33	0.33	0.81	0.40	1.66	0.68	0.18	0.74	0.47
scal. [×]	41.8	16.5	15.6	20.5	11.0	34.0	29.1	29.6	33.7	26.4	8.4

Table 4.2: TPC-H (scale factor 100) performance on Sandy Bridge EP

aware processing, most data is accessed locally, which results in lower latency and higher bandwidth. From the "QPI" column[6], which shows the saturation of the most heavily used QPI link, one can conclude that the bandwidth of the QPI links is sufficient on this system. The table also shows that Vectorwise is not NUMA optimized: most queries have high percentages of remotely accessed memory. For instance, the 75% remote accesses in query 1 shows that its buffer manager is not NUMA-aware. However, the QPI links are utilized fairly evenly, as the database relations seem to be spread over all 4 NUMA nodes. This prevents a single memory controller and the QPI links to it from becoming the bottleneck.

Most experiments so far used our NUMA-aware storage layout, NUMA-local scans, the NUMA-aware partitioning, which reduces remote accesses in joins, and the fact that all operators try to keep data NUMA-local whenever possible. To show the overall performance benefit of NUMA-awareness we also experimented with plausible alternatives: "OS default", where the placement is performed by the operating system[7], and "interleaved", where all memory is allocated round robin over all nodes. We report the geometric mean and maximum speedup of our NUMA-aware approach on TPC-H:

	Nehalem EX		Sandy Bridge EP	
	geo. mean	max	geo. mean	max
OS default	1.57×	4.95×	2.40×	5.81×
interleaved	1.07×	1.24×	1.58×	5.01×

Clearly, the default placement of the operating system is sub-optimal, as the memory controller of one NUMA node and the QPI links to it become the bottleneck. These results also show that on Nehalem EX, simply interleaving the memory is a reasonable, though not optimal strategy, whereas on Sandy Bridge EP NUMA-awareness is much more important for good performance. The reason is that these two systems are quite different in their NUMA behavior, as can be seen from a micro benchmark that compares NUMA-local accesses with a random mix of 25% local and 75% remote (including 25% two-hop accesses on Sandy Bridge EP) accesses:

	bandwidth [GB/s]		latency [ns]	
	local	mix	local	mix
Nehalem EX	93	60	161	186
Sandy Bridge EP	121	41	101	257

On Sandy Bridge EP only a small fraction of the theoretical memory bandwidth can

[6]The QPI links are used both for sending the actual data, as well as for broadcasting cache coherency requests, which is unavoidable and happens even for local accesses. Query 1, for example, reads 82.6 GB/s, 99% of it locally, but still uses 40% of the QPI link bandwidth.

[7]In practice, the database itself is located on a single NUMA node, because the data is read from disk by a single thread. Other allocations are local to the thread that first wrote to that memory. Thus, hash tables are distributed randomly over the nodes.

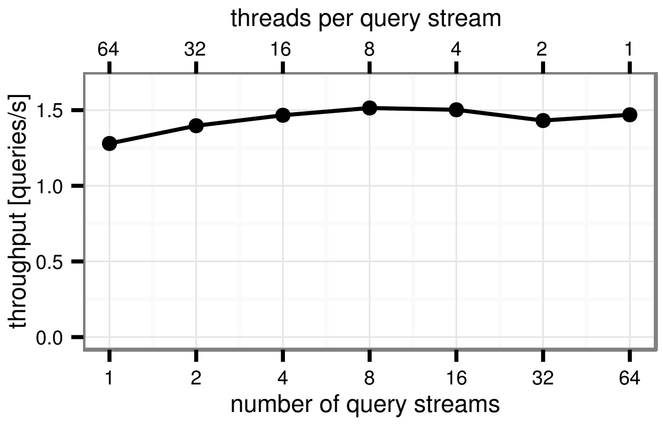

Figure 4.13: Intra- vs. inter-query parallelism with 64 threads

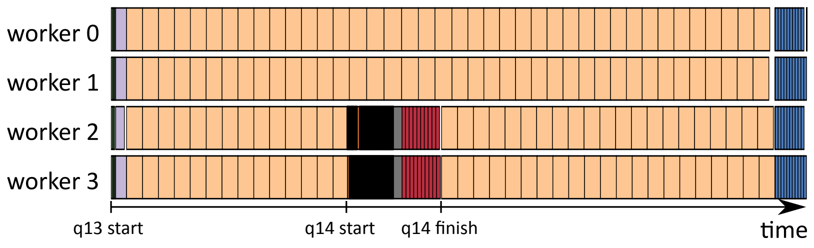

Figure 4.14: Illustration of morsel-wise processing and elasticity

be reached unless most accesses are local, and the latency it 2.5× higher than for local accesses. On Nehalem EX, in contrast, these effects are much smaller, which explains why the positive effect of NUMA-awareness is smaller on this system. The importance of NUMA-awareness clearly depends on the speed and number of the cross-socket interconnects.

4.6.4 Elasticity

To demonstrate the elasticity of our approach, we performed an experiment where we varied the number parallel query streams. The 64 available hardware threads are distributed uniformly over the streams, and each stream executes random permutations of the TPC-H queries. Figure 4.13 shows that the throughput stays high even if few streams (but many cores per stream) are used. This allows to minimize response time for high priority queries without sacrificing too much throughput.

Figure 4.14 illustrates morsel-wise processing by showing an annotated execution trace from our parallel profiler. Each color represents one pipeline stage and each block is one morsel. For graphical reasons we used only 4 threads in this experiment. We started by executing TPC-H query 13, which received 4 threads; after some time, TPC-H query 14 was started. As the trace shows, once the current morsels of worker

SSB #	time [s]	scal. [×]	read [GB/s]	write [GB/s]	remote [%]	QPI [%]
1.1	0.10	33.0	35.8	0.4	18	29
1.2	0.04	41.7	85.6	0.1	1	44
1.3	0.04	42.6	85.6	0.1	1	44
2.1	0.11	44.2	25.6	0.7	13	17
2.2	0.15	45.1	37.2	0.1	2	19
2.3	0.06	36.3	43.8	0.1	3	25
3.1	0.29	30.7	24.8	1.0	37	21
3.2	0.09	38.3	37.3	0.4	7	22
3.3	0.06	40.7	51.0	0.1	2	27
3.4	0.06	40.5	51.9	0.1	2	28
4.1	0.26	36.5	43.4	0.3	34	34
4.2	0.23	35.1	43.3	0.3	28	33
4.3	0.12	44.2	39.1	0.3	5	22

Table 4.3: Star Schema Benchmark (scale 50) on Nehalem EX

thread 2 and 3 are finished, these threads switch to query 14 until it is finished, and finally continue working on query 13. This experiment shows that it is possible to dynamically reassign worker threads to other queries, i.e., that our parallelization scheme is fully elastic.

As mentioned in the introduction, the Volcano approach typically assigns work to threads statically. To compare with this approach, we emulated it in our morsel-driven scheme by splitting the work into as many chunks as there are threads, i.e., we set the morsel size to n/t, where n is the input size and t is the number of threads. As long as we only execute a single TPC-H query at a time, this change alone does not significantly decrease performance, because the input data is uniformly distributed on this workload. However, if we add some interference from other processes, this picture changes. For example, when we ran the TPC-H queries while another, unrelated single-threaded process occupied one core, query performance dropped by 36.8% with static approach, but only 4.7% with dynamic morsel assignment.

4.6.5 Star Schema Benchmark

Besides TPC-H, we also measured the performance and scalability of our system on the Star Schema Benchmark (SSB) [144], which mimics data warehousing scenarios. Table 4.3 shows that our parallelization framework works very well on this workload, achieving a speedup of over 40 for most queries. The scalability is higher than on TPC-H, because TPC-H is a much more complex and challenging workload. TPC-H contains a very diverse set of queries: queries that only scan a single table, queries with complex joins, queries with simple and with complex aggregations, etc. It is quite challenging to obtain good performance *and* scalability on such a workload, as all operators must be scalable and capable of efficiently handling very diverse input distributions. All SSB queries, in contrast, join a large fact table with multiple smaller dimension tables where the pipelining capabilities of our hash join algorithm are very beneficial. Most of the data comes from the large fact table, which can be read NUMA-locally (cf. column "remote" in Figure 4.3), the hash tables of the dimensions are much smaller than the fact table, and the aggregation is quite cheap in comparison with the rest of the query.

4.7 Related Work

This work is related to three distinct lines of work: papers that focus on multi-core join or aggregation processing in isolation, full systems descriptions, and parallel execution frameworks, most notably Volcano.

The radix hash join was originally designed to increase locality [128]. Kim et al. proposed it for parallel processing based on repeatedly partitioning the input relations [90]. Blanas et al. [17] were the first to compare the radix join with a simple, single global hash table join. Balkesen et al. [10, 9] and Schuh et al. [160] comprehensively investigated hash- and sort-based join algorithms. Ye et al. evaluated parallel aggregation algorithms on multi-core CPUs [183]. Polychroniou and Ross designed an aggregation algorithm to efficiently aggregate heavy hitters (frequent items) [149].

A number of papers specifically focus on NUMA. In one of the first paper that pinpoints the relevance of NUMA-locality, Teubner and Müller [169] presented a NUMA-aware window-based stream join. In another early NUMA paper, Albutiu et al. designed a NUMA-aware parallel sort merge join [3]. Li et al. refined this algorithm by explicitly scheduling the shuffling of the sorted runs in order to avoid cross traffic in the NUMA interconnection network [117]. However, despite its locality-preserving nature this algorithm turned out to be less efficient than hash joins due to the high cost of sorting [9, 96]. Lang et al. [96] devised a low synchronization overhead NUMA-aware hash join, which is similar to our algorithm. It relies on a single latch-free hash table interleaved across all NUMA nodes into which all threads insert the build input.

Unfortunately, the conclusiveness of these single-operator studies for full-fledged query engines is limited because the micro-benchmarks used for testing usually have single simple keys (sometimes even containing hash values), and typically use very small payloads (one column only). Furthermore, each operator was analyzed in isolation, which ignores how data is passed between operators and therefore, for example, ignores the different pipelining capabilities of the algorithms. In our morsel-driven database system, we have concentrated on (non-materializing) pipelined hash joins, since in practice, often one of the join sides is much larger than the others. Therefore, teams of pipelined joins are often possible and effective. Further, for certain often-traversed large joins (such as orders-lineitem in TPC-H), pre-partitioned data storage can achieve NUMA locality on large joins without need for materialization.

The IBM BLU query engine [156] and Microsoft's Apollo project [101] are two prominent commercial projects to exploit modern multi-core servers for parallel query processing. IBM BLU processes data in "Vectorwise" fashion, a so-called stride at a time. In this respect there is some resemblance to our morsel-wise processing technique. However, there was no indication that the strides are maintained NUMA-locally across processing steps/pipelines. In addition, the full elasticity w.r.t. the degree of parallelism that we propose was not covered. Very similar to Volcano-style parallelization, in Oracle the individual operators are largely unaware of parallelism. [15] addresses some problems of this model, in particular reliance on query optimizer estimates, by adaptively changing data distribution decisions during query execution. In an experimental study Kiefer et al. [89] showed that NUMA-awareness can improve database performance considerably. Porobic et al. investigated [152] and improved NUMA-placement in OLTP systems by partitioning the data and internal data structures in a NUMA-aware way [151]. Heimel et al. presented a hardware-oblivious approach to parallelization that allows operators to be compiled to different hardware platforms like CPUs or GPUs [65]. In this work we focus on classical, query-centric parallelization, i.e., parallelizing individual queries in isolation. Another fruitful approach is to exploit common work from multiple queries. This operator-centric approach is used by QPipe [64] and SharedDB [51].

The seminal Volcano model [52] forms the basis of most current query evaluation engines enabling multi-core as well as distributed [53] parallelism. Note that Volcano in a non-parallel context is also associated with an interpreted iterator execution paradigm where results are pulled upwards through an operator tree, by calling the *next()* method on each operator, which delivers the next tuple. Such a tuple-at-a-time execution model, while elegant in its implementation, has been shown to introduce significant interpretation overhead [139]. With the advent of high-performance analytical query engines, systems have been moving from this model towards vector or batch-oriented execution, where each *next()* method works on hundreds or thousands of tuples. This vector-wise execution model appears in Vectorwise [6], but also in the batch-mode execution offered by ColumnStore Index tables in SQL Server [101] (the Apollo project), as well as in stride-at-a-time execution in IBM's BLU engine for DB2 [156]. In HyPer we rely on a compiled query evaluation approach as first postulated by Krikellas et al. [94] and later refined by Neumann [139] to obtain the same, or even higher raw execution performance.

As far as parallelism is concerned, Volcano differentiates between vertical parallelism, where essentially the pipeline between two operators is transformed into an asynchronous producer/consumer model, and horizontal parallelism, where one operator is parallelized by partitioning the input data and have each parallel thread work on one of the partitions. Most systems have implemented horizontal parallelism, since vertical and bushy parallelism are less useful due to their unbalanced nature, as we observed earlier. Examples of such horizontal Volcano parallelism are found in e.g., Microsoft SQL Server and Vectorwise [6].

While there may be (undisclosed) implementation differences between these systems, morsel-driven execution differentiates itself by making parallel query scheduling fine-grained, adaptive at run-time and NUMA-aware. The parallel query engine described here relies on chunking of the input data into fine-grained morsels. A morsel resides completely in a single NUMA partition. The dispatcher assigns the processing of a morsel to a thread running on a core of the same socket in order to preserve NUMA locality. The morsel-wise processing also facilitates the full elasticity, meaning that the degree of parallelism can be adjusted at any time, e.g., at mid-query processing. As soon as a morsel is finished, the thread can be assigned a morsel belonging to the same query pipeline or be assigned a different task of, e.g., another more important query. This way the dispatcher controls parallelism explicitly as opposed to the recently proposed approach by Psaroudakis et al. [153] where the number of threads is changed based on the core utilization.

4.8 Summary

We presented the morsel-driven query evaluation framework for parallel query processing. It is targeted at solving the major bottlenecks for analytical query performance in the many-core age, which are load-balancing, thread synchronization, memory access locality, and resource elasticity. We demonstrated the good scalability of this framework in HyPer on the full TPC-H and SSB query workloads. It is important to highlight, that at the time of this writing, the presented results are by far the fastest achieved (barring the hand-written queries on a fully indexed and customized storage scheme [36][8]) on a single-server architecture. This is not being noted to claim a performance record—these are academic and non-audited results—but rather to underline the effectiveness of the morsel-driven framework in achieving scalability. In particular, one needs to keep in mind that it is much easier to provide linear scalability on computationally slow systems than it is on fast systems such as HyPer. The comparison with the state-of-the-art Vectorwise system, which uses a classical implementation of Volcano-style parallelism [6], shows that beyond 8 cores, in many-core territory, the morsel-driven framework speeds ahead; and we believe that its principles

[8] The paper by Dees and Sanders [36], while interesting as an extreme take on TPC-H, visibly violates many of its implementation rules, including the use of precomputed joins, precomputed aggregates, and full-text indexing. It generally presents a storage structure that is very expensive to update.

in fine-grained scheduling, full operator parallelization, low-overhead synchronization and NUMA-aware scheduling can be used to improve the many-core scaling in other systems as well.

The work presented in this chapter focused on single-node scalability. Work by Wolf Rödiger et al. investigated how to achieve scalability on multiple nodes. Building on top of HyPer, their work achieves excellent scalability and performance by implementing Exchange operators optimized for high-speed networks. They also show that, when Exchange operators are used for single- as well as multi-node parallelism, the quadratic number of communication channels (cores times nodes) becomes a major performance problem. Thus, indirectly, our approach contributes to improving multi-node scalability.

5 Window Function Processing in SQL

Parts of this chapter have previously been published in [111].

5.1 Introduction

Window functions, which are also known as analytic OLAP functions, are part of the SQL:2003 standard. This SQL feature is widely used: The TPC-DS benchmark [136], for example, uses window functions in 9 out of 99 queries and a recent study [77] (of non-expert SQL users) reports that 4% of all queries use this feature. Almost all major database systems, including Oracle [1], Microsoft SQL Server [2], IBM DB2 [3], SAP HANA [4], Vertica [5], PostgreSQL [6], Actian Vectorwise [72], Cloudera Impala [93], and MonetDB [7] implement the functionality described in the SQL standard—or at least some subset thereof.

Window functions allow one to easily formulate certain business intelligence queries that include time series analysis, ranking, top-k, percentiles, moving averages, cumulative sums, etc. Without window function support, such queries either require difficult to formulate and inefficient correlated subqueries, or must be implemented at the application level.

In the following we present example queries that highlight the usefulness and versatility of the window operator. The first example query, which might be used to detect outliers in a time series, illustrates the use of window functions in SQL:

[1] `http://docs.oracle.com/database/121/DWHSG/analysis.htm`
[2] `http://msdn.microsoft.com/en-us/library/ms189461(v=sql.120).aspx`
[3] `http://www-01.ibm.com/support/knowledgecenter/SSEPGG_10.5.0/com.ibm.db2.luw.sql.ref.doc/doc/r0023461.html`
[4] `http://help.sap.de/hana/SAP_HANA_SQL_and_System_Views_Reference_en.pdf`
[5] `https://my.vertica.com/docs/7.1.x/HTML/Content/Authoring/SQLReferenceManual/Functions/Analytic/AnalyticFunctions.htm`
[6] `http://www.postgresql.org/docs/9.4/static/tutorial-window.html`
[7] `https://www.monetdb.org/Documentation/Manuals/SQLreference/WindowFunctions`

```
  select location, time, value, abs(value-
    (avg(value) over w))/(stddev(value) over w)
  from measurement
  window w as (
     partition by location
     order by time
     range between 5 preceding and 5 following)
```

The query normalizes each measurement by subtracting the average and dividing by the standard deviation. Both aggregates are computed over a window of 5 time units around the time of the measurement and at the same location. Without window functions, it is possible to state the query as follows:

```
select location, time, value, abs(value-
  (select avg(value)
   from measurement m2
   where m2.time between m.time-5 and m.time+5
         and m.location = m2.location))
/ (select stddev(value)
   from measurement m3
   where m3.time between m.time-5 and m.time+5
         and m.location = m3.location)
from measurement m
```

In this formulation, correlated subqueries are used to compute the aggregates, which in most query processing engines results in very slow execution times due to quadratic complexity. The example also illustrates that to implement window functions efficiently, a new relational operator is required. Window expressions cannot be replaced by simple aggregation (i.e., `group by`) because each measurement defines a separate window.

The second example query determines medalists for an Olympic-style competition where the same number of points results in the same medal (and an omitted lesser medal):

```
select name, (case rank when 1 then 'Gold'
       when 2 then 'Silver'
       else 'Bronze' end)
from (select name, rank() over w as rank
      from results
      window w as (order by points desc))
where rank <= 3
```

The percentile of each participant in a competition, partitioned by gender can be computed as follows:

```
select name, gender,
   percent_rank() over (partition by gender order by time)
from competition
```

Finally, the rate of change for each measurement in comparison with the previous measurement (e.g., "transactions per second") is also easy to compute:

```
select time,
    (value - lag(value) over w) / (time - lag(time) over w)
from measurement
window w as (order by time)
```

Despite the usefulness and prevalence of window functions "in the wild", the window operator has mostly been neglected in the literature. One exception is the pioneering paper by Cao et al. [26], which shows how to optimize *multiple* window functions that occur *in one query* by avoiding unnecessary sorting or partitioning steps. In this work, we instead focus on the core algorithm for efficient window function computation itself. The optimization techniques from [26] are therefore orthogonal and should be used in conjunction.

To the best of our knowledge, we present the first detailed description of a complete algorithm for the window operator. Our algorithm is universally applicable, efficient in practice, and asymptotically superior to algorithms currently employed by commercial systems. This is achieved by utilizing a specialized data structure, the *Segment Tree*, for window function evaluation. The design of the window operator is optimized for high-performance main-memory databases like HyPer [87], which is optimized for modern multi-core CPUs [106].

As commodity server CPUs with dozens of cores are becoming widespread, it becomes more and more important to parallelize *all* operations that depend on the size of the input data. Therefore, our algorithm is designed to be highly scalable: instead of only supporting inter-partition parallelism, which is a best-effort approach that is simple to implement but not applicable to all queries, we show how to parallelize *all* phases of our algorithm. At the same time, we opportunistically use low-overhead, partitioning-based parallelization when possible. As a result, our implementation is fast and scales even for queries without a partitioning clause and for arbitrary, even highly skewed, input distributions.

The rest of the chapter is organized as follows: Section 5.2 gives an overview of the syntax and semantics of window functions in SQL. The core of our window operator and our parallelization strategy is presented in Section 5.3. The actual computation of window function expressions, which is the last phase of our operator, is discussed in

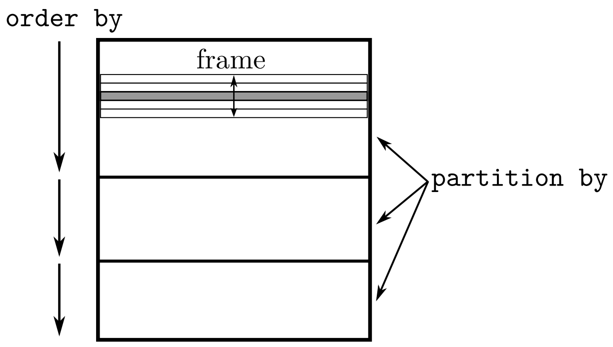

Figure 5.1: Window function concepts: partitioning, ordering, framing. The current (gray) row can access rows in its frame. The frame of a tuple can only encompass tuples from that partition

Section 5.4. Section 5.5 describes how to integrate the algorithm into database systems. In Section 5.6 we experimentally evaluate our algorithm under a wide range of settings and compare it with other implementations. Finally, after presenting related work in Section 5.7, we summarize the results in Section 5.8.

5.2 Window Functions in SQL

One of the core principles of SQL is that the output tuple order of all operators (except for sort) is undefined. This design decision enables many important optimizations, but makes queries that depend on the tuple order (e.g., ranking) or that refer to neighboring tuples (e.g., cumulative sums) quite difficult to state. By making it possible to refer to neighboring tuples (the “window”) directly, window functions allow one to easily express such queries.

In this section, we introduce the syntax and semantics of SQL window functions. To understand the semantics two observations are important. Firstly, window function expressions are computed after most other clauses (including `group by` and `having`), but before the final sorting `order by` and duplicate removal `distinct` clauses. Secondly, the window operator only computes additional attributes for each input tuple but does not change or filter its input otherwise. Therefore, window expressions are only allowed in the `select` and `order by` clauses, but not in the `where` clause.

5.2.1 Partitioning

Window function evaluation is based on three simple and orthogonal concepts: partitioning, ordering, and framing. Figure 5.1 illustrates these concepts graphically. The `partition by` clause partitions the input by one or more expressions into independent groups, and thereby restricts the window of a tuple. In contrast to normal

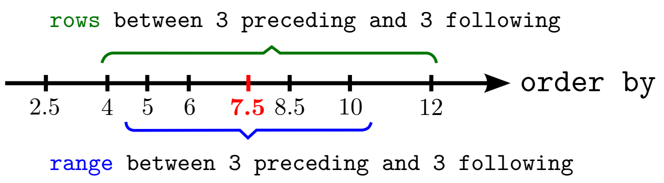
rows between 3 preceding and 3 following
order by
2.5
4
5
6
7.5
8.5
10
12
range between 3 preceding and 3 following

Figure 5.2: Illustration of the `range` and `rows` modes for framing. Each tick represents the value of a tuple's `order by` expression

aggregation (`group by`), the window operator does not reduce all tuples of a group to a single tuple, but only logically partitions tuples into groups. If no partitioning clause is specified, all input rows are considered as belonging to the same partition.

5.2.2 Ordering

Within each partition, the rows can be ordered using the `order by` clause. Semantically, the `order by` clause defines how the input tuples are logically ordered during window function evaluation. For example, if a ranking window function is used, the rank is computed with respect to the specified order. Note that the ordering only affects window function processing but not necessarily the final order of the result. If no ordering is specified, the result of some window functions (e.g., `row_number`) is non-deterministic.

5.2.3 Framing

Besides the partitioning clause, window functions have a *framing clause* which allows restricting the tuples that a window function acts on further. The frame specifies which tuples in the proximity of the current row (based on the specified ordering) belong to its frame. Figure 5.2 illustrates the two available modes.

- `rows` mode directly specifies how many rows before or after the current row belong to the frame. In the figure, the 3 rows before and after the current row are part of the frame, which also includes the current row therefore consists of the values 4, 5, 6, 7.5, 8.5, 10, and 12. It is also possible to specify a frame that does not include the current row, e.g., `rows between 5 preceding and 2 preceding`.

- In `range` mode, the frame bounds are computed by decrementing/incrementing the `order by` expression of the current row[8]. In the figure, the `order by` expression of the current row is 7.5, the window frame bounds are 4.5 (7.5 − 3) and 10.5 (7.5 − 3). Therefore, the frame consists of the values 5, 6, 7.5, 8.5, and 10.

[8]`range` mode is only possible if the query has exactly one numeric order by expression.

In both modes, the framing bounds do not have to be constants, but can be arbitrary expressions and may even depend on attributes of the current row. Most implementations only support constant values for framing bounds, whereas our implementation supports non-constant framing bounds efficiently. All rows in the same partition that have the same `order by` expression values are considered *peers*. The peer concept is only used by some window functions, but ignored by others. For example, all peers have the same `rank()` but a different `row_number()`.

Besides `preceding` and `following`, the frame bounds can also be set to the following values:

- `current row`: the current row (including all peers in `range` mode)
- `unbounded preceding`: the frame starts at the first row in the partition
- `unbounded following`: the frame ends with the last row in the partition

If no window frame was specified and there is an `order by` clause, the default frame specification is `range between unbounded preceding and current row`. This results in a window frame that consists of all rows from the start of the current partition to the current row and all its peers, and is useful for computing cumulative sums. Queries without an `order by` clause, are evaluated over the entire partition, as if having the frame specification `range between unbounded preceding and unbounded following`. Finally, it is important to note that the framing clause only affects some window functions, namely intra-window navigation functions (`first_value`, `last_value`, `nth_value`), and non-distinct aggregate functions (`min`, `max`, `count`, `sum`, `avg`). The remaining window functions (`row_number`, `rank`, `lead`, ...) and distinct aggregates are always evaluated on the entire partition.

For syntactic convenience and as already shown in the first example of the introduction, SQL allows one to name a particular combination of partitioning, ordering, and framing clauses. By referring to this name the window specification can then be reused by multiple window expressions to avoid repeating the clauses, which often improves the readability of the query, as shown in the following example:

```
select min(value) over w1, max(value) over w1,
       min(value) over w2, max(value) over w2
from measurement
window w1 as (order by time
              range between 5 preceding and 5 following),
       w2 as (order by time
              range between 3 preceding and 3 following)
```

5.2.4 Window Expressions

SQL:2011 defines a number of window functions for different purposes. The following functions ignore framing, i.e., they are always evaluated on the entire partition:

- ranking:
  - `rank()`: rank of the current row with gaps
  - `dense_rank()`: rank of the current row without gaps
  - `row_number()`: row number of the current row
  - `ntile(num)`: distribute evenly over buckets (returns integer from 1 to `num`)
- distribution:
  - `percent_rank()`: relative rank of the current row
  - `cume_dist()`: relative rank of peer group
- navigation in partition:
  - `lead(expr, offset, default)`: evaluate `expr` on preceding row in partition
  - `lag(expr, offset, default)`: evaluate `expr` on following row in partition
- distinct aggregates: `min`, `max`, `sum`, ...: compute distinct aggregate over partition

There are also window functions that are evaluated on the current frame, i.e., a subset of the partition:

- navigation in frame:
  - `first_expr(expr)`, `last_expr(expr)`, `nth_expr(expr, nth)`: evaluate `expr` on first/last/`nth` row of the frame
- aggregates: `min`, `max`, `sum`, ...: compute aggregate over all tuples in the current frame

As the argument lists of these functions indicate, most functions require an arbitrary expression (the `expr` argument) and other additional parameters as input.

To syntactically distinguish normal aggregation functions (computed by the `group by` operator) from their window function cousins, which have the same name but are computed by the aggregation operator, window function expressions must be followed by the `over` keyword and a (potentially empty) window frame specification. In the following query, the average is computed using the window operator, whereas the sum aggregate is computed by the aggregation operator:

```
select cid, year, month, sum(price),
    avg(sum(price)) over (partition by customer_id)
from orders
group by customer_id, year, month
```

For each customer and month, the query computes the sum of all purchases of this customer (using aggregation) and the average of all monthly expenditures of this customer (using window aggregation without framing).

In some cases, window function queries can directly be translated to aggregation queries:

```
select location, time, value,
       avg(value) over ()
from measurement
```

In this query, the average is computed using the window operator over the entire input because no `partition by` or `order by` clauses were specified. Therefore the query can be rewritten using aggregation as follows:

```
select location, time, value,
      (select avg(value) from measurement)
from measurement
```

This transformation avoids the sorting phase and should be performed when the frame encompasses the entire partition.

Distinct aggregates, which in contrast to normal aggregates cannot be used with framing, are always best executed without using the window operator. Instead, distinct aggregates can be executed efficiently using normal aggregation and an additional join. For example, the query

```
select sum(distinct x) over (partition by y)
from r
```

is equivalent to:

```
select d.cd from r,
     (select sum(distinct x) as cd, y
      from r group by y) d
where r.y = d.y
```

5.3 The Window Operator

Depending on the window function and the partitioning, ordering, and framing clause specified (or omitted) in a particular query, the necessary algorithmic steps differ greatly. In order to incorporate all aspects into a single operator we present our algorithm in a modular fashion. Some phases can simply be omitted if they are not needed for a particular query.

The basic algorithm for window function processing directly follows from the high-level syntactic structure discussed in Section 5.2 and involves the following phases:

1. *Partitioning*: partition the input relation using the `partition by` attributes
2. *Sorting*: sort each partition using the `order by` attributes
3. *Window function computation*: for each tuple
   a) *Compute window frame*: Determine window frame (a subset of the partition)
   b) *Evaluate window function*: Evaluate window function on the window frame and output tuple

In this section we focus on the first two phases, partitioning and sorting. Phase 3, window function evaluation, is discussed in Section 5.4.

5.3.1 Partitioning and Sorting

For the initial partitioning and sorting phases there are two traditional methods:

1. The *hash-based* approach fully partitions the input using hash values of the `partition by` attributes before sorting each partition independently using only the `order by` attributes.
2. The *sort-based* approach first sorts the input by both the `partition by` and the `order by` attributes. The partition boundaries are determined "on-the-fly" during the window function evaluation phase (phase 3), e.g., using binary search.

From a purely theoretical point of view, the hash-based approach is preferable. Assuming there are n input rows and $O(n)$ partitions, the overall complexity of the hash-based approach is $O(n)$, whereas the sort-based approach results in $O(n \log n)$ complexity. Nevertheless, the *sort-based* approach is often used in commercial systems—perhaps because it requires less implementation effort, as a sorting phase is required anyway. In order to achieve good performance *and* scalability we use combination of both methods.

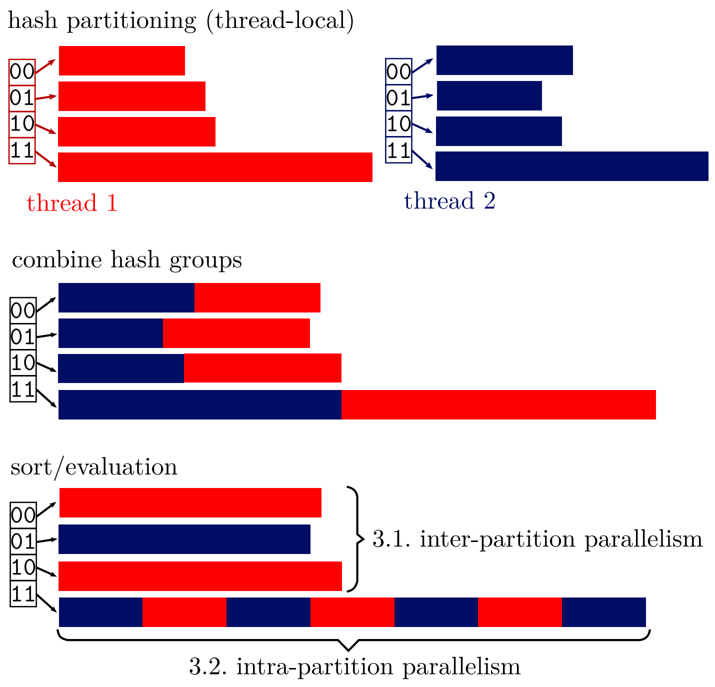
hash partitioning (thread-local)
00
01
10
11
thread 1
thread 2
combine hash groups
sort/evaluation
3.1. inter-partition parallelism
3.2. intra-partition parallelism

Figure 5.3: Overview of the phases of the window operator. The colors represent the two threads

In single-threaded execution, it is usually best to first fully partition the input data using a hash table. With parallel execution, a concurrent hash table would be required for this approach. We have found, however, that concurrent, dynamically-growing hash tables (e.g., split-ordered lists [162]) have a significant overhead in comparison with unsynchronized hash tables. The sort-based approach, without partitioning first, is also very expensive. Therefore, to achieve high scalability and low overhead, we use a hybrid approach that combines the two methods.

5.3.2 Pre-Partitioning into Hash Groups

Our approach is to partition the input data into a constant number (e.g., 1024) of *hash groups*, regardless of how many partitions the input data has. The number of hash groups should be a power of 2 and larger than the number of threads but small enough to make partitioning efficient on modern CPUs. This form of partitioning can be done very efficiently in parallel due to limited synchronization requirements: As illustrated in Figure 5.3, each thread (distinguished using different colors) initially has its own array of hash groups (4 in the figure)[9]. After all threads have partitioned their input

[9]In our implementation in HyPer, the thread-local hash groups physically consist of multiple, chained arrays, since no random access is necessary and the chunks are copied into a combined array anyway.

data, the corresponding hash groups from all threads are copied into a combined array. This can be done in parallel and without synchronization because at this point the sizes and offsets of all threads' hash groups are known. After copying, each combined hash group is stored in a contiguous array, which allows for efficient random access to each tuple.

After the hash groups copied, the next step is to sort them by both the partitioning and the ordering expressions. As a result, all tuples with the same partitioning key are adjacent in the same hash group, although of course a hash group may contain multiple partitioning keys. When necessary, the actual partition boundaries can be determined using binary search as in the sort-based approach during execution of the remaining window function evaluation step.

5.3.3 Inter- and Intra-Partition Parallelism

At first glance, the window operator seems to be embarrassingly parallel, as partitioning can be done in parallel and all hash groups are independent from each other: Since sorting and window function evaluation for different hash groups is independent, the available threads can simply work on different hash groups without needing any synchronization. Database systems that parallelize window functions usually use this strategy, as it is easy to implement and can offer very good performance for "good-natured" queries.

However, this approach is not sufficient for queries with no partitioning clause, when the number of partitions is much smaller than the number of threads, or if the partition sizes are heavily skewed (i.e., one partition has a large fraction of all tuples). Therefore, to fully utilize modern multi- and many-core CPUs, which often have dozens of cores, the simple *inter-partition* parallelism approach alone is not sufficient. For some queries, it is additionally necessary to support *intra-partition* parallelism, i.e., to parallelize within hash groups.

We use intra-partition parallelism only for large hash groups. When there are enough hash groups for the desired number of threads and none of these hash groups is too large, inter-partition parallelism is sufficient and most efficient. Since the sizes of all hash groups are known after the partitioning phase, we can dynamically assign each hash group into either the inter- or the intra-partition parallelism class. This classification takes the size of the hash group, the total amount of work, and the number of threads into account. In Figure 5.3, intra-partition parallelism is only used for hash group 11, whereas the other hash groups use inter-partition parallelism. Our approach is resistant to skew and always utilizes the available hardware parallelism while ex-

Furthermore, all types conceptually have a fixed size (variable-length types like strings are stored as pointers), which allows the partitioning and sorting phases to work on the tuples directly instead of pointers.

ploiting low-overhead inter-partition parallelism when possible.

When intra-partition parallelism is used, a parallel sorting algorithm must be used. Additionally, the window function evaluation phase itself must be parallelized, as we describe in the next section.

5.4 Window Function Evaluation

As mentioned before, some window functions are affected by framing and some ignore it. Consequently, their implementations are quite different and we discuss them separately. We start with those window functions that are affected by framing.

5.4.1 Basic Algorithmic Structure

After the partitioning and sorting phases, all tuples that have the same partitioning key are stored adjacently, and the tuples are sorted by the `order by` expressions. Based on this representation, window function evaluation can be performed in parallel by assigning different threads to different subranges of the hash group. In single-threaded execution or with inter-partition parallelism the entire hash group is assigned to one thread.

To compute a window function, the following steps are necessary for each tuple:

1. determine partition boundaries
2. determine window frame
3. compute window function over the frame and output tuple

The first step, computing the partition boundaries, is necessary because a hash group can contain multiple (logical) partitions, and is done using binary search. The two remaining steps, determining the window frame bounds and window function evaluation, which is the main algorithmic challenge, are discussed in the following two sections.

Figure 5.4 shows the algorithmic template for window functions that are affected by framing in more detail. The code computes the result for a sub-range in a hash group (from `begin` below `end`). This interface allows one to parallelize window function evaluation within a hash group by assigning threads to different ranges, e.g., using a `parallel_for` construct that dynamically distributes the range of values between threads. In single-threaded execution, `begin` and `end` can be set to the start and end of the hash group. Since a hash group can contain multiple partitions, the code starts by computing the partition bounds (line 2 and 3), and then updates them as needed (lines 5, 6, and 7). In line 10 one of the aggregation algorithms in Section 5.4.3 can be used.

```
evalOverFrame(begin, end)
   pBegin = findPartitionBegin(0, begin+1)
   pEnd = findPartitionEnd(begin)
   for (pos from begin below end)
      if (pos = pEnd)
         pBegin = pos
         pEnd = findPartitionEnd(pos)
      wBegin = findWindowBegin(pos,pBegin)
      wEnd = findWindowEnd(pos, pEnd)
      result[pos] = eval(wBegin, wEnd)
```

Figure 5.4: Basic code structure for window functions with framing

5.4.2 Determining the Window Frame Bounds

For window functions that are affected by framing, for each tuple it is necessary to determine the indexes of the window frame bounds. Since we store the tuples in arrays, the tuples in the frame can then easily be accessed. The implementation of `rows` mode is obvious and fast; one simply needs to add/subtract the index of the current row to the bounds while ensuring that the bounds remain in the current partition.

`range` mode is slightly more complicated. If the bounds are constant, one can keep track of the previous window and advance the start and end window one-by-one as needed[10]. It is clear that the frame start only advances by at most n rows in total (and analogously for the frame end). Therefore, the complexity for finding the frame for n tuples is $O(n)$. If, in `range` mode, the bounds are not constant, the window can grow and shrink arbitrarily. For this case, the solution is to first add/subtract the bounds from the current ordering key, and then to use binary search which results in a complexity of $O(n \log n)$. The complexity of computing the window frame for n rows can be summarized as follows:

mode	constant	non-constant
`rows`	$O(n)$	$O(n)$
`range`	$O(n)$	$O(n \log n)$

5.4.3 Aggregation Algorithms

Once the window frame bounds have been computed for a particular tuple, the final step is to evaluate the desired window function on that frame. For the navigation functions `first_expr`, `last_expr`, and `nth_expr` this evaluation is simple and cheap

[10]Note that the incremental approach may lead to redundant work during intra-partition parallelism and with large frame sizes. Thus, to achieve better scalability with intra-partition parallelism, binary search should be employed even for constant frame bounds.

($O(1)$), because these functions merely select one row in the window and evaluate an expression on it. Aggregate functions, in contrast, need to be (conceptually) evaluated *over all* rows of the current window, which makes them more expensive. Therefore, we present and analyze 4 algorithms with different performance characteristics for computing aggregates over window frames.

Naïve Aggregation

The naïve approach is to simply loop over all tuples in the window frame and compute the aggregate. The inherent problem of this algorithm is that it often performs redundant work, resulting in quadratic runtime. In a running-sum query like `sum(b) over (order by a rows between unbounded preceding and current row)`, for example, for each row of the input relation all values from the first to the current row are added—each time starting anew from the first row, and doing the same work all over again.

Cumulative Aggregation

The running-sum query suggests an improved algorithm, which tries to avoid redundant work instead of recomputing the aggregate from scratch for each tuple. The cumulative algorithm keeps track of the previous aggregation result and previous frame bounds. As long as the window grows (or does not change), only the additional rows are aggregated using the previous result. This algorithm is used by PostgreSQL and works well for some frequently occurring queries, e.g., the default framing specification (`range between unbounded preceding and current row`).

However, this approach only works well as long as the window frame grows. For queries where the window frame can both grow and shrink (e.g., `sum(b) over (order by a rows between 5 preceding and 5 following)`), one can still get quadratic runtime, because the previous aggregate must be discarded every time.

Removable Cumulative Aggregation

The removable cumulative algorithm, which is used by some commercial database systems, is a further algorithmic refinement. Instead of only allowing the frame to grow before recomputing the aggregate, it permits removal of rows from the previous aggregate. For the `sum`, `count`, and `avg` aggregates, removing rows from the current aggregate can easily be achieved by subtracting. For the `min` and `max` aggregates, it is necessary to maintain an ordered search tree of all entries in the previous window. For each tuple this data structure is updated by adding and removing entries as necessary, which makes these aggregates significantly more expensive.

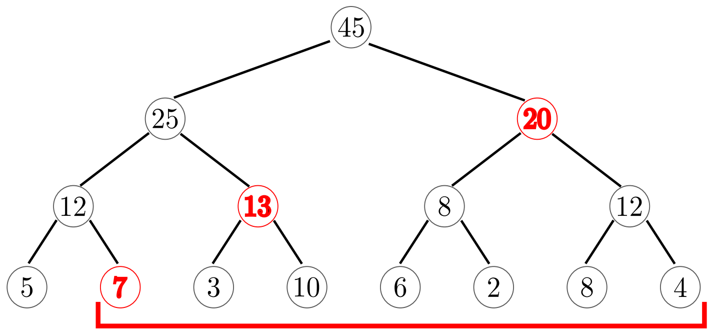

Figure 5.5: Segment Tree for `sum` aggregation. Only the red nodes (7, 13, 20) have to be aggregated to compute the sum of 7, 3, 10, 6, 2, 8, 4

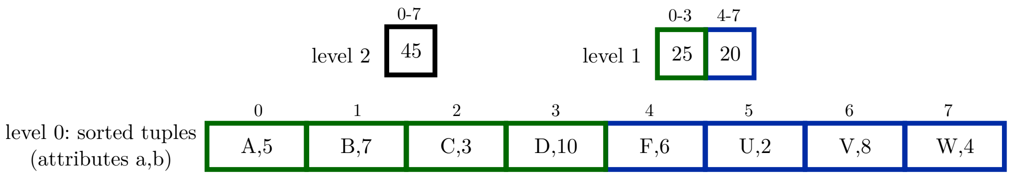

Figure 5.6: Physical Segment Tree representation with fanout 4 for `sum(b) over (order by a)`

The removable cumulative approach works well for many queries, in particular for `sum` and `avg` window expressions, which are more common than `min` or `max` in window expressions. However, queries with non-constant frame bounds (e.g., `sum(b) over (order by a rows between x preceding and y following)`) can be a problem: In the worst case, the frame bounds vary very strongly between neighboring tuples, such that the runtime becomes $O(n^2)$.

Segment Tree Aggregation

As we saw in the previous section, even the removable cumulative algorithm can result in quadratic execution time because caching the result of the previous window does not help when the window frame changes arbitrarily for each tuple. We therefore introduce an additional data structure, the Segment Tree, which allows evaluating an aggregate over an arbitrary frame in $O(\log n)$. The Segment Tree stores aggregates for sub ranges of the entire hash group, as shown in Figure 5.5. In the figure `sum` is used as the aggregate, thus the root node stores the sum of all leaf nodes. The two children of the root store the sums for two equi-width sub ranges, and so on. The Segment Tree allows computing the aggregate over an arbitrary range in logarithmic time by using the associativity of aggregates. For example, to compute the sum for the last 7 values of the sequence, we need to compute the sum of the red nodes 7, 13, and 20.

For illustration purposes, Figure 5.5 shows the Segment Tree as a binary tree with

```
1  traverseSTree(levels, begin, end)
2     agg = initAggregate()
3     for (level in levels)
4        parentBegin = begin / fanout
5        parentEnd = end / fanout
6        if (parentBegin = parentEnd)
7           for (pos from begin below end)
8              agg = aggregate(level[pos])
9           return agg
10       groupBegin = parentBegin * fanout
11       if (begin != groupBegin)
12          limit = groupBegin + fanout
13          for (pos from begin below limit)
14             agg = aggregate(level[pos])
15          parentBegin = parentBegin + 1
16       groupEnd = parentEnd * fanout
17       if (end != groupEnd)
18          for (pos from groupEnd below end)
19             agg = aggregate(level[pos])
20       begin = parentBegin
21       end = parentEnd
```

Figure 5.7: Aggregating from `begin` below `end` using a Segment Tree

pointers. In fact, our implementation stores all nodes of each tree level in an array and without any pointers, as shown in Figure 5.6. In this compact representation, which is similar to that of a standard binary heap, the tree structure is implicit and the child and parent of a node can be determined using arithmetic operations. Furthermore, to save even more space, the lowest level of the tree is the sorted input data itself, and we use a larger fanout (4 in the figure). These optimizations make the additional space consumption for the Segment Tree negligible. Additionally, the higher fanout improves performance, as we show in an experiment that is described in Section 5.6.7.

In order to compute an aggregate for a given range, the Segment Tree is traversed bottom up starting from *both window frame bounds*. Both traversals are done simultaneously until the traversals arrive at the same node. As a result, this procedure stops early for small ranges and always aggregates the minimum number of nodes.

The pseudo code in Figure 5.7 computes the aggregate for the range from `begin` below `end` using a Segment Tree. Line 3 loops over the levels of the Segment Tree starting at the bottom-most level and proceeding upwards. In line 4 and 5 the parent entries of `begin` and `end` are computed using integer division, which can be implemented as bit shifting if fanout is a power of 2. If the parent entries are equal, the range of values between `begin` and `end` is aggregated and the search terminates (lines 6-9). Otherwise, the search continues at the next level with the parent nodes becoming

`rows between ...`	Case
`1 preceding and current row`	1
`unbounded preceding and current row`	2
`CONST preceding and CONST following`	3
`VAR preceding and VAR following`	4

Case	Naïve	Cumulative	Removable Cumulative	Segment Tree
1	$O(n)$	$O(n)$	$O(n)$	$O(n \log n)$
2	$O(n^2)$	$O(n)$	`sum`: $O(n)$, `min`: $O(n \log n)$	$O(n \log n)$
3	$O(n^2)$	$O(n^2)$	`sum`: $O(n)$, `min`: $O(n \log n)$	$O(n \log n)$
4	$O(n^2)$	$O(n^2)$	`sum`: $O(n^2)$, `min`: $O(n^2 \log n)$	$O(n \log n)$

Table 5.1: Worst-case complexity of computing aggregates for n tuples

the new `begin` and `end` boundaries. It is first necessary, however, to aggregates any "protruding" values at the current level (lines 10-18).

In addition to improving worst-case efficiency, another important benefit of the Segment Tree is that it allows parallelizing arbitrary aggregates, even for running sum queries like `sum(b) over (order by a rows between unbounded preceding and current row)`. This is particularly important for queries without a partitioning clause, which can only use intra-partition parallelism to avoid executing this phase of the algorithm serially. The Segment Tree itself can easily be constructed in parallel and without any synchronization, in a bottom-up fashion: All available threads scan adjacent ranges of the same Segment Tree level (e.g., using a `parallel_for` construct) and store the computed aggregates into the level above it.

For aggregate functions like `min`, `max`, `count`, and `sum`, the Segment Tree uses the obvious corresponding aggregate function. For derived aggregate functions like `avg` or `stddev`, it is more efficient to store all needed values (e.g., the sum and the count) in the same Segment Tree instead of having two such trees. Interestingly, besides efficient aggregation, the Segment Tree is also useful for parallelizing the `dense_rank` function, which computes a rank without gaps. To compute the `dense_rank` of a particular tuple, the number of distinct values that precede this tuple must be known. A Segment Tree where each segment counts the number of distinct child values is easy to construct[11], and allows threads to work in parallel on different ranges of the partition.

Algorithm Choice

Table 5.1 summarizes the worst-case complexities of the 4 algorithms. The naïve algorithm results in quadratic runtime for many common window function queries. The cumulative algorithm works well as long as the window frame only grows. Additionally, queries with frames like `current row and unbounded following` or `1 preceding and unbounded following` can also be executed efficiently using the cumulative algorithm by first reversing the sort order. The removable algorithm further expands the set of queries that can be executed efficiently, but requires an additional ordered tree structure for `min` and `max` aggregates and can still result in quadratic runtime if the frame bounds are not constant.

Therefore, the analysis might suggest that the Segment Tree algorithm should always be chosen, as it avoids quadratic runtime in all cases. However, for many simple queries like `rows between 1 preceding and current row`, the simpler algorithms perform better in practice because the Segment Tree can incur a significant overhead both for constructing and traversing the tree structure. Intuitively, the Segment Tree approach is only beneficial if the frame frequently changes by a large amount in comparison with the previous tuple's frame. Unfortunately, in many cases, the optimal algorithm cannot be chosen based on the query structure alone, because the data distribution determines whether building a Segment Tree will pay off. Furthermore, choosing the optimal algorithm becomes even more difficult when one also considers parallelism, because, as mentioned before, the Segment Tree algorithm *always* scales well in the intra-partition parallelism case whereas the other algorithms do not.

Fortunately, we have found that the majority of the overall query time is spent in the partitioning and sorting phases (cf. Figure 5.2 and Figure 5.13), thus erring on the side of the Segment Tree is always a safe choice. We therefore propose an opportunistic approach: A simple algorithm like cumulative aggregation is only chosen when there is no risk of $O(n^2)$ runtime *and* no risk of insufficient parallelism. This method only uses the static query structure, and does not rely on cardinality estimates from the query optimizer. A query like `sum(b) over (order by a rows between unbounded preceding and current row)`, for example, can always safely and efficiently be evaluated using the cumulative algorithm. Additionally, we choose the algorithm for inter-partition parallelism and the intra-partition parallelism hash groups separately. For example, the small hash groups of a query might use the cumulative algorithm, whereas the large hash groups might be evaluated using the Segment Tree to make sure evaluation scales well. This approach always avoids quadratic run-

[11] Each node of the Segment Tree for `dense_rank` stores the number of distinct values for its segment. To combine two adjacent segments, one simply needs to add their distinct value counts and subtract 1 if the neighboring tuples are equal. Note that the Segment Tree is only used for computing the first result.

```
1  //rank of the current row with gaps
2  rank(begin, end)
3     pBegin = findPartitionBegin(0, begin+1)
4     pEnd = findPartitionEnd(begin)
5     p=findFirstPeer(pBegin,begin)-pBegin+1
6     result[begin] = p
7     for (pos from begin+1 below end)
8        if (pos = pEnd)
9           pBegin = pos
10          pEnd = findPartitionEnd(pos)
11       if (isPeer(pos, pos-1))
12          result[pos] = result[pos-1]
13       else
14          result[pos] = pos-pBegin+1
```

Figure 5.8: Pseudo code for the `rank` function, which ignores framing

time, scales well on systems with many cores, while achieving optimal performance for many common queries.

5.4.4 Window Functions without Framing

Window functions that are not affected by framing are less complicated than aggregates as they do not require any complex aggregation algorithms and do not need to compute the window frame. Nevertheless, the high-level structure is similar due to supporting intra-partition parallelism and the need to compute partition boundaries. Generally, the implementation on window functions that are not affected by framing consists of two steps: In the first step, the result for the first tuple in the work range is computed. In the second step, the remaining results are computed sequentially by using the previously computed result.

Figure 5.8 shows the pseudo code of the `rank` function, which we use as an example. To compute the rank of an arbitrary tuple at index `begin`, the index of the first peer is computed using binary search (done by `findFirstPeer` in line 5). All tuples that are in the same partition and have the same order by key(s) are considered peers. Given this first result, all remaining rank computations can then assume that the previous rank has been computed (lines 10-13). All window functions without framing are quite cheap to compute, since they consist of a sequential scan that only looks at neighboring tuples.

Figure 5.9 shows additional examples for window functions that are always evaluated on the entire partition. Most of the remaining functions have a structure similar to one of these examples.

```
// the row number
row_number(begin, end)
   pBegin = findPartitionBegin(0, begin+1)
   pEnd = findPartitionEnd(begin)
   for (pos from begin below end)
      if (pos = pEnd)
         pBegin = pos
         pEnd = findPartitionEnd(pos)
      result[pos] = pos-pBegin+1

//relative rank
percent_rank(begin, end)
   pBegin = findPartitionBegin(0, begin+1)
   pEnd = findPartitionEnd(begin)
   firstPeer = findFirstPeer(pBegin, begin)
   rank = (firstPeer-pBegin)+1
   pSize = pEnd - pBegin
   result[begin] = (rank-1) / (pSize-1)
   for (pos from begin+1 below end)
      if (pos = pEnd)
         pBegin = pos
         pEnd = findPartitionEnd(pos)
         pSize = pEnd-pBegin
      if (isPeer(pos, pos-1))
         result[pos] = result[pos-1]
      else
         rank = pos+1
         result[pos] = (rank-1) / (pSize-1)

// evaluate expr at preceding row
lag(expr, offset, default, begin, end)
   pBegin = findPartitionBegin(0, begin+1)
   pEnd = findPartitionEnd(begin)
   for (pos from begin below end)
      if (pos = pEnd)
         pBegin = pos
         pEnd = findPartitionEnd(pos)
      if (pos-offset < pBegin)
         result[pos] = default
      else
         result[pos] = expr(pos-offset)
```

Figure 5.9: Pseudo code for the `row_number`, `percent_rank`, and `lag` window functions, which ignore framing

5.5 Database Integration

In this section we describe how to integrate the algorithm described above and further optimizations and use cases.

5.5.1 Query Engine

Our window function algorithm can be integrated into different database query engines, including query engines that use the traditional tuple-at-a-time model (Volcano iterator model), vector-at-a-time execution [20], or push-based query compilation [139]. Of course, the code structure heavily depends on the specific query engine. The pseudo code in Figure 5.8 is very similar to the code generated by our implementation, which is integrated into HyPer and uses push-based query compilation.

The main difference is that in our implementation and in contrast to the pseudo code shown, we do not store the computed result in a vector (lines 6,12,14), but directly push the tuple to the next operator. This is both faster and uses less space. Also note that, regardless of the execution model, the window function operator is a full pipeline breaker, i.e., it must consume all input tuples before it can produce results. Only during the final window function evaluation phase, can tuples be produced on the fly.

The parallelization strategy described in Section 5.3 also fits into HyPer's parallel execution framework, which breaks up work into constant-sized work units ("morsels"). These morsels are scheduled dynamically using work stealing, which allows distributing work evenly between the cores and to quickly react to workload changes. The morsel-driven approach can be used for the initial partitioning and copying phases, as well as the final window function computation phase.

5.5.2 Multiple Window Function Expressions

For simplicity of presentation, we have so far assumed that the query contains only one window function expression. Queries that contain multiple window function expressions, can be computed by adding successive window operators for each expression. HyPer currently uses this approach, which is simple and general but wastes optimization opportunities for queries where the partitioning and ordering clauses are shared between multiple window expressions. Since partitioning and sorting usually dominate the overall query execution time, avoiding these phases can be very beneficial.

Cao et al. [26] discuss optimizations that avoid unnecessary partitioning and sorting steps in great detail. In our compilation-based query engine, the final evaluation phase (as shown in Figure 5.8), could directly compute all window expressions with shared partitioning/ordering clauses. We plan to incorporate this feature into HyPer in the future.

5.5.3 Ordered-Set Aggregates

Ordered-set aggregates are an SQL feature that allows one to compute common summary statistics like median and mode. The following example query computes the mode of the column a[12] for each group of b:

```
select b, mode() within group (order by a)
from r
group by b
```

Another use case is to compute percentiles using percentile_disc(fraction) or percentile_cont(fraction). The first is the discrete variant, which can be used for arbitrary data types, whereas the latter version is continuous and linearly interpolates when the number of entries is even. The parameter fraction specifies the desired percentile (from 0 to 1). A fraction of 0.5 thus computes the median.

Semantically, ordered-set aggregates are a mix between window functions and normal aggregates. Like normal aggregates, they only produce one result per group. Like window functions, they require full materialization (and sorting) of the input tuples. In systems like HyPer that rely on hash-based (not sort-based) aggregation, one elegant way to implement ordered-set aggregates is by combining both operators. In this approach mode, percentile_disc, and percentile_cont are implemented as window functions. The group by operator receives this result and aggregates it. In effect, the example query is rewritten as follows:

```
select b, any(m)
from (select b, mode() over (partition by b order by a) m
      from r)
group by b
```

Note that in this approach the window function operator is placed *below* the aggregation, whereas normally it must be placed above it. The additional overhead of the aggregation is usually very small, as the tuples arrive at the aggregation in an order that makes pre-aggregation very effective.

5.6 Evaluation

We have integrated the window operator into HyPer. In this section, we experimentally evaluate our implementation and compare its performance with other systems.

[12]Only one attribute can be specified in the order by clause.

5.6.1 Implementation

HyPer uses the data-centric query compilation approach for query processing [139, 142]. Therefore, our implementation of the window operator is a compiler that uses the LLVM compiler infrastructure to generate machine code for arbitrary window function queries instead of directly computing them "iterator style". One great advantage of compilation is that it allows omitting steps of an algorithm that may be necessary in general but not needed for a particular query. For example, if the framing end is set to `unbounded following`, it never changes within a partition. Therefore, there is no need to generate code that recomputes the frame end for each tuple. Due to its versatile nature, the window function operator offers many opportunities like this for "optimizing away" unnecessary parts of the algorithm. However, it would also be possible to integrate our algorithm into iterator-based or vectorized [20] query engines.

For sorting large hash groups (intra-partition parallelism), we use the parallel multi-way merge sort implementation from the GNU libstdc++ library ("Parallel Mode") [154].

5.6.2 Experimental Setup

We initially experimented with the TPC-DS benchmark, which contains some queries with window functions. However, in these queries expensive joins dominate and the window expressions are quite simple (no framing clauses). Therefore, in this evaluation, we use a synthetically-generated data set which allows us to evaluate our implementation under a wide range of query types and input distributions. Most queries are executed with 10 million input tuples that consist of two 8-byte integer columns, named `a` and `b`. The values of `b` are uniformly distributed and unique, whereas the number of unique values and the distribution of `a` differs between the experiments.

The experiments were performed on a system with an Intel Core i7 3930K processor, which has 6 cores (12 hardware threads) at 3.2 GHz and 3.8 GHz turbo frequency. The system has 12 MB shared, last-level cache and quad-channel DDR3-1600 RAM. We used Linux as operating system and GCC 4.9 as compiler.

For comparison, we report results for a number of database systems with varying degrees of window function support. Vectorwise (version 2.5) is very fast in comparison with other commercial systems, but has limited support for window functions (framing is not supported). PostgreSQL 9.4 is slower than Vectorwise but offers more complete support (`range` mode support is incomplete and non-constant frame bounds are not supported). Finally, we also experimented with a commercial system (labeled "DBMS") that has full window function support.

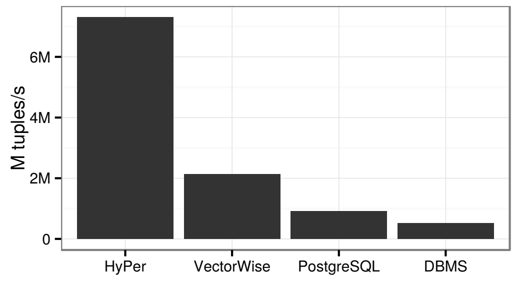

Figure 5.10: Single-threaded performance of `rank` query (with 100 partitions)

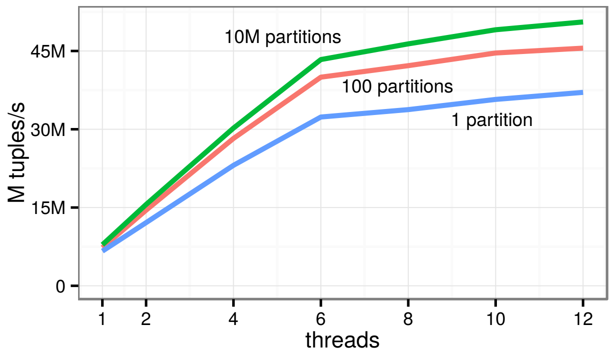

Figure 5.11: Scalability of `rank` query

5.6.3 Performance and Scalability

To highlight the properties of our algorithm, we initially use the following ranking query:

```
select rank() over (partition by a order by b) from r
```

Figure 5.10 compares the performance of the ranking query. HyPer is 3.4× faster than Vectorwise, 8× faster than PostgreSQL, and 14.1× faster than the commercial system. Note that we used single-threaded execution in this experiment, because PostgreSQL does not support intra-query parallelism at all and Vectorwise does not support it for the window operator. Other window functions that, like `rank`, are also not affected by framing have similar performance; only aggregation functions with frames can be significantly more expensive (cf., Figure 5.15).

In the next experiment, we look at the scalability of our implementation. We used different distributions for attribute `a` creating 10 million partitions, 100 partitions, or only 1 partition. The partitions have approximately the same size, so our algorithm chooses inter-partition parallelism with 10 million and 100 partitions, and intra-partition parallelism with 1 partition. Figure 5.11 shows that our implementation scales almost linearly up to 6 threads. After that, HyperThreading gives an additional performance boost.

	10M partitions		100 partitions		1 partition	
	time	speedup	time	speedup	time	speedup
phase	[ms]		[ms]		[ms]	
partition	46	2.5×	32	2.9×	32	2.3×
sort	139	7.7×	184	6.7×	198	6.9×
rank	12	7.0×	6	5.9×	10	7.4×
= total	197	6.5×	223	6.2×	239	6.3×

Table 5.2: Performance and scalability for the different phases of the window operator (`rank` query)

5.6.4 Algorithm Phases

To better understand the behavior of the different phases of our algorithm, we measured the runtime with 12 threads and the speedups over single-threaded execution for the three phases of our algorithm. The results are shown in Table 5.2. The overall speedup is over 6× for all data distributions, which is a very good result with 6 cores and 12 HyperThreads. The majority of the query execution time is spent in the sorting and partitioning phases, because the evaluation of the `rank` function consists of a very fast and simple sequential scan. The table also shows that, all else being equal, input distributions with more partitions result in higher overall performance. This is because sorting becomes significantly more expensive with larger partitions due to both asymptotic and caching reasons. The partitioning phase, on the other hand, becomes only slightly more expensive with many partitions since we only partition into 1024 hash groups, which is always very efficient.

When many threads are used for the partitioning phase, the available memory bandwidth is exhausted, which explains the slightly lower speedup during partitioning. Of course, systems with higher memory bandwidth can achieve higher speedups. We also experimented with tuples larger than 16 bytes, which increases execution time due to higher data movement costs. However, the effect is not linear; using 64-byte tuples instead of 16-byte tuples reduces performance by 1.6×.

5.6.5 Skewed Partitioning Keys

In the previous experiments, each query used either inter-partition parallelism (100 or 10M partitions) or intra-partition parallelism (1 partition), but never a combination of the two. To show that inter-partition parallelism alone is not sufficient, we created an extremely skewed data set where 50% of all tuples belong to the largest partition, 25% to the second largest, and so on. Despite the fact that there are more partitions than threads, when we enforced inter-partition parallelism alone, we achieved a speedup of only 1.9× due to load imbalances. In contrast, when we enabled our automatic

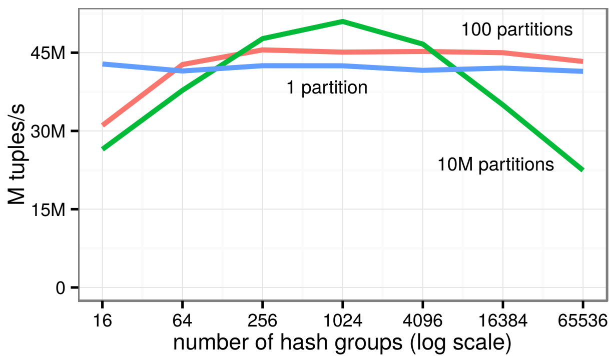

Figure 5.12: Varying the number of hash groups for `rank` query.

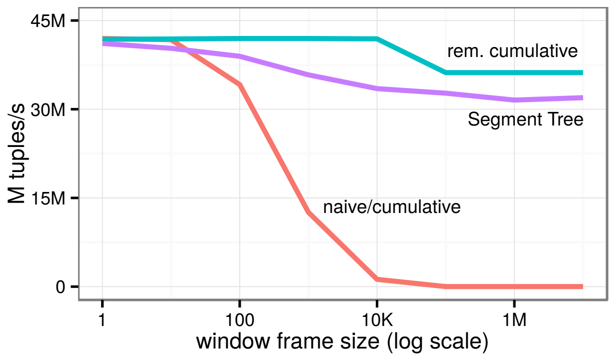

Figure 5.13: Performance of `sum` query with constant frame bounds for different frame sizes

classification scheme that uses intra-partition parallelism for the largest partitions and inter-partition parallelism for the smaller partitions we measured a speedup of 5.9×.

5.6.6 Number of Hash Groups

So far, all experiments used 1024 hash groups. Figure 5.12 shows the overall performance of the `rank` query with a varying number of hash groups. Having more hash groups can result in slower partitioning due to cache and TLB misses but faster sorting due to smaller partitions. Using 1024 hash groups results in performance close to optimal regardless of the number of partitions, because on modern x86 CPUs 1024 is small enough to allow for very cache- and TLB-friendly partitioning. Therefore, we argue that there is no need to rely on the query optimizer to choose the number of hash groups, and a value around 1024 generally seems to be a good setting.

5.6.7 Aggregation with Framing

In the next experiment, we investigate the performance characteristics of the 4 different aggregation algorithms, which we implemented in C++ for this experiment because HyPer only implements the cumulative and the Segment Tree algorithm. Using 12 threads, we execute the following query with different constants for the placeholder:

```
select sum(a) over
   (order by b
    rows between ? preceding and current row)
from r
```

By using different constants, we obtain queries with different frame sizes (from 1 tuple to 10M tuples). The frame "lags behind" the current row and should therefore be ideal for the removable cumulative aggregation algorithm, whereas the naïve and cumulative algorithms must recompute the result for each tuple.

Figure 5.13 shows that for very small frame sizes (<10 tuples), even the simple naïve and cumulative algorithms perform very well. The Segment Tree approach is slightly slower in this range of frame sizes as it must pay the price of initially constructing the tree that is quite useless for such small frames. However, the overhead is quite small in comparison with the sorting and partitioning phases which dominate the execution time. For larger window sizes (10 to $10,000$ tuples), the naïve and cumulative algorithms become very slow due to their quadratic behavior in this query. This also happens when we run such queries in PostgreSQL (not shown in the graph), which uses the cumulative algorithm.

As expected, the removable cumulative algorithm has good performance for the entire range, as the amount of work per tuple is constant and no ordered tree is necessary because the aggregation is a sum and not a minimum or maximum. However, for very large window sizes (>10,000 tuples), where the query, in effect, becomes a running sum over the entire partition, the removable cumulative algorithm does not scale and becomes as slow as single-threaded execution. The reason is that each thread must initially compute a running sum over the majority of all preceding tuples. We repeated this experiment on a 60-core system, where the Segment Tree algorithm surpasses the removable cumulative algorithm for large frames with around 20 threads. The performance of Segment Tree traversal cost decreases only slightly with increasing frame sizes and is always high.

In the previous experiment, for each query the frame bound was a constant. In the experiment shown in Figure 5.14, the frame bound is an expression that depends on the current row and varies very strongly in comparison with the previous frame bound. Nevertheless, the Segment Tree algorithm performs well even for large and extremely fluctuating frames. The performance of the other algorithms, in contrast, approaches 0 tuples/s for larger frame sizes due to quadratic behavior. We observed the same

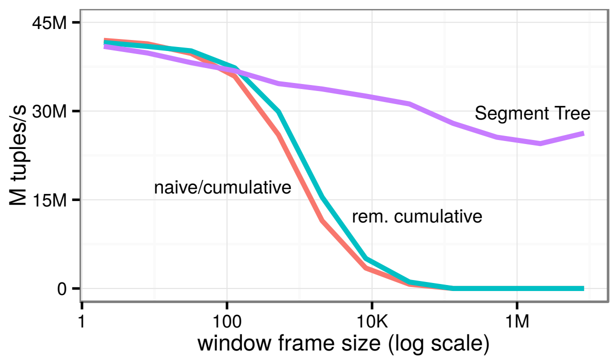

Figure 5.14: Performance of `sum` query with variable frame bounds for different frame sizes

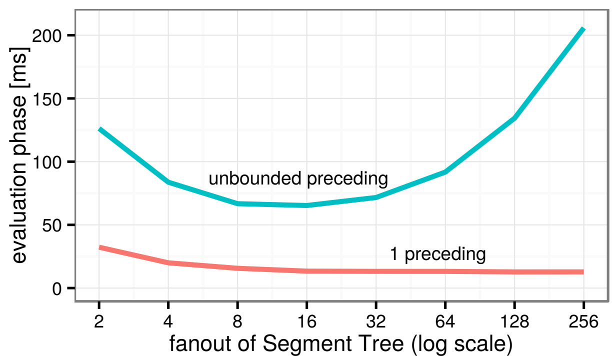

Figure 5.15: Segment Tree performance for `sum` query under varying fanout settings

behavior with the commercial database system, whereas PostgreSQL does not support such queries at all.

To summarize, the Segment Tree approach usually has higher overhead than the simpler algorithms, and it certainly makes sense to choose a different algorithm *if* the query structure allows one to statically determine that this is beneficial. However, this not possible for many queries. The Segment Tree has the advantage of being very robust in all cases, and is dominated by the partitioning and sorting phases for all possible frame sizes. Additionally, the Segment Tree always scales very well, whereas the other approaches cannot scale for large window sizes, which becomes more important on large systems with many cores.

5.6.8 Segment Tree Fanout

The previous experiments used a Segment Tree fanout of 16. The next experiment investigates the influence of the fanout of the Segment Tree on the performance of aggregation and tree construction. Figure 5.15 uses the same `sum` query as before but varies the fanout of the Segment Tree for two very extreme workloads. The time shown includes both the window function evaluation and Segment Tree construction. For queries where the frame size is very small (cf., curve labeled as "1 preceding"), using a higher fanout is always beneficial. The reason is that such queries build a Segment Tree but do not actually use it during aggregation due to the small frame size. For queries with large frames (cf., curve labeled as "unbounded preceding"), a fanout of around 16 is optimal. For both query variants, the Segment Tree construction time alone (without evaluation, not shown in the graph) starts at 23ms with a fanout of 2 and decreases to 5ms with a fanout of 16 or higher.

Another advantage of a higher fanout is that the additional space consumption for the Segment Tree is reduced. For the example query, the input tuples use around 153 MB. The additional space overhead for the Segment Tree with a fanout of 2 is 76 MB (50%). The space consumption is reduced to 5 MB (3.3%) with a fanout of 16, and to 0.6 MB (0.4%) with a fanout of 128. Thus, a value close to 16 generally seems to be a good setting that offers a good balance between space consumption and performance.

5.7 Related Work

Window functions were introduced as an (optional) amendment to SQL:1999 and were finally fully incorporated into SQL:2003 [186]. SQL:2011 added support for window functions for referring to neighboring tuples in a window frame. Oracle has been the first database system to implement window function support in 1999, followed by IBM DB2 LUW in 2000. Successively, all major commercial and open source database systems, including Microsoft SQL Server (in 2005), PostgreSQL (in 2009), and SAP HANA followed[13].

As mentioned before, we feel there is a gap between the importance of window functions in practice and the amount of research on this topic in the database systems community, for example in comparison with other analytic SQL constructs like rollup and cube [61]. An early Oracle technical report [14] contains motivating query examples, optimization opportunities, and parallel execution strategies for window functions. In a more recent paper, Bellamkonda et al. [15] observed that using partitioning only to achieve good scalability is not sufficient if the number of distinct groups is lower than the desired degree of parallelism. They proposed to artificially enlarge the partitioning key with additional attributes ("extended distribution keys") to achieve a larger number of partitions and therefore increased parallelism. However, this approach incurs additional work due to having an additional window consolidator phase and relies on cardinality estimates. We sidestep these problems by directly and fully parallelizing

[13]Two widely-used systems that do not yet offer window function support are MySQL/MariaDB and SQLite.

each phase of the window operator and by using intra-partition parallelism when necessary.

There are a number of query optimization papers that relate to the window operator. Cao et al. [26] focus on optimizing multiple window functions occurring in one query. They found that often the majority of the execution time for the window operator is spent in the partitioning and sorting phases. Therefore, it is often possible to avoid some of the partitioning and/or sorting work by optimizing the order of the window expressions. The paper shows that finding the optimal sequence is NP-hard and presents a useful heuristic algorithm for this problem. Though the window operator is very useful its own right, other papers [188, 13] propose to introduce window expressions for de-correlating subqueries. In such scenarios, a fast implementation of the window operator is important even for queries that do not originally contain window functions. Due to a different approach for unnesting [141], HyPer currently does not introduce window operators when unnesting queries. In the future, we plan to investigate whether might be beneficial with our approach. Window functions have also been used to speed up the translation of XQuery to SQL [18].

Yang and Widom [182] introduced the Segment B-Tree for temporal aggregation, which is very similar to our Segment Tree except that we do not need to handle updates and can therefore represent the structure more efficiently without pointers.

5.8 Summary

We have presented an algorithm for window function computation that is very efficient in practice and avoids quadratic runtime in all cases. Furthermore, we have shown how to execute window functions in parallel on multi-core CPUs, even when the query has no partitioning clause. We have demonstrated both the high performance and the excellent scalability in a number of experiments that cover very different query types and input distributions.

6 Evaluation of Join Order Optimization for In-Memory Workloads

Parts of this chapter have previously been published in [107].

6.1 Introduction

The problem of finding a good join order is one of the most studied problems in the database field. Figure 6.1 illustrates the classical, cost-based approach, which dates back to System R [161]. To obtain an efficient query plan, the query optimizer enumerates some subset of the valid join orders, for example using dynamic programming. Using cardinality estimates as its principal input, the cost model then chooses the cheapest alternative from semantically equivalent plan alternatives.

Theoretically, as long as the cardinality estimations and the cost model are accurate, this architecture obtains the optimal query plan. In reality, cardinality estimates are usually computed based on simplifying assumptions like uniformity and independence. In real-world data sets, these assumptions are *frequently* wrong, which may lead to sub-optimal and sometimes disastrous plans.

In this chapter we investigate the three main components of the classical query optimization architecture in order to answer the following questions:

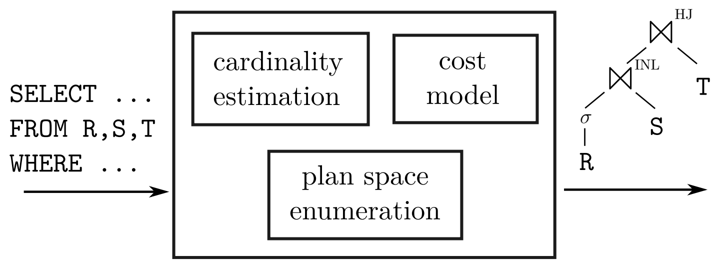

Figure 6.1: Traditional query optimizer architecture

- How good are cardinality estimators and when do bad estimates lead to slow queries?
- How important is an accurate cost model for the overall query optimization process?
- How large does the enumerated plan space need to be?

To answer these questions, we use a novel methodology that allows us to isolate the influence of the individual optimizer components on query performance. Our experiments are conducted using a real-world data set and 113 multi-join queries that provide a challenging, diverse, and realistic workload. Another novel aspect of this work is that it focuses on the increasingly common main-memory scenario, where all data fits into RAM.

The main contributions of this chapter are listed in the following:

- Based on the IMDB data set, we design a challenging workload named *Join Order Benchmark (*JOB*)*. The benchmark is publicly available to facilitate further research.
- To the best of our knowledge, we present the first end-to-end study of the join ordering problem using a real-world data set and realistic queries.
- By quantifying the contributions of cardinality estimation, the cost model, and the plan enumeration algorithm on query performance, we provide guidelines for the complete design of a query optimizer. We also show that many disastrous plans can easily be avoided.

The rest of this chapter is organized as follows: We first discuss important background and our new benchmark in Section 6.2. Section 6.3 shows that the cardinality estimators of major relational database systems produce bad estimates for many realistic queries, in particular for multi-join queries. The conditions under which these bad estimates cause slow performance are analyzed in Section 6.4. We show that it very much depends on how much the query engine relies on these estimates and on how complex the physical database design is, i.e., the number of indexes available. Query engines that mainly rely on hash joins and full table scans, are quite robust even in the presence of large cardinality estimation errors. The more indexes are available, the harder the problem becomes for the query optimizer resulting in runtimes that are far away from the optimal query plan. Section 6.5 shows that with the currently-used cardinality estimation techniques, the influence of cost model errors is dwarfed by cardinality estimation errors and that even quite simple cost models seem to be sufficient. Section 6.6 investigates different plan enumeration algorithms and shows that—despite large cardinality misestimates and sub-optimal cost models—exhaustive join order enumeration improves performance and that using heuristics leaves performance on the table. Finally, after discussing related work in Section 6.7, we present our conclusions in Section 6.8.

6.2 Background and Methodology

Many query optimization papers ignore cardinality estimation and only study search space exploration for join ordering with randomly generated, synthetic queries (e.g., [138, 47]). Other papers investigate only cardinality estimation in isolation either theoretically (e.g., [75]) or empirically (e.g., [184]). As important and interesting both approaches are for understanding query optimizers, they do not necessarily reflect real-world user experience.

The goal of this work is to investigate the contribution of all relevant query optimizer components to end-to-end query performance in a realistic setting. We therefore perform our experiments using a workload based on a real-world data set and the widely-used PostgreSQL system. PostgreSQL is a relational database system with a fairly traditional architecture making it a good subject for our experiments. Furthermore, its open source nature allows one to inspect and change its internals. In this section we introduce the Join Order Benchmark, describe all relevant aspects of PostgreSQL, and present our methodology.

6.2.1 The IMDB Data Set

Many research papers on query processing and optimization use standard benchmarks like TPC-H, TPC-DS, or the Star Schema Benchmark (SSB). While these benchmarks have proven their value for evaluating query engines, we argue that they are not good benchmarks for the cardinality estimation component of query optimizers. The reason is that in order to easily be able to scale the benchmark data, the data generators are using the very same simplifying assumptions (uniformity, independence, principle of inclusion) that query optimizers make. Real-world data sets, in contrast, are full of correlations and non-uniform data distributions, which makes cardinality estimation much harder. Section 6.3.3 shows that PostgreSQL's simple cardinality estimator indeed works unrealistically well for TPC-H. TPC-DS is slightly harder in that it has a number of non-uniformly distributed (skewed) attributes, but is still too easy due to not having correlations between attributes.

Therefore, instead of using a synthetic data set, we chose the *Internet Movie Data Base*[1] *(IMDB)*. It contains a plethora of information about movies and related facts about actors, directors, production companies, etc. The data is freely available[2] for

[1]`http://www.imdb.com/`
[2]`ftp://ftp.fu-berlin.de/pub/misc/movies/database/`

non-commercial use as text files. In addition, we used the open source *imdbpy*[3] package to transform the text files into a relational database with 21 tables. The data set allows one to answer queries like “Which actors played in movies released between 2000 and 2005 with ratings above 8?”. Like most real-world data sets IMDB is full of correlations and non-uniform data distributions, and is therefore much more challenging than most synthetic data sets. Our snapshot is from May 2013 and occupies 3.6 GB when exported to CSV files. The two largest tables, `cast_info` and `movie_info` have 36 M and 15 M rows, respectively.

6.2.2 The JOB Queries

Based on the IMDB database, we have constructed analytical SQL queries. Since we focus on join ordering, which arguably is the most important query optimization problem, we designed the queries to have between 3 and 16 joins, with an average of 8 joins per query. Query 13d, which finds the ratings and release dates for all movies produced by US companies, is a typical example:

```
SELECT cn.name, mi.info, miidx.info
FROM company_name cn, company_type ct,
     info_type it, info_type it2, title t,
     kind_type kt, movie_companies mc,
     movie_info mi, movie_info_idx miidx
WHERE cn.country_code = '[us]'
AND ct.kind = 'production companies'
AND it.info = 'rating'
AND it2.info = 'release dates'
AND kt.kind = 'movie'
AND ... -- (11 join predicates)
```

Each query consists of one select-project-join block[4]. The join graph of the query is shown in Figure 6.2. The solid edges in the graph represent key/foreign key edges ($1 : n$) with the arrow head pointing to the primary key side. Dotted edges represent foreign key/foreign key joins ($n : m$), which appear due to transitive join predicates. Our query set consists of 33 query structures, each with 2-6 variants that differ in their selections only, resulting in a total of 113 queries. Note that depending on the selectivities of the base table predicates, the variants of the same query structure have different optimal

[3] `https://bitbucket.org/alberanid/imdbpy/get/5.0.zip`

[4] Since in this work we do not model or investigate aggregation, we omitted `GROUP BY` from our queries. To avoid communication from becoming the performance bottleneck for queries with large result sizes, we wrap all attributes in the projection clause with `MIN(...)` expressions when executing (but not when estimating). This change has no effect on PostgreSQL’s join order selection because its optimizer does not push down aggregations.

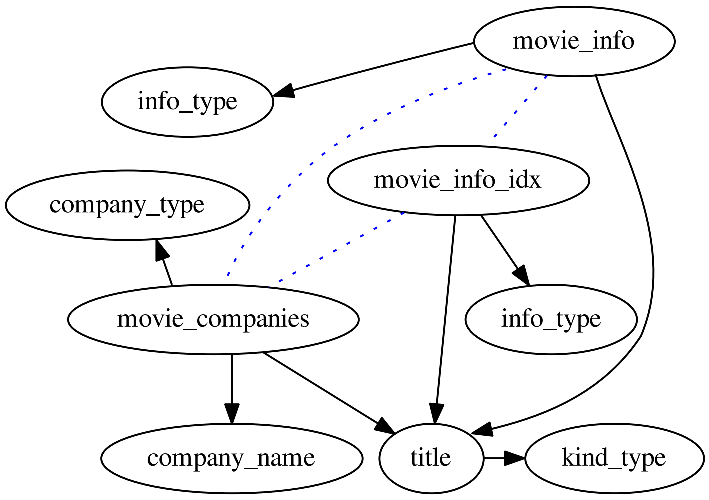

Figure 6.2: Typical query graph of our workload

query plans that yield widely differing (sometimes by orders of magnitude) runtimes. Also, some queries have more complex selection predicates than the example (e.g., disjunctions or substring search using `LIKE`).

Our queries are "realistic" and "ad hoc" in the sense that they answer questions that may reasonably have been asked by a movie enthusiast. We also believe that despite their simple SPJ-structure, the queries model the core difficulty of the join ordering problem. For cardinality estimators the queries are challenging due to the significant number of joins and the correlations contained in the data set. However, we did not try to "trick" the query optimizer, e.g., by picking attributes with extreme correlations. Also, we intentionally did not include more complex join predicates like inequalities or non-surrogate-key predicates, because cardinality estimation for this workload is already quite challenging.

We propose JOB for future research in cardinality estimation and query optimization. The query set is available online:
`http://www-db.in.tum.de/~leis/qo/job.tgz`

6.2.3 PostgreSQL

PostgreSQL's optimizer follows the traditional textbook architecture. Join orders, including bushy trees but excluding trees with cross products, are enumerated using dynamic programming. The cost model, which is used to decide which plan alternative is cheaper, is described in more detail in Section 6.5.1. The cardinalities of base tables are estimated using histograms (quantile statistics), most common values with their frequencies, and domain cardinalities (distinct value counts). These per-attribute statistics are computed by the `analyze` command using a sample of the relation. For complex predicates, where histograms can not be applied, the system resorts to ad hoc methods that are not theoretically grounded ("magic constants"). To combine conjunctive predicates for the same table, PostgreSQL simply assumes independence and multiplies the selectivities of the individual selectivity estimates.

The result sizes of joins are estimated using the formula

$$|T_1 \bowtie_{x=y} T_2| = \frac{|T_1||T_2|}{\max(\mathrm{dom}(x), \mathrm{dom}(y))},$$

where T_1 and T_2 are arbitrary expressions and $\mathrm{dom}(x)$ is the domain cardinality of attribute x, i.e., the number of distinct values of x. This value is the principal input for the join cardinality estimation. To summarize, PostgreSQL's cardinality estimator is based on the following assumptions:

- uniformity: all values, except for the most-frequent ones, are assumed to have the same number of tuples
- independence: predicates on attributes (in the same table or from joined tables) are independent
- principle of inclusion: the domains of the join keys overlap such that the keys from the smaller domain have matches in the larger domain

The query engine of PostgreSQL takes a physical operator plan and executes it using Volcano-style interpretation. The most important access paths are full table scans and lookups in unclustered B+Tree indexes. Joins can be executed using either nested loops (with or without index lookups), in-memory hash joins, or sort-merge joins where the sort can spill to disk if necessary. The decision which join algorithm is used is made by the optimizer and cannot be changed at runtime.

6.2.4 Cardinality Extraction and Injection

We loaded the IMDB data set into 5 relational database systems: PostgreSQL, HyPer, and 3 commercial systems. Next, we ran the statistics gathering command of each database system with default settings to generate the database-specific statistics (e.g., histograms or samples) that are used by the estimation algorithms. We then obtained the cardinality estimates for all intermediate results of our test queries using database-specific commands (e.g., using the `EXPLAIN` command for PostgreSQL). We will later use these estimates of different systems to obtain optimal query plans (w.r.t. respective systems) and run these plans in PostgreSQL. For example, the intermediate results of the chain query

$$\sigma_{x=5}(A) \bowtie_{A.bid=B.id} B \bowtie_{B.cid=C.id} C$$

are $\sigma_{x=5}(A)$, $\sigma_{x=5}(A) \bowtie B$, $B \bowtie C$, and $\sigma_{x=5}(A) \bowtie B \bowtie C$. Additionally, the availability of indexes on foreign keys and index-nested loop joins introduces the need for additional intermediate result sizes. For instance, if there exists a non-unique index on the foreign key $A.bid$, it is also necessary to estimate $A \bowtie B$ and $A \bowtie B \bowtie C$. The reason is that the selection $A.x = 5$ can only be applied *after* retrieving all matching tuples from the index on $A.bid$, and therefore the system produces two intermediate results, before and after the selection. Besides cardinality estimates from the different systems, we also obtain the true cardinality for each intermediate result by executing `SELECT COUNT(*)` queries[5].

We further modified PostgreSQL to enable cardinality injection of arbitrary join expressions, allowing PostgreSQL's optimizer to use the estimates of other systems (or the true cardinality) instead of its own. This allows one to directly measure the influence of cardinality estimates from different systems on query performance. Note that IBM DB2 allows a limited form of user control over the estimation process by allowing users to explicitly specify the selectivities of predicates. However, selectivity injection cannot fully model inter-relation correlations and is therefore less general than the capability of injecting cardinalities for arbitrary expressions.

6.2.5 Experimental Setup

The cardinalities of the commercial systems were obtained using a laptop running Windows 7. All performance experiments were run on a server with two Intel Xeon X5570 CPUs (2.9 GHz) and a total of 8 cores running PostgreSQL 9.4 on Linux. PostgreSQL does not parallelize queries, so that only a single core was used during query processing. The system has 64 GB of RAM, which means that the entire IMDB database is fully cached in RAM. Intermediate query processing results (e.g., hash tables) also easily fit into RAM, unless a very bad plan with extremely large intermediate results is chosen.

We set the memory limit per operator (`work_mem`) to 2 GB, which results in much better performance due to the more frequent use of in-memory hash joins instead of external memory sort-merge joins. Additionally, we set the buffer pool size (`shared_buffers`) to 4 GB and the size of the operating system's buffer cache used by PostgreSQL (`effective_cache_size`) to 32 GB. For PostgreSQL it is generally recommended to use OS buffering in addition to its own buffer pool and keep most of the memory on the OS side. The defaults for these three settings are very low (MBs, not GBs), which is why increasing them is generally recommended. Finally, by increasing the `geqo_threshold` parameter to 18 we forced PostgreSQL to always use dynamic programming instead of falling back to a heuristic for queries with more

[5]For our workload it was still feasible to do this naïvely. For larger data sets the approach by Chaudhuri et al. [32] may become necessary.

	median	90th	95th	max
PostgreSQL	1.00	2.08	6.10	207
DBMS A	1.01	1.33	1.98	43.4
DBMS B	1.00	6.03	30.2	104000
DBMS C	1.06	1677	5367	20471
HyPer	1.02	4.47	8.00	2084

Table 6.1: Q-errors for base table selections

than 12 joins.

6.3 Cardinality Estimation

Cardinality estimates are the most important ingredient for finding a good query plan. Even exhaustive join order enumeration and a perfectly accurate cost model are worthless unless the cardinality estimates are (roughly) correct. It is well known, however, that cardinality estimates are sometimes wrong by orders of magnitude, and that such errors are usually the reason for slow queries. In this section, we experimentally investigate the quality of cardinality estimates in relational database systems by comparing the estimates with the true cardinalities.

6.3.1 Estimates for Base Tables

To measure the quality of base table cardinality estimates, we use the *q-error*, which is the factor by which an estimate differs from the true cardinality. For example, if the true cardinality of an expression is 100, the estimates of 10 or 1000 both have a q-error of 10. Using the ratio instead of an absolute or quadratic difference captures the intuition that for making planning decisions only relative differences matter. The q-error furthermore provides a theoretical upper bound for the plan quality if the q-errors of a query are bounded [132].

Table 6.1 shows the 50th, 90th, 95th, and 100th percentiles of the q-errors for the 629 base table selections in our workload. The median q-error is close to the optimal value of 1 for all systems, indicating that the majority of all selections are estimated correctly. However, all systems produce misestimates for some queries, and the quality of the cardinality estimates differs strongly between the different systems.

Looking at the individual selections, we found that DBMS A and HyPer can usually predict even complex predicates like substring search using `LIKE` very well. To estimate the selectivities *for base tables* HyPer uses a random sample of 1000 rows per table and applies the predicates on that sample. This allows one to get accurate estimates for arbitrary base table predicates as long as the selectivity is not too low. When we looked at the selections where DBMS A and HyPer produce errors above 2, we found that most of them have predicates with extremely low true selectivities (e.g., 10^{-5} or 10^{-6}). This routinely happens when the selection yields zero tuples on the sample, and the system falls back on an ad-hoc estimation method ("magic constants"). It therefore appears to be likely that DBMS A also uses the sampling approach.

The estimates of the other systems are worse and seem to be based on per-attribute histograms, which do not work well for many predicates and cannot detect (anti-)correlations between attributes. Note that we obtained all estimates using the default settings after running the respective statistics gathering tool. Some commercial systems support the use of sampling for base table estimation, multi-attribute histograms ("column group statistics"), or ex post feedback from previous query runs [165]. However, these features are either not enabled by default or are not fully automatic.

6.3.2 Estimates for Joins

Let us now turn our attention to the estimation of intermediate results for joins, which are more challenging because neither sampling nor histograms work well across joins. Figure 6.3 summarizes over 100,000 cardinality estimates in a single figure. For each intermediate result of our query set, we compute the factor by which the estimate differs from the true cardinality, distinguishing between over- and underestimation. The graph shows one "boxplot" (note the legend in the bottom-left corner) for each intermediate result size, which allows one to compare how the errors change as the number of joins increases. The vertical axis uses a logarithmic scale to encompass underestimates by a factor of 10^8 and overestimates by a factor of 10^4.

Despite the better base table estimates of DBMS A, the overall variance of the join estimation errors, as indicated by the boxplot, is similar for all systems with the exception of DBMS B. For all systems we routinely observe misestimates by a factor of 1000 or more. Furthermore, as witnessed by the increasing height of the box plots, the errors grow exponentially (note the logarithmic scale) as the number of joins increases [75]. For PostgreSQL 16% of the estimates for 1 join are wrong by a factor of 10 or more. This percentage increases to 32% with 2 joins, and to 52% with 3 joins. For DBMS A, which has the best estimator of the systems we compared, the corresponding percentages are only marginally better at 15%, 25%, and 36%.

Another striking observation is that all tested systems—though DBMS A to a lesser degree—tend to systematically underestimate the results sizes of queries with multiple joins. This can be deduced from the median of the error distributions in Figure 6.3. For our query set, it is indeed the case that the intermediate results tend to decrease with an increasing number of joins because more base table selections get applied. However, the true decrease is less than the independence assumption used by PostgreSQL (and apparently by the other systems) predicts. Underestimation is most pronounced with

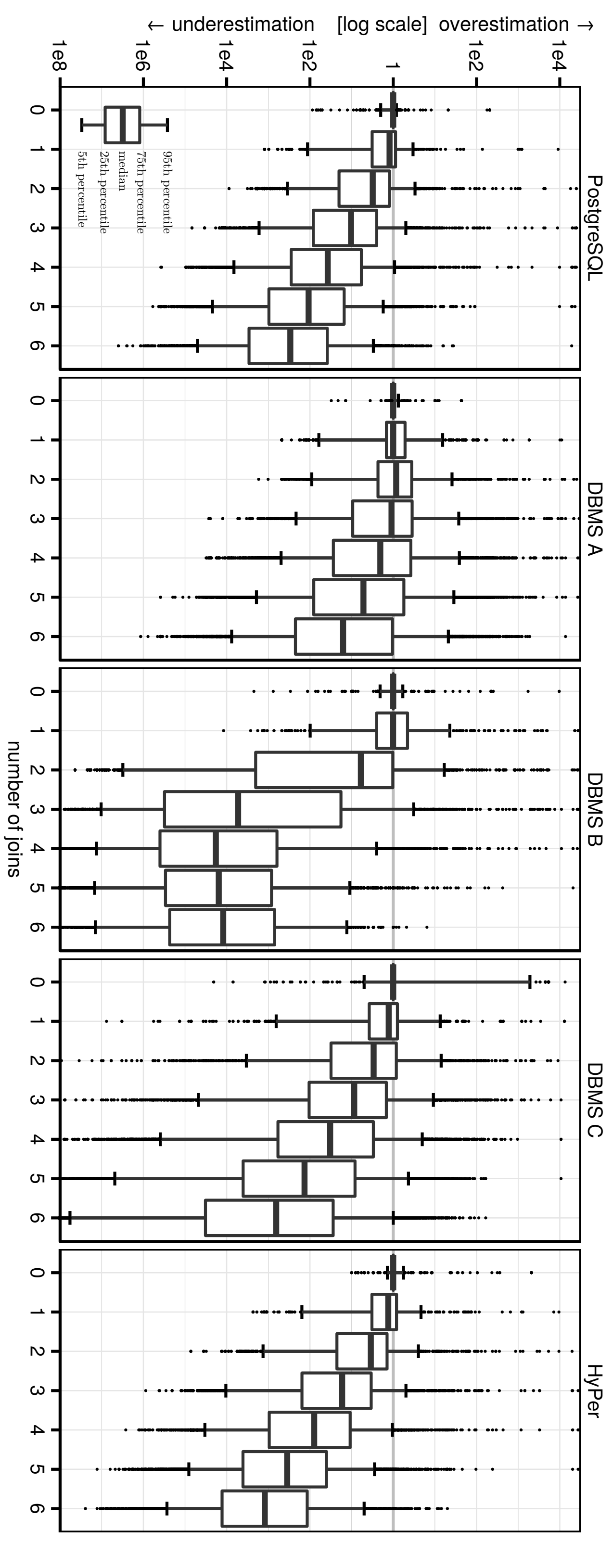

Figure 6.3: Quality of cardinality estimates for multi-join queries in comparison with the true cardinalities. Each boxplot summarizes the error distribution of all subexpressions with a particular size (over all queries in the workload)

DBMS B, which frequently estimates 1 row for queries with more than 2 joins. The estimates of DBMS A, on the other hand, have medians that are much closer to the truth, despite their variance being similar to some of the other systems. We speculate that DBMS A uses a damping factor that depends on the join size, similar to how many optimizers combine multiple selectivities. Many estimators combine the selectivities of multiple predicates (e.g., for a base relation or for a subexpression with multiple joins) not by assuming full independence, but by adjusting the selectivities "upwards", using a damping factor. The motivation for this stems from the fact that the more predicates need to be applied, the less certain one should be about their independence.

Given the simplicity of PostgreSQL's join estimation formula (cf. Section 6.2.3) and the fact that its estimates are nevertheless competitive with the commercial systems, we can deduce that the current join size estimators are based on the independence assumption. No system tested was able to detect join-crossing correlations. Furthermore, cardinality estimation is highly brittle, as illustrated by the significant number of extremely large errors we observed (factor 1000 or more) and the following anecdote: In PostgreSQL, we observed different cardinality estimates of the same simple 2-join query depending on the *syntactic* order of the relations in the `from` and/or the join predicates in the `where` clauses! Simply by swapping predicates or relations, we observed the estimates of 3, 9, 128, or 310 rows for the same query (with a true cardinality of 2600)[6].

Note that this section does not benchmark the query optimizers of the different systems. In particular, our results do not imply that the DBMS B's optimizer or the resulting query performance is necessarily worse than that of other systems, despite larger errors in the estimator. The query runtime heavily depends on how the system's optimizer uses the estimates and how much trust it puts into these numbers. A sophisticated engine may employ adaptive operators (e.g., [23, 33]) and thus mitigate the impact of misestimations. The results do, however, demonstrate that the state-of-the-art in cardinality estimation is far from perfect.

6.3.3 Estimates for TPC-H

We have stated earlier that cardinality estimation in TPC-H is a rather trivial task. Figure 6.4 substantiates that claim by showing the distributions of PostgreSQL estimation errors for 3 of the larger TPC-H queries and 4 of our JOB queries. Note that in the figure we report estimation errors for *individual* queries (not for all queries like in Figure 6.3). Clearly, the TPC-H query workload does not present many hard challenges for cardinality estimators. In contrast, our workload contains queries that routinely

[6] The reasons for this surprising behavior are two implementation artifacts: First, estimates that are less than 1 are rounded up to 1, making subexpression estimates sensitive to the (usually arbitrary) join enumeration order, which is affected by the `from` clause. The second is a consistency problem caused by incorrect domain sizes of predicate attributes in joins with multiple predicates.

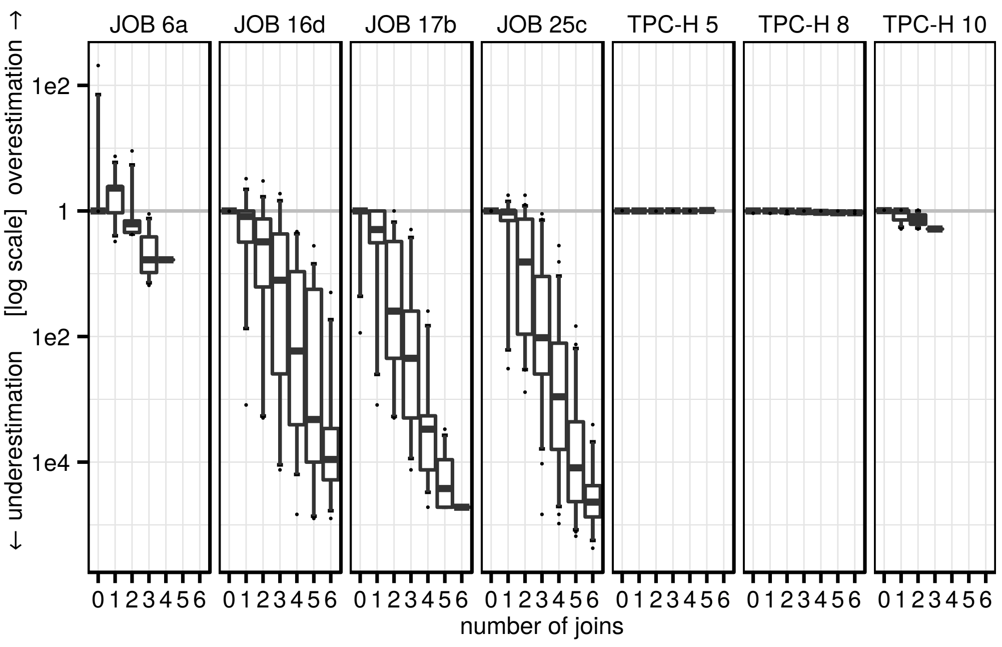

Figure 6.4: PostgreSQL cardinality estimates for 4 JOB queries and 3 TPC-H queries

lead to severe overestimation and underestimation errors, and hence can be considered a challenging benchmark for cardinality estimation.

6.3.4 Better Statistics for PostgreSQL

As mentioned in Section 6.2.3, the most important statistic for join estimation in PostgreSQL is the number of distinct values. These statistics are estimated from a fixed-sized sample, and we have observed severe underestimates for large tables. To determine if the misestimated distinct counts are the underlying problem for cardinality estimation, we computed these values precisely and replaced the estimated with the true values.

Figure 6.5 shows that the true distinct counts slightly improve the variance of the errors. Surprisingly, however, the trend to underestimate cardinalities becomes even more pronounced. The reason is that the original, underestimated distinct counts resulted in higher estimates, which, accidentally, are closer to the truth. This is an example for the proverbial “two wrongs that make a right”, i.e., two errors that (partially) cancel each other out. Such behavior makes analyzing and fixing query optimizer problems very frustrating because fixing one query might break another.

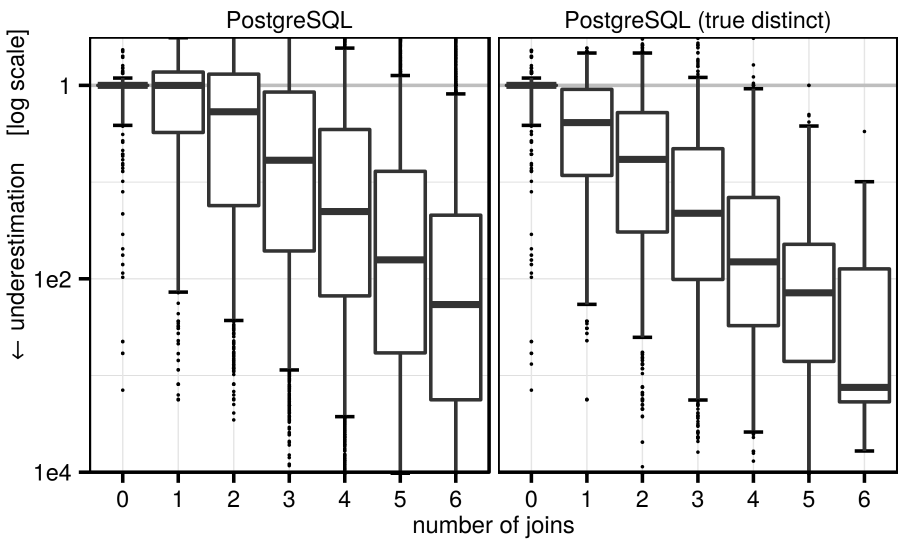

Figure 6.5: PostgreSQL cardinality estimates based on the default distinct count estimates, and the true distinct counts

6.4 When Do Bad Cardinality Estimates Lead to Slow Queries?

While the large estimation errors shown in the previous section are certainly sobering, large errors do *not necessarily* lead to slow query plans. For example, the misestimated expression may be cheap in comparison with other parts of the query, or the relevant plan alternative may have been misestimated by a similar factor thus "canceling out" the original error. In this section we investigate the conditions under which bad cardinalities are likely to cause slow queries.

One important observation is that query optimization is closely intertwined with the physical database design: the type and number of indexes heavily influence the plan search space, and therefore affects how sensitive the system is to cardinality misestimates. We therefore start this section with experiments using a relatively robust physical design with only primary key indexes and show that in such a setup the impact of cardinality misestimates can largely be mitigated. After that, we demonstrate that for more complex configurations with many indexes, cardinality misestimation makes it much more likely to miss the optimal plan by a large margin.

6.4.1 The Risk of Relying on Estimates

To measure the impact of cardinality misestimation on query performance we injected the estimates of the different systems into PostgreSQL and then executed the resulting plans. Using the same query engine allows one to compare the cardinality estimation components in isolation by (largely) abstracting away from the different query execution engines. Additionally, we inject the true cardinalities, which computes the—with respect to the cost model—optimal plan. We group the runtimes based on their slowdown w.r.t. the optimal plan, and report the distribution in the following table, where each column corresponds to a group:

	<0.9	[0.9,1.1)	[1.1,2)	[2,10)	[10,100)	>100
PostgreSQL	1.8%	38%	25%	25%	5.3%	5.3%
DBMS A	2.7%	54%	21%	14%	0.9%	7.1%
DBMS B	0.9%	35%	18%	15%	7.1%	25%
DBMS C	1.8%	38%	35%	13%	7.1%	5.3%
HyPer	2.7%	37%	27%	19%	8.0%	6.2%

A small number of queries become slightly slower using the true instead of the erroneous cardinalities. This effect is caused by cost model errors, which we discuss in Section 6.5. However, as expected, the vast majority of the queries are slower when estimates are used. Using DBMS A's estimates, 78% of the queries are less than 2$\times$ slower than using the true cardinalities, while for DBMS B this is the case for only 53% of the queries. This corroborates the findings about the relative quality of cardinality estimates in the previous section. Unfortunately, all estimators occasionally lead to plans that take an unreasonable time and lead to a timeout. Surprisingly, however, many of the observed slowdowns are easily avoidable despite the bad estimates as we show in the following.

When looking at the queries that did not finish in a reasonable time using the estimates, we found that most have one thing in common: PostgreSQL's optimizer decides to introduce a nested-loop join (without an index lookup) because of a very low cardinality estimate, whereas in reality the true cardinality is larger. As we saw in the previous section, systematic underestimation happens very frequently, which occasionally results in the introduction of nested-loop joins.

The underlying reason why PostgreSQL chooses nested-loop joins is that it picks the join algorithm on a purely cost-based basis. For example, if the cost estimate is 1,000,000 with the nested-loop join algorithm and 1,000,001 with a hash join, PostgreSQL will always prefer the nested-loop algorithm even if there is a equality join predicate, which allows one to use hashing. Of course, given the $O(n^2)$ complexity of nested-loop join and $O(n)$ complexity of hash join, and given the fact that underestimates are quite frequent, this decision is extremely risky. And even if the estimates happen to be correct, any potential performance advantage of a nested-loop join in comparison with a hash join is very small, so taking this *high risk* can only result in a *very small payoff*.

Therefore, we disabled nested-loop joins (but not index-nested-loop joins) in all following experiments. As Figure 6.6b shows, when rerunning all queries without these

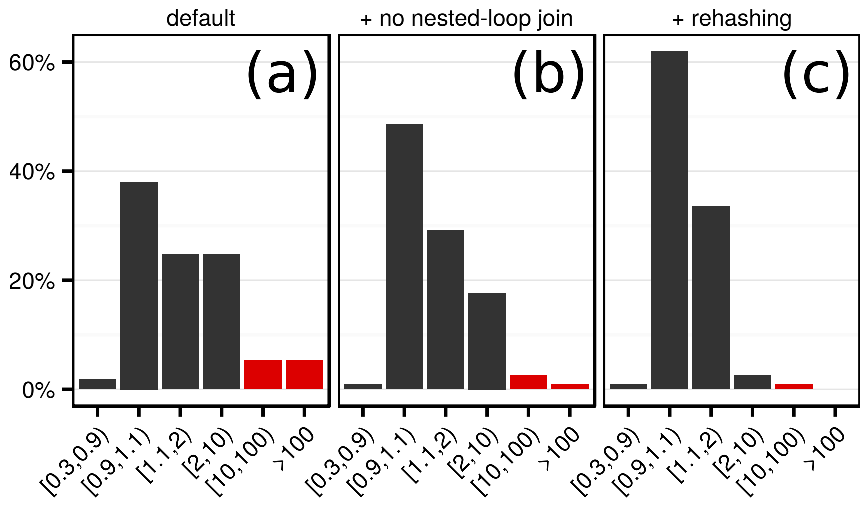

Figure 6.6: Slowdown of queries using PostgreSQL estimates w.r.t. using true cardinalities (primary key indexes only)

risky nested-loop joins, we observed no more timeouts despite using PostgreSQL's estimates.

Also, none of the queries performed slower than before despite having less join algorithm options, confirming our hypothesis that nested-loop joins (without indexes) seldom have any upside. However, this change does not solve all problems, as there are still a number of queries that are more than a factor of 10 slower (cf., red bars) in comparison with the true cardinalities.

When investigating the reason why the remaining queries still did not perform as well as they could, we found that most of them contain a hash join where the size of the build input is underestimated. PostgreSQL up to and including version 9.4 chooses the size of the in-memory hash table based on the cardinality estimate. Underestimates can lead to undersized hash tables with very long collisions chains and therefore bad performance. The upcoming version 9.5 resizes the hash table at runtime based on the number of rows actually stored in the hash table. We back-ported this patch to our code base, which is based on 9.4, and enabled it for all remaining experiments. Figure 6.6c shows the effect of this change in addition with disabled nested-loop joins. Less than 4% of the queries are off by more than $2\times$ in comparison with the true cardinalities.

To summarize, being "purely cost-based", i.e., not taking into account the inherent uncertainty of cardinality estimates and the asymptotic complexities of different algorithm choices, can lead to very bad query plans. Algorithms that seldom offer a large benefit over more robust algorithms should not be chosen. Furthermore, query processing algorithms should, if possible, automatically determine their parameters at runtime instead of relying on cardinality estimates.

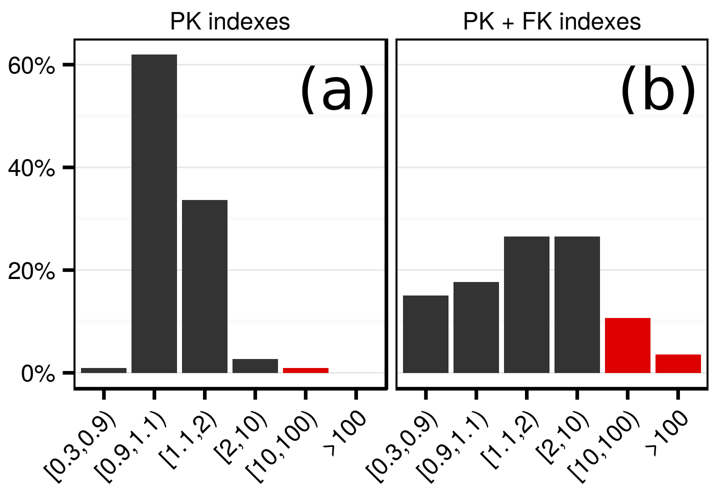

Figure 6.7: Slowdown of queries using PostgreSQL estimates w.r.t. using true cardinalities (different index configurations)

6.4.2 Good Plans Despite Bad Cardinalities

The query runtimes of plans with different join orders often vary by many orders of magnitude (cf. Section 6.6.1). Nevertheless, when the database has only primary key indexes, as in all in experiments so far, and once nested loop joins have been disabled and rehashing has been enabled, the performance of most queries is close to the one obtained using the true cardinalities. Given the bad quality of the cardinality estimates, we consider this to be a surprisingly positive result. It is worthwhile to reflect on why this is the case.

The main reason is that without foreign key indexes, most large ("fact") tables need to be scanned using full table scans, which dampens the effect of different join orders. The join order still matters, but the results indicate that the cardinality estimates are usually good enough to rule out all disastrous join order decisions like joining two large tables using an unselective join predicate. Another important reason is that in main memory picking an index-nested-loop join where a hash join would have been faster is never disastrous. With all data and indexes fully cached, we measured that the performance advantage of a hash join over an index-nested-loop join is at most $5\times$ with PostgreSQL and $2\times$ with HyPer. Obviously, when the index must be read from disk, random IO may result in a much larger factor. Therefore, the main-memory setting is much more forgiving.

6.4.3 Complex Access Paths

So far, all query executions were performed on a database with indexes on primary key attributes only. To see if the query optimization problem becomes harder when there are more indexes, we additionally indexed all foreign key attributes. Figure 6.7b shows the effect of additional foreign key indexes. We see large performance differences with 40% of the queries being slower by a factor of 2! Note that these results do not mean that adding more indexes decreases performance (although this can occasionally happen). Indeed overall performance generally increases significantly, but the more indexes are available the harder the job of the query optimizer becomes.

6.4.4 Join-Crossing Correlations

There is consensus in our community that estimation of intermediate result cardinalities in the presence of *correlated* query predicates is a frontier in query optimization research. The JOB workload studied in this work consists of real-world data and its queries contain many correlated predicates. Our experiments that focus on *single-table* subquery cardinality estimation quality (cf. Table 6.1) show that systems that keep table samples (HyPer and presumably DBMS A) can achieve almost perfect estimation results, even for correlated predicates (inside the same table). As such, the cardinality estimation research challenge appears to lie in queries where the correlated predicates involve columns from *different* tables, connected by joins. These we call "join-crossing correlations". Such correlations frequently occur in the IMDB data set, e.g., actors born in Paris are likely to play in French movies.

Given these join-crossing correlations one could wonder if there exist complex access paths that allow one to exploit these. One example relevant here despite its original setting in XQuery processing is ROX [82]. It studied runtime join order query optimization in the context of DBLP co-authorship queries that count how many `Authors` had published `Papers` in three particular venues, out of many. These queries joining the author sets from different venues clearly have join-crossing correlations, since authors who publish in `VLDB` are typically database researchers, likely to also publish in `SIGMOD`, but not—say—in `Nature`.

In the DBLP case, `Authorship` is a $n : m$ relationship that links the relation `Authors` with the relation `Papers`. The optimal query plans in [82] used an index-nested-loop join, looking up each `author` into `Authorship.author` (the indexed primary key) followed by a filter restriction on `Paper.venue`, which needs to be looked up with yet another join. This filter on venue would normally have to be calculated *after* these two joins. However, the physical design of [82] stored `Authorship` *partitioned by* `Paper.venue`.[7] This partitioning has startling effects: instead of one `Authorship` table and primary key index, one physically has many, one for each `venue` partition. This means that by accessing the right partition, the filter is implic-

[7] In fact, rather than relational table partitioning, there was a separate XML document per venue, e.g., separate documents for `SIGMOD`, `VLDB`, `Nature` and a few thousand more venues. Storage in a separate XML document has roughly the same effect on access paths as partitioned tables.

itly enforced (for free), *before* the join happens. This specific physical design therefore causes the optimal plan to be as follows: first join the smallish authorship set from `SIGMOD` with the large set for `Nature` producing almost no result tuples, making the subsequent nested-loops index lookup join into `VLDB` very cheap. If the tables would not have been partitioned, index lookups from all `SIGMOD` authors into `Authorships` would first find all co-authored papers, of which the great majority is irrelevant because they are about database research, and were not published in `Nature`. Without this partitioning, there is no way to avoid this large intermediate result, and there is no query plan that comes close to the partitioned case in efficiency: even if cardinality estimation would be able to predict join-crossing correlations, there would be no physical way to profit from this knowledge.

The lesson to draw from this example is that the effects of query optimization are always gated by the available options in terms of access paths. Having a partitioned index on a *join-crossing predicate* as in [82] is a non-obvious physical design alternative which even modifies the schema by bringing in a join-crossing column (`Paper.venue`) as partitioning key of a table (`Authorship`). The partitioned DBLP set-up is just one example of how one particular join-crossing correlation can be handled, rather than a generic solution. Join-crossing correlations remain an open frontier for database research involving the interplay of physical design, query execution and query optimization. In our JOB experiments we do not attempt to chart this mostly unknown space, but rather characterize the impact of (join-crossing) correlations on the current state-of-the-art of query processing, restricting ourselves to standard PK and FK indexing.

6.5 Cost Models

The cost model guides the selection of plans from the search space. The cost models of contemporary systems are sophisticated software artifacts that are resulting from 30+ years of research and development, mostly concentrated in the area of traditional disk-based systems. PostgreSQL's cost model, for instance, is comprised of over 4000 lines of C code, and takes into account various subtle considerations, e.g., it takes into account partially correlated index accesses, interesting orders, tuple sizes, etc. It is interesting, therefore, to evaluate how much a complex cost model actually contributes to the overall query performance.

First, we will experimentally establish the correlation between PostgreSQL's cost model—a typical cost model of a disk-based DBMS—and the query runtime. Then, we will compare PostgreSQL's cost model with two other cost functions. The first cost model is a tuned version of PostgreSQL's model for a main-memory setup where all data fits into RAM. The second cost model is an extremely simple function that only takes the number of tuples produced during query evaluation into account. We show that, unsurprisingly, the difference between the cost models is dwarfed by the cardinality estimates errors. We conduct our experiments on a database instance with foreign key indexes. We begin with a brief description of a typical disk-oriented complex cost model, namely the one of PostgreSQL.

6.5.1 The PostgreSQL Cost Model

PostgreSQL's disk-oriented cost model combines CPU and I/O costs with certain weights. Specifically, the cost of an operator is defined as a weighted sum of the number of accessed disk pages (both sequential and random) and the amount of data processed in memory. The cost of a query plan is then the sum of the costs of all operators. The default values of the weight parameters used in the sum (*cost variables*) are set by the optimizer designers and are meant to reflect the relative difference between random access, sequential access and CPU costs.

The PostgreSQL documentation contains the following note on cost variables:

> "Unfortunately, there is no well-defined method for determining ideal values for the cost variables. They are best treated as averages over the entire mix of queries that a particular installation will receive. This means that changing them on the basis of just a few experiments is very risky."

For a database administrator, who needs to actually set these parameters these suggestions are not very helpful; no doubt most will not change these parameters. This comment is of course, not PostgreSQL-specific, since other systems feature similarly complex cost models. In general, tuning and calibrating cost models (based on sampling, various machine learning techniques etc.) has been a subject of a number of papers (e.g, [180, 120]). It is important, therefore, to investigate the impact of the cost model on the overall query engine performance. This will indirectly show the contribution of cost model errors on query performance.

6.5.2 Cost and Runtime

The main virtue of a cost function is its ability to predict which of the alternative query plans will be the fastest, given the cardinality estimates; in other words, what counts is its correlation with the query runtime. The correlation between the cost and the runtime of queries in PostgreSQL is shown in Figure 6.8a. Additionally, we consider the case where the engine has the true cardinalities injected, and plot the corresponding data points in Figure 6.8b. For both plots, we fit the linear regression model (displayed as a straight line) and highlight the standard error. The predicted cost of a query correlates with its runtime in both scenarios. Poor cardinality estimates, however, lead to a large number of outliers and a very wide standard error area in Figure 6.8a. Only using the

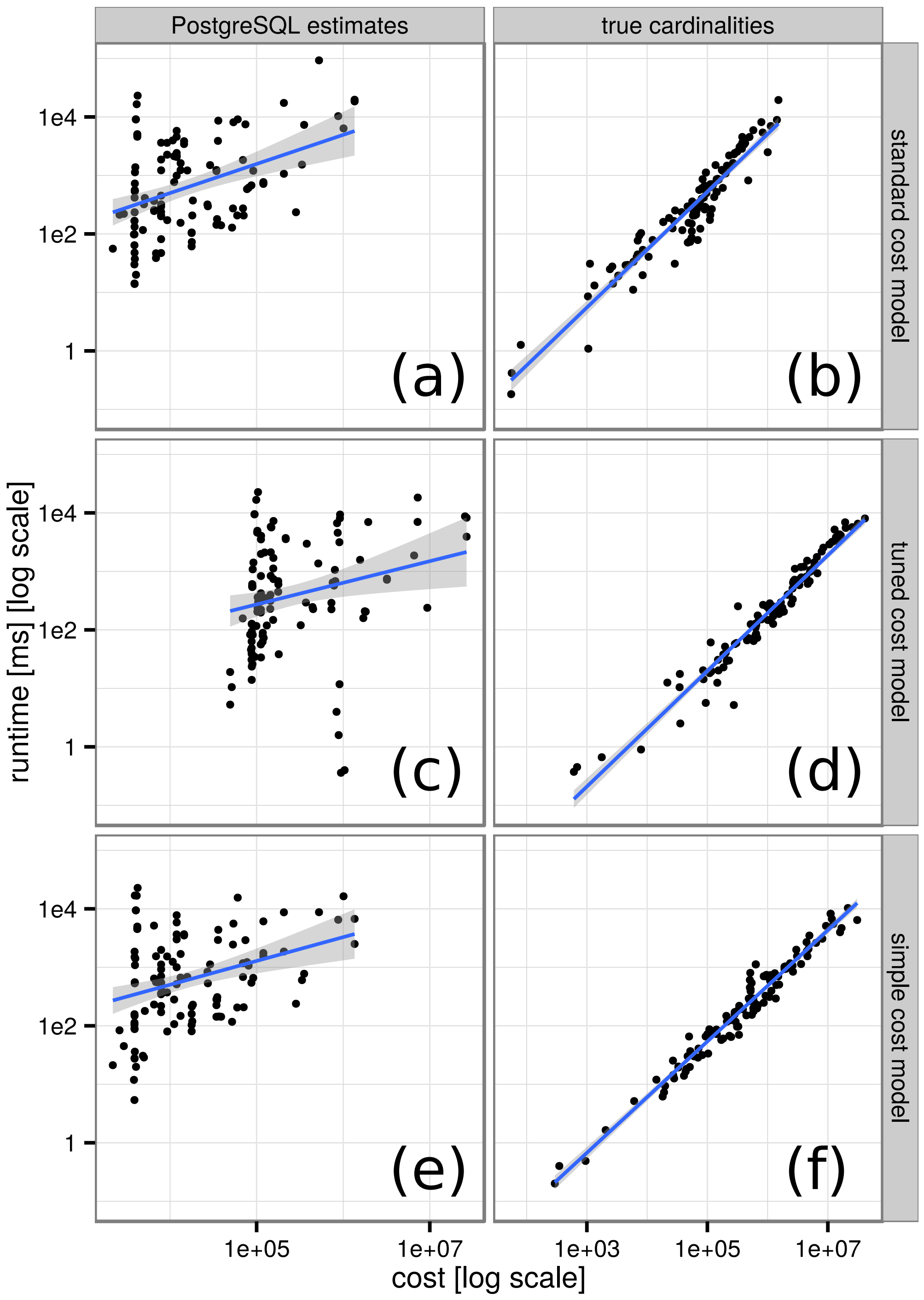

Figure 6.8: Predicted cost vs. runtime for different cost models

true cardinalities makes PostgreSQL's cost model a reliable predictor of the runtime, as has been observed previously [180].

Intuitively, a straight line in Figure 6.8 corresponds to an ideal cost model that always assigns (predicts) higher costs for more expensive queries. Naturally, any monotonically increasing function would satisfy that requirement, but the linear model provides the simplest and the closest fit to the observed data. We can therefore interpret the deviation from this line as the *prediction error* of the cost model. Specifically, we consider the absolute percentage error of a cost model for a query Q: $\epsilon(Q) = \frac{|T_{\text{real}}(Q) - T_{\text{pred}}(Q)|}{T_{\text{real}}(Q)}$, where T_{real} is the observed runtime, and T_{pred} is the runtime predicted by our linear model. Using the default cost model of PostgreSQL and the true cardinalities, the median error of the cost model is 38%.

6.5.3 Tuning the Cost Model for Main Memory

As mentioned above, a cost model typically involves parameters that are subject to tuning by the database administrator. In a disk-based system such as PostgreSQL, these parameters can be grouped into *CPU cost parameters* and *I/O cost parameters*, with the default settings reflecting an expected proportion between these two classes in a hypothetical workload.

In many settings the default values are sub optimal. For example, the default parameter values in PostgreSQL suggest that processing a tuple is 400x cheaper than reading it from a page. However, modern servers are frequently equipped with very large RAM capacities, and in many workloads the data set actually fits entirely into available memory (admittedly, the core of PostgreSQL was shaped decades ago when database servers only had few megabytes of RAM). This does not eliminate the page access costs entirely (due to buffer manager overhead), but significantly bridges the gap between the I/O and CPU processing costs.

Arguably, the most important change that needs to be done in the cost model for a main-memory workload is to decrease the proportion between these two groups. We have done so by multiplying the *CPU cost* parameters by a factor of 50. The results of the workload run with improved parameters are plotted in the two middle subfigures of Figure 6.8. Comparing Figure 6.8b with d, we see that tuning does indeed improve the correlation between the cost and the runtime. On the other hand, as is evident from comparing Figure 6.8c and d, parameter tuning improvement is still overshadowed by the difference between the estimated and the true cardinalities. Note that Figure 6.8c features a set of outliers for which the optimizer has accidentally discovered very good plans (runtimes around 1 ms) without realizing it (hence very high costs). This is another sign of "oscillation" in query planning caused by cardinality misestimates.

In addition, we measure the prediction error ϵ of the tuned cost model, as defined in Section 6.5.2. We observe that tuning improves the predictive power of the cost model:

the median error decreases from 38% to 30%.

6.5.4 Are Complex Cost Models Necessary?

As discussed above, PostgreSQL's cost model is quite complex. Presumably, this complexity should reflect various factors influencing query execution, such as the speed of a disk seek and read, CPU processing costs, etc. In order to find out whether this complexity is actually necessary in a main-memory setting, we will contrast it with a very simple cost function C_{mm}. This cost function is tailored for the *main-memory* setting in that it does not model I/O costs, but only counts the number of tuples that pass through each operator during query execution:

$$C_{\text{mm}}(T) = \begin{cases} \tau \cdot |R| & \text{if } T = R \vee T = \sigma(R) \\ |T| + C_{\text{mm}}(T_1) + C_{\text{mm}}(T_2) & \text{if } T = T_1 \bowtie^{\text{HJ}} T_2 \\ C_{\text{mm}}(T_1) + & \text{if } T = T_1 \bowtie^{\text{INL}} T_2, \\ \quad \lambda \cdot |T_1| \cdot \max(\frac{|T_1 \bowtie R|}{|T_1|}, 1) & (T_2 = R \vee T_2 = \sigma(R)) \end{cases}$$

In the formula above R is a base relation, and $\tau \leq 1$ is a parameter that discounts the cost of a table scan in comparison with joins. The cost function distinguishes between hash $\bowtie^{\text{HJ}}$ and index-nested loop $\bowtie^{\text{INL}}$ joins: the latter scans T_1 and performs index lookups into an index on R, thus avoiding a full table scan of R. A special case occurs when there is a selection on the right side of the index-nested loop join, in which case we take into account the number of tuple lookups in the base table index and essentially discard the selection from the cost computation (hence the multiplier $\max(\frac{|T_1 \bowtie R|}{|T_1|}, 1)$). For index-nested loop joins we use the constant $\lambda \geq 1$ to approximate by how much an index lookup is more expensive than a hash table lookup. Specifically, we set $\lambda = 2$ and $\tau = 0.2$. As in our previous experiments, we disable nested loop joins when the inner relation is not an index lookup (i.e., non-index nested loop joins).

The results of our workload run with C_{mm} as a cost function are depicted in Figure 6.8e and f. We see that even our trivial cost model is able to fairly accurately predict the query runtime using the true cardinalities. To quantify this argument, we measure the improvement in the runtime achieved by changing the cost model for true cardinalities: In terms of the geometric mean over all queries, our tuned cost model yields 41% faster runtimes than the standard PostgreSQL model, but even a simple C_{mm} makes queries 34% faster than the built-in cost function. This improvement is not insignificant, but on the other hand, it is dwarfed by improvement in query runtime observed when we replace estimated cardinalities with the real ones (cf. Figure 6.6b). This allows us to reiterate our main message that cardinality estimation is much more crucial than the cost model.

6.6 Plan Space

Besides cardinality estimation and the cost model, the final important query optimization component is a plan enumeration algorithm that explores the space of semantically equivalent join orders. Many different algorithms, both exhaustive (e.g., [131, 46]) as well as heuristic (e.g, [164, 138]) have been proposed. These algorithms consider a different number of candidate solutions (that constitute the *search space*) when picking the best plan. In this section we investigate how large the search space needs to be in order to find a good plan.

The experiments of this section use a standalone query optimizer, which implements Dynamic Programming (DP) and a number of heuristic join enumeration algorithms. Our optimizer allows the injection of arbitrary cardinality estimates. In order to fully explore the search space, we do not actually execute the query plans produced by the optimizer in this section, as that would be infeasible due to the number of joins our queries have. Instead, we first run the query optimizer using the estimates as input. Then, we recompute the cost of the resulting plan with the true cardinalities, giving us a very good approximation of the runtime the plan would have in reality. We use the in-memory cost model from Section 6.5.4 and assume that it perfectly predicts the query runtime, which, for our purposes, is a reasonable assumption since the errors of the cost model are negligible in comparison the cardinality errors. This approach allows us to compare a large number of plans without executing all of them.

6.6.1 How Important Is the Join Order?

We use the Quickpick [174] algorithm to visualize the costs of different join orders. Quickpick is a simple, randomized algorithm that picks joins edges at random until all joined relations are fully connected. Each run produces a correct, but usually slow, query plan. By running the algorithm 10,000 times per query and computing the costs of the resulting plans, we obtain an approximate distribution for the costs of random plans. Figure 6.9 shows density plots for 5 representative example queries and for three physical database designs: no indexes, primary key indexes only, and primary+foreign key indexes. The costs are normalized by the optimal plan (with foreign key indexes), which we obtained by running dynamic programming and the true cardinalities.

The graphs, which use a logarithmic scale on the horizontal cost axis, clearly illustrate the importance of the join ordering problem: The slowest or even median cost is generally multiple orders of magnitude more expensive than the cheapest plan. The shapes of the distributions are quite diverse. For some queries, there are many good plans (e.g., 25c), for others few (e.g., 16d). The distribution are sometimes wide (e.g., 16d) and sometimes narrow (e.g., 25c). The plots for the “no indexes” and the “PK indexes” configurations are very similar implying that for our workload primary key

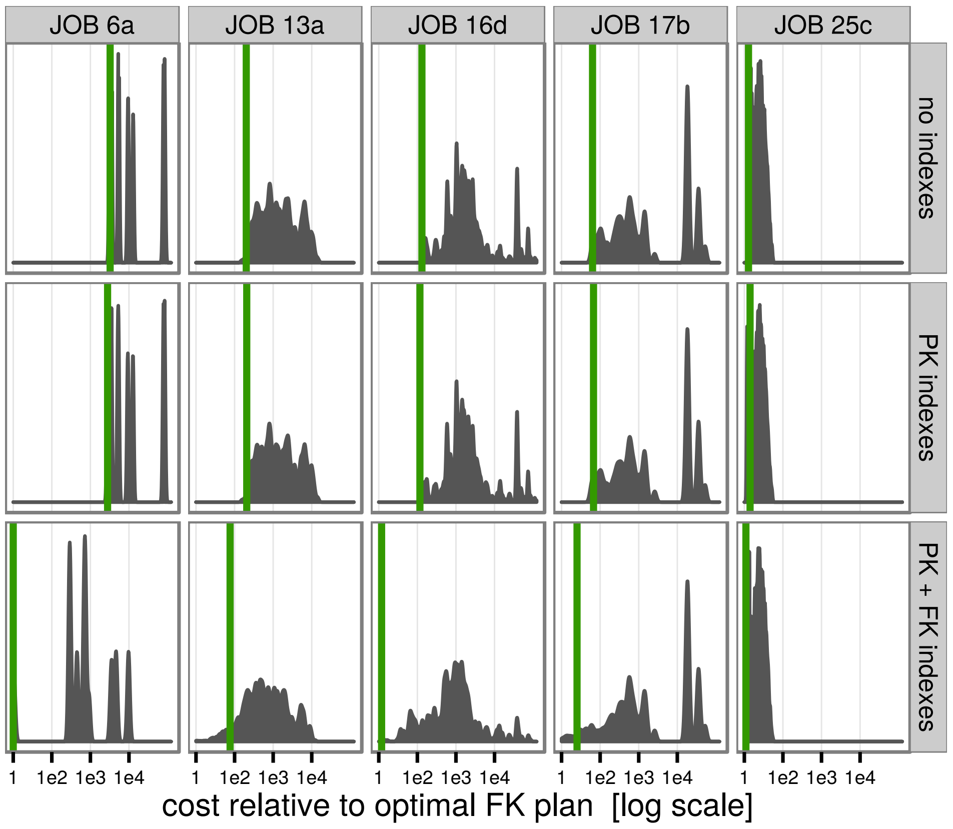

Figure 6.9: Cost distributions for 5 queries and different index configurations. The vertical green lines represent the cost of the optimal plan

indexes alone do not improve performance very much, since we do not have selections on primary key columns. In many cases the "PK+FK indexes" distributions have additional small peaks on the left side of the plot, which means that the optimal plan in this index configuration is much faster than in the other configurations.

We also analyzed the entire workload to confirm these visual observations: The percentage of plans that are at most $1.5\times$ more expensive than the optimal plan is 44% without indexes, 39% with primary key indexes, but only 4% with foreign key indexes. The average fraction between the worst and the best plan, i.e., the width of the distribution, is $101\times$ without indexes, $115\times$ with primary key indexes, and $48120\times$ with foreign key indexes. These summary statistics highlight the dramatically different search spaces of the three index configurations.

6.6.2 Are Bushy Trees Necessary?

Most join ordering algorithms do not enumerate all possible tree shapes. Virtually all optimizers ignore join orders with cross products, which results in a dramatically

	PK indexes			PK + FK indexes		
	median	95%	max	median	95%	max
zig-zag	1.00	1.06	1.33	1.00	1.60	2.54
left-deep	1.00	1.14	1.63	1.06	2.49	4.50
right-deep	1.87	4.97	6.80	47.2	30931	738349

Table 6.2: Slowdown for restricted tree shapes in comparison to the optimal plan (true cardinalities)

reduced optimization time with only negligible query performance impact. Oracle goes even further by not considering bushy join trees [2]. In order to quantify the effect of restricting the search space on query performance, we modified our DP algorithm to only enumerate *left-deep*, *right-deep*, or *zig-zag* trees.

Aside from the obvious tree shape restriction, each of these classes implies constraints on the join method selection. We follow the definition by Garcia-Molina et al.'s textbook, which is reverse from the one in Ramakrishnan and Gehrke's book: Using hash joins, right-deep trees are executed by first creating hash tables out of each relation except one before probing in all of these hash tables in a pipelined fashion, whereas in left-deep trees, a new hash table is built from the result of each join. In zig-zag trees, which are a super set of all left- and right-deep trees, each join operator must have at least one base relation as input. For index-nested loop joins we additionally employ the following convention: the left child of a join is a source of tuples that are looked up in the index on the right child, which must be a base table.

Using the true cardinalities, we compute the cost of the optimal plan for each of the three restricted tree shapes. We divide these costs by the optimal tree (which may have any shape, including "bushy") thereby measuring how much performance is lost by restricting the search space. The results in Table 6.2 show that zig-zag trees offer decent performance in most cases, with the worst case being $2.54\times$ more expensive than the best bushy plan. Left-deep trees are worse than zig-zag trees, as expected, but still result in reasonable performance. Right-deep trees, on the other hand, perform much worse than the other tree shapes and thus should not be used exclusively. The bad performance of right-deep trees is caused by the large intermediate hash tables that need to be created from each base relation and the fact that only the bottom-most join can be done via index lookup.

6.6.3 Are Heuristics Good Enough?

So far, in our experiments we have used the dynamic programming algorithm, which computes the optimal join order. However, given the bad quality of the cardinality estimates, one may reasonably ask whether an exhaustive algorithm is even necessary. We therefore compare dynamic programming with a randomized and a greedy heuristics.

	PK indexes					
	PostgreSQL estimates			true cardinalities		
	median	95%	max	median	95%	max
Dynamic Programming	1.03	1.85	4.79	1.00	1.00	1.00
Quickpick-1000	1.05	2.19	7.29	1.00	1.07	1.14
Greedy Operator Ordering	1.19	2.29	2.36	1.19	1.64	1.97
	PK + FK indexes					
	PostgreSQL estimates			true cardinalities		
	median	95%	max	median	95%	max
Dynamic Programming	1.66	169	186367	1.00	1.00	1.00
Quickpick-1000	2.52	365	186367	1.02	4.72	32.3
Greedy Operator Ordering	2.35	169	186367	1.20	5.77	21.0

Table 6.3: Comparison of exhaustive dynamic programming with the Quickpick-1000 (best of 1000 random plans) and the Greedy Operator Ordering heuristics. All costs are normalized by the optimal plan of that index configuration

The "Quickpick-1000" heuristics is a randomized algorithm that chooses the cheapest (based on the estimated cardinalities) 1000 random plans. Among all greedy heuristics, we pick Greedy Operator Ordering (GOO) since it was shown to be superior to other deterministic approximate algorithms [44]. GOO maintains a set of join trees, each of which initially consists of one base relation. The algorithm then combines the pair of join trees with the lowest cost to a single join tree. Both Quickpick-1000 and GOO can produce bushy plans, but obviously only explore parts of the search space. All algorithms in this experiment internally use the PostgreSQL cardinality estimates to compute a query plan, for which we compute the "true" cost using the true cardinalities.

Table 6.3 shows that it is worthwhile to fully examine the search space using dynamic programming despite cardinality misestimation. However, the errors introduced by estimation errors cause larger performance losses than the heuristics. In contrast to some other heuristics (e.g., [25]), GOO and Quickpick-1000 are not really aware of indexes. Therefore, GOO and Quickpick-1000 work better when few indexes are available, which is also the case when there are more good plans.

To summarize, our results indicate that enumerating all bushy trees exhaustively offers moderate but not insignificant performance benefits in comparison with algorithms that enumerate only a sub set of the search space. The performance potential from good cardinality estimates is certainly much larger. However, given the existence of exhaustive enumeration algorithms that can find the optimal solution for queries with dozens of relations very quickly (e.g., [131, 46]), there are few cases where resorting to heuristics or disabling bushy trees should be necessary.

6.7 Related Work

Our cardinality estimation experiments show that systems which keep table samples for cardinality estimation predict single-table result sizes considerably better than those which apply the independence assumption and use single-column histograms [74]. We think systems should be adopting table samples as a simple and robust technique, rather than earlier suggestions to explicitly detect certain correlations [71] to subsequently create multi-column histograms [150] for these.

However, many of our JOB queries contain join-crossing correlations, which single-table samples do not capture, and where the current generation of systems still apply the independence assumption. There is a body of existing research work to better estimate result sizes of queries with join-crossing correlations, mainly based on join samples [60], possibly enhanced against skew (end-biased sampling [42], correlated samples [184]), using sketches [159] or graphical models [173]. This work confirms that without addressing join-crossing correlations, cardinality estimates deteriorate strongly with more joins [75], leading to both the over- and underestimation of result sizes (mostly the latter), so it would be positive if some of these techniques would be adopted by systems.

Another way of learning about join-crossing correlations is by exploiting query feedback, as in the LEO project [165], though there it was noted that deriving cardinality estimations based on a mix of exact knowledge and lack of knowledge needs a sound mathematical underpinning. For this, maximum entropy (MaxEnt [130, 85]) was defined, though the costs for applying maximum entropy are high and have prevented its use in systems so far. We found that the performance impact of estimation mistakes heavily depends on the physical database design; in our experiments the largest impact is in situations with the richest designs. From the ROX [82] discussion in Section 6.4.4 one might conjecture that to truly unlock the potential of correctly predicting cardinalities for join-crossing correlations, we also need new physical designs and access paths.

Another finding in this work is that the adverse effects of cardinality misestimations can be strongly reduced if systems would be "hedging their bets" and not only choose the plan with the cheapest expected cost, but take the probabilistic distribution of the estimate into account, to avoid plans that are marginally faster than others but bear a high risk of strong underestimation. There has been work both on doing this for cardinality estimates purely [132], as well as combining these with a cost model (cost distributions [8]).

The problem with fixed hash table sizes for PostgreSQL illustrates that cost misestimation can often be mitigated by making the runtime behavior of the query engine more "performance robust". This links to a body of work to make systems adaptive to estimation mistakes, e.g., dynamically switch sides in a join, or change between hashing and sorting (GJoin [55]), switch between sequential scan and index lookup (smooth scan [23]), adaptively reordering join pipelines during query execution [116], or change aggregation strategies at runtime depending on the actual number of group-by values [135] or partition-by values [15].

A radical approach is to move query optimization to runtime, when actual value-distributions become available [140, 40]. However, runtime techniques typically restrict the plan search space to limit runtime plan exploration cost, and sometimes come with functional restrictions such as to only consider (sampling through) operators which have pre-created indexed access paths (e.g., ROX [82]).

Our experiments with the second query optimizer component besides cardinality estimation, namely the cost model, suggest that tuning cost models provides less benefits than improving cardinality estimates, and in a main-memory setting even an extremely simple cost-model can produce satisfactory results. This conclusion resonates with some of the findings in [180] which sets out to improve cost models but shows major improvements by refining cardinality estimates with additional sampling.

For testing the final query optimizer component, plan enumeration, we borrowed in our methodology from the Quickpick method used in randomized query optimization [174] to characterize and visualize the search space. Another well-known search space visualization method is Picasso [62], which visualizes query plans as areas in a space where query parameters are the dimensions. Interestingly, [174] claims in its characterization of the search space that good query plans are easily found, but our tests indicate that the richer the physical design and access path choices, the rarer good query plans become.

Query optimization is a core database research topic with a huge body of related work, that cannot be fully represented in this section. After decades of work still having this problem far from resolved [121], some have even questioned it and argued for the need of optimizer application hints [31]. This work introduces the Join Order Benchmark based on the highly correlated IMDB real-world data set and a methodology for measuring the accuracy of cardinality estimation. Its integration in systems proposed for testing and evaluating the quality of query optimizers [175, 59, 48, 124] is hoped to spur further innovation in this important topic.

6.8 Summary

In this work we have provided quantitative evidence for conventional wisdom that has been accumulated in three decades of practical experience with query optimizers. We have shown that query optimization is essential for efficient query processing and that exhaustive enumeration algorithms find better plans than heuristics. We have also shown that relational database systems produce large estimation errors that quickly grow as the number of joins increases, and that these errors are usually the reason for bad plans. In contrast to cardinality estimation, the contribution of the cost model to the overall query performance is limited.

The unsatisfactory quality of cardinality estimators has been observed before [121], and we hope that this important problem will receive more attention in the future. Nevertheless, the cardinality estimates contain information that is often sufficient for avoiding very bad query plans. Query optimizers can therefore usually find decent join orders for most queries. However, the more access paths a database offers, the harder it becomes to find a plan close to the optimum. We also showed that it is better to use estimates only when necessary (e.g., for determining the join orders), but not to set parameters that can be determined automatically at runtime (e.g., hash table sizes).

7 Future Work

In this work we have shown that a modern database system that is carefully optimized for modern hardware can achieve orders of magnitude higher performance than a traditional design. However, there are still many unsolved problems, some of which we plan to address in the future.

One important research frontier nowadays lies in supporting mixed workloads in a single database. Many systems that start out as pure OLTP systems, over time add OLAP features thus blurring the distinction between the two system types. Even in HyPer, which was a mixed-workload system from the start [87], the research focus shifted from topics like indexing [108] to parallel query processing [106, 158] and compression [97]. While there may be sound technical reasons for running OLTP and OLAP in separate systems, in reality, OLTP and OLAP are more platonic ideals than truly separate applications. Therefore, there will always be pressure to support both workloads. One major consequence is that, even for main-memory database systems, the convenient assumption that *all* data fits into RAM generally does not hold. There has been lots of research into supporting data sets larger than RAM in main-memory database systems (e.g., [35, 113, 4, 41, 57, 49, 166]). Nevertheless, we believe that the general problem of efficiently maintaining a global replacement strategy over relational as well as index data is still not fully solved.

Major changes are also happening on the hardware side and database systems must keep evolving to benefit from these changes. One aspect is the ever increasing number of cores per CPU. While it is not clear whether servers with 1000 cores will be common in the near future—if this indeed happens—it will have a major effect on database architecture. It is a general rule, that the higher the degree of parallelism, the more difficult scalability becomes [185]. Any efficient system that scales up to, for example, 100 cores, will likely require some major changes to scale up to 1000 cores. Thus, some of the architectural decisions may need to be revised if the many-core trend continues.

A potentially even greater challenge is the increasing heterogeneity of modern hardware, which has the potential of disrupting the architecture of database systems. The following trends can already be observed now:

- The Single Instruction, Multiple Data (SIMD) register width of modern CPUs is increasing and will soon reach 512 bits (with Intel's Skylake EP).

- Graphics Processing Units (GPUs) have much higher nominal computational power as well as memory bandwidth than general-purpose CPUs.
- Accelerated Processing Units (APUs), which combine a CPU with a GPU on a single chip, in contrast, have lower communication cost between the two devices but less memory bandwidth than GPUs.
- Special purpose accelerators like Oracle's SPARC M7 on-chip data analytics accelerator offer database-specific functionality like selection or decompression in hardware.
- The emerging FPGA technology blurs the line between hardware and software.

In the past hardware evolved quickly too, but this mainly manifested in higher clock frequency, higher bandwidth, etc. From the point of view of a software developer, over time, software became faster "automatically". The hardware technologies mentioned above have, however, one thing in common: Programmers have to invest effort to get any benefit from them. Programming for SIMD, GPUs, or FPGAs is very different (and more difficult) than using the instruction set of a conventional, general-purpose CPU. Therefore, as has been observed by Mark D. Hill, software is becoming a *producer of performance*[1] instead of a consumer of performance.

Consider a scenario in the not too far future, where a database server is equipped with a 100-core CPU, 512-bit-wide SIMD instructions, a hardware accelerator for data-intensive operations, a 10 TFLOP GPU, and an FPGA. Although much research has been done on how to process data using these technologies (e.g., [65, 148, 170]), designing a database system that effectively uses a mix of devices poses many additional challenges. A database system will have to decide which part of a query should be executed on which device, all while managing the data movement between the devices and the energy/heat budget of the overall system. Put simply, no one currently knows how to do this and no doubt it will take at least a decade of research to find a satisfactory solution.

Whereas the technologies mentioned above promise faster computation, new storage technologies like PCIe-attached NAND flash and non-volatile memory (NVM) [7, 123, 91, 145] like Phase Change Memory threaten to disrupt the way data is stored and accessed. In order to avoid changing the software stack much, it is certainly possible to hide modern storage devices behind a conventional block device interface, which was originally designed for rotating disks. However, this approach leaves performance on the table as it ignores the specific physical properties like the block erase requirement of NAND flash or the byte-addressability of non-volatile memory. Thus, research is

[1] `http://www.systems.ethz.ch/sites/default/files/file/TALKS/Gustavo/GA-Keynote-ICDE-2013.pdf`

required to find out how these new storage technologies are best utilized by database systems.

Finally, even the venerable field of query optimization still has many unsolved problems. One promising approach is to rely more heavily on sampling (e.g., [180, 181]), which is much cheaper than in the past when CPU cycles were costly and random disk I/O would have been required. Sampling, for example across indexes, opens up new ways to estimate the cardinality of multi-way joins, which after decades of research, is still done naively in most systems.

8 Bibliography

[1] D. Abadi, P. A. Boncz, S. Harizopoulos, S. Idreos, and S. Madden. The design and implementation of modern column-oriented database systems. *Foundations and Trends in Databases*, 5(3):197–280, 2013.

[2] R. Ahmed, R. Sen, M. Poess, and S. Chakkappen. Of snowstorms and bushy trees. *PVLDB*, 7(13):1452–1461, 2014.

[3] M.-C. Albutiu, A. Kemper, and T. Neumann. Massively parallel sort-merge joins in main memory multi-core database systems. *PVLDB*, 5(10), 2012.

[4] K. Alexiou, D. Kossmann, and P. Larson. Adaptive range filters for cold data: Avoiding trips to Siberia. *PVLDB*, 6(14):1714–1725, 2013.

[5] G. Alonso. Hardware killed the software star. In *ICDE*, 2013.

[6] K. Anikiej. Multi-core parallelization of vectorized query execution. Master's thesis, University of Warsaw and VU University Amsterdam, 2010. `http://homepages.cwi.nl/~boncz/msc/2010-KamilAnikijej.pdf`.

[7] J. Arulraj, A. Pavlo, and S. Dulloor. Let's talk about storage & recovery methods for non-volatile memory database systems. In *SIGMOD*, pages 707–722, 2015.

[8] B. Babcock and S. Chaudhuri. Towards a robust query optimizer: A principled and practical approach. In *SIGMOD*, pages 119–130, 2005.

[9] C. Balkesen, G. Alonso, J. Teubner, and M. T. Özsu. Multi-core, main-memory joins: Sort vs. hash revisited. *PVLDB*, 7(1), 2013.

[10] C. Balkesen, J. Teubner, G. Alonso, and M. T. Özsu. Main-memory hash joins on multi-core CPUs: Tuning to the underlying hardware. In *ICDE*, 2013.

[11] R. Bayer and E. M. McCreight. Organization and maintenance of large ordered indices. *Acta Informatica*, 1:173–189, 1972.

[12] R. Bayer and M. Schkolnick. Concurrency of operations on B-trees. *Acta Informatica*, 9, 1977.

[13] S. Bellamkonda, R. Ahmed, A. Witkowski, A. Amor, M. Zaït, and C. C. Lin. Enhanced subquery optimizations in Oracle. *PVLDB*, 2(2):1366–1377, 2009.

[14] S. Bellamkonda, T. Bozkaya, B. Ghosh, A. Gupta, J. Haydu, S. Subramanian, and A. Witkowski. Analytic functions in Oracle 8i. Technical report, Oracle, 2000.

[15] S. Bellamkonda, H.-G. Li, U. Jagtap, Y. Zhu, V. Liang, and T. Cruanes. Adaptive and big data scale parallel execution in Oracle. *PVLDB*, 6(11):1102–1113, 2013.

[16] P. A. Bernstein, V. Hadzilacos, and N. Goodman. *Concurrency Control and Recovery in Database Systems*. Addison-Wesley, 1987.

[17] S. Blanas, Y. Li, and J. M. Patel. Design and evaluation of main memory hash join algorithms for multi-core CPUs. In *SIGMOD*, 2011.

[18] P. Boncz, T. Grust, M. van Keulen, S. Manegold, J. Rittinger, and J. Teubner. Pathfinder: XQuery - the relational way. In *VLDB*, pages 1322–1325, 2005.

[19] P. Boncz, T. Neumann, and O. Erling. TPC-H analyzed: Hidden messages and lessons learned from an influential benchmark. In *TPCTC*, 2013.

[20] P. Boncz, M. Zukowski, and N. Nes. MonetDB/X100: Hyper-pipelining query execution. In *CIDR*, pages 225–237, 2005.

[21] P. A. Boncz, S. Manegold, and M. L. Kersten. Database architecture evolution: Mammals flourished long before dinosaurs became extinct. *PVLDB*, 2(2):1648–1653, 2009.

[22] P. A. Boncz, W. Quak, and M. L. Kersten. Monet and its geographic extensions: A novel approach to high performance GIS processing. In *EDBT*, pages 147–166, 1996.

[23] R. Borovica-Gajic, S. Idreos, A. Ailamaki, M. Zukowski, and C. Fraser. Smooth scan: Statistics-oblivious access paths. In *ICDE*, pages 315–326, 2015.

[24] N. G. Bronson, J. Casper, H. Chafi, and K. Olukotun. A practical concurrent binary search tree. In *PPOPP*, pages 257–268, 2010.

[25] N. Bruno, C. A. Galindo-Legaria, and M. Joshi. Polynomial heuristics for query optimization. In *ICDE*, pages 589–600, 2010.

[26] Y. Cao, C.-Y. Chan, J. Li, and K.-L. Tan. Optimization of analytic window functions. *PVLDB*, 5(11):1244–1255, 2012.

[27] M. J. Carey. *Modeling and evaluation of database concurrency control algorithms*. PhD thesis, 1983.

[28] C. Cascaval, C. Blundell, M. M. Michael, H. W. Cain, P. Wu, S. Chiras, and S. Chatterjee. Software transactional memory: why is it only a research toy? *Commun. ACM*, 51(11), 2008.

[29] D. Cervini, D. Porobic, P. Tözün, and A. Ailamaki. Applying HTM to an OLTP system: No free lunch. In *DaMoN*, 2015.

[30] S. K. Cha, S. Hwang, K. Kim, and K. Kwon. Cache-conscious concurrency control of main-memory indexes on shared-memory multiprocessor systems. In *VLDB*, 2001.

[31] S. Chaudhuri. Query optimizers: time to rethink the contract? In *SIGMOD*, pages 961–968, 2009.

[32] S. Chaudhuri, V. R. Narasayya, and R. Ramamurthy. Exact cardinality query optimization for optimizer testing. *PVLDB*, 2(1):994–1005, 2009.

[33] M. Colgan. Oracle adaptive joins. `https://blogs.oracle.com/optimizer/entry/what_s_new_in_12c`, 2013.

[34] C. Curino, Y. Zhang, E. P. C. Jones, and S. Madden. Schism: a workload-driven approach to database replication and partitioning. *PVLDB*, 3(1), 2010.

[35] J. DeBrabant, A. Pavlo, S. Tu, M. Stonebraker, and S. B. Zdonik. Anti-caching: A new approach to database management system architecture. *PVLDB*, 6(14):1942–1953, 2013.

[36] J. Dees and P. Sanders. Efficient many-core query execution in main memory column-stores. In *ICDE*, 2013.

[37] C. Diaconu, C. Freedman, E. Ismert, P. Larson, P. Mittal, R. Stonecipher, N. Verma, and M. Zwilling. Hekaton: SQL server's memory-optimized OLTP engine. In *SIGMOD*, pages 1243–1254, 2013.

[38] D. Dice, O. Shalev, and N. Shavit. Transactional locking II. In *DISC*, 2006.

[39] N. Diegues and P. Romano. Self-tuning intel transactional synchronization extensions. In *ICAC*, 2014.

[40] A. Dutt and J. R. Haritsa. Plan bouquets: query processing without selectivity estimation. In *SIGMOD*, pages 1039–1050, 2014.

[41] A. Eldawy, J. J. Levandoski, and P. Larson. Trekking through Siberia: Managing cold data in a memory-optimized database. *PVLDB*, 7(11):931–942, 2014.

[42] C. Estan and J. F. Naughton. End-biased samples for join cardinality estimation. In *ICDE*, page 20, 2006.

[43] F. Färber, S. K. Cha, J. Primsch, C. Bornhövd, S. Sigg, and W. Lehner. SAP HANA database: data management for modern business applications. *SIGMOD Record*, 40(4), 2011.

[44] L. Fegaras. A new heuristic for optimizing large queries. In *DEXA*, pages 726–735, 1998.

[45] P. Felber, C. Fetzer, P. Marlier, and T. Riegel. Time-based software transactional memory. *IEEE Trans. Parallel Distrib. Syst.*, 21(12), 2010.

[46] P. Fender and G. Moerkotte. Counter strike: Generic top-down join enumeration for hypergraphs. *PVLDB*, 6(14):1822–1833, 2013.

[47] P. Fender, G. Moerkotte, T. Neumann, and V. Leis. Effective and robust pruning for top-down join enumeration algorithms. In *ICDE*, pages 414–425, 2012.

[48] C. Fraser, L. Giakoumakis, V. Hamine, and K. F. Moore-Smith. Testing cardinality estimation models in SQL Server. In *DBtest*, 2012.

[49] F. Funke, A. Kemper, and T. Neumann. Compacting transactional data in hybrid OLTP&OLAP databases. *PVLDB*, 5(11):1424–1435, 2012.

[50] H. Garcia-Molina and K. Salem. Main memory database systems: An overview. *IEEE Trans. Knowl. Data Eng.*, 4(6):509–516, 1992.

[51] G. Giannikis, G. Alonso, and D. Kossmann. SharedDB: Killing one thousand queries with one stone. *PVLDB*, 5(6), 2012.

[52] G. Graefe. Encapsulation of parallelism in the Volcano query processing system. In *SIGMOD*, 1990.

[53] G. Graefe. Query evaluation techniques for large databases. *ACM Comput. Surv.*, 25(2), 1993.

[54] G. Graefe. A survey of B-tree locking techniques. *ACM Trans. Database Syst.*, 35(3), 2010.

[55] G. Graefe. A generalized join algorithm. In *BTW*, pages 267–286, 2011.

[56] G. Graefe. Modern B-tree techniques. *Foundations and Trends in Databases*, 3(4):203–402, 2011.

[57] G. Graefe, H. Volos, H. Kimura, H. A. Kuno, J. Tucek, M. Lillibridge, and A. C. Veitch. In-memory performance for Big Data. *PVLDB*, 8(1):37–48, 2014.

[58] J. Gray and A. Reuter. *Transaction Processing: Concepts and Techniques*. Morgan Kaufmann, 1993.

[59] Z. Gu, M. A. Soliman, and F. M. Waas. Testing the accuracy of query optimizers. In *DBTest*, 2012.

[60] P. J. Haas, J. F. Naughton, S. Seshadri, and A. N. Swami. Selectivity and cost estimation for joins based on random sampling. *J Computer System Science*, 52(3):550–569, 1996.

[61] V. Harinarayan, A. Rajaraman, and J. D. Ullman. Implementing data cubes efficiently. In *SIGMOD*, pages 205–216, 1996.

[62] J. R. Haritsa. The Picasso database query optimizer visualizer. *PVLDB*, 3(2):1517–1520, 2010.

[63] S. Harizopoulos, D. J. Abadi, S. Madden, and M. Stonebraker. OLTP through the looking glass, and what we found there. In *SIGMOD*, 2008.

[64] S. Harizopoulos, V. Shkapenyuk, and A. Ailamaki. QPipe: A simultaneously pipelined relational query engine. In *SIGMOD*, 2005.

[65] M. Heimel, M. Saecker, H. Pirk, S. Manegold, and V. Markl. Hardware-oblivious parallelism for in-memory column-stores. *PVLDB*, 6(9), 2013.

[66] J. M. Hellerstein, M. Stonebraker, and J. R. Hamilton. Architecture of a database system. *Foundations and Trends in Databases*, 1(2):141–259, 2007.

[67] J. L. Hennessy and D. A. Patterson. *Computer Architecture - A Quantitative Approach (5. ed.).* Morgan Kaufmann, 2012.

[68] M. Herlihy. Fun with hardware transactional memory. In *SIGMOD*, 2014.

[69] M. Herlihy and J. E. B. Moss. Transactional memory: Architectural support for lock-free data structures. In *ISCA*, 1993.

[70] M. Herlihy and N. Shavit. *The art of multiprocessor programming*. Morgan Kaufmann, 2008.

[71] I. F. Ilyas, V. Markl, P. J. Haas, P. Brown, and A. Aboulnaga. CORDS: automatic discovery of correlations and soft functional dependencies. In *SIGMOD*, pages 647–658, 2004.

[72] D. Inkster, M. Zukowski, and P. Boncz. Integration of VectorWise with Ingres. *SIGMOD Record*, 40(3):45–53, 2011.

[73] Intel architecture instruction set extensions programming reference. `http://software.intel.com/file/41417`, 2013.

[74] Y. E. Ioannidis. The history of histograms (abridged). In *VLDB*, pages 19–30, 2003.

[75] Y. E. Ioannidis and S. Christodoulakis. On the propagation of errors in the size of join results. In *SIGMOD*, 1991.

[76] C. Jacobi, T. J. Slegel, and D. F. Greiner. Transactional memory architecture and implementation for IBM system z. In *MICRO*, 2012.

[77] S. Jain, D. Moritz, D. Halperin, B. Howe, and E. Lazowska. SQLShare: Results from a multi-year SQL-as-a-service experiment. In *SIGMOD*, 2016.

[78] R. Johnson and I. Pandis. The bionic DBMS is coming, but what will it look like? In *CIDR*, 2013.

[79] R. Johnson, I. Pandis, and A. Ailamaki. Improving OLTP scalability using speculative lock inheritance. *PVLDB*, 2(1), 2009.

[80] E. Jones and A. Pavlo. A specialized architecture for high-throughput OLTP applications. HPTS, 2009.

[81] E. P. C. Jones, D. J. Abadi, and S. Madden. Low overhead concurrency control for partitioned main memory databases. In *SIGMOD*, 2010.

[82] R. A. Kader, P. A. Boncz, S. Manegold, and M. van Keulen. ROX: run-time optimization of XQueries. In *SIGMOD*, pages 615–626, 2009.

[83] R. Kallman, H. Kimura, J. Natkins, A. Pavlo, A. Rasin, S. B. Zdonik, E. P. C. Jones, S. Madden, M. Stonebraker, Y. Zhang, J. Hugg, and D. J. Abadi. H-store: a high-performance, distributed main memory transaction processing system. *PVLDB*, 1(2), 2008.

[84] T. Karnagel, R. Dementiev, R. Rajwar, K. Lai, T. Legler, B. Schlegel, and W. Lehner. Improving in-memory database index performance with intel® transactional synchronization extensions. In *HPCA*, 2014.

[85] R. Kaushik, C. Ré, and D. Suciu. General database statistics using entropy maximization. In *DBPL*, pages 84–99, 2009.

[86] A. Kemper and T. Neumann. HyPer - hybrid OLTP&OLAP high performance database system. Technical report, TUM, 2010.

[87] A. Kemper and T. Neumann. HyPer: A hybrid OLTP&OLAP main memory database system based on virtual memory snapshots. In *ICDE*, 2011.

[88] A. Kemper, T. Neumann, J. Finis, F. Funke, V. Leis, H. Mühe, T. Mühlbauer, and W. Rödiger. Transaction processing in the hybrid OLTP & OLAP main-memory database system HyPer. *IEEE Data Eng. Bull.*, 36(2):41–47, 2013.

[89] T. Kiefer, B. Schlegel, and W. Lehner. Experimental evaluation of NUMA effects on database management systems. In *BTW*, 2013.

[90] C. Kim, E. Sedlar, J. Chhugani, T. Kaldewey, A. D. Nguyen, A. D. Blas, V. W. Lee, N. Satish, and P. Dubey. Sort vs. hash revisited: Fast join implementation on modern multi-core CPUs. *PVLDB*, 2(2), 2009.

[91] H. Kimura. FOEDUS: OLTP engine for a thousand cores and NVRAM. In *SIGMOD*, pages 691–706, 2015.

[92] T. Kissinger, B. Schlegel, D. Habich, and W. Lehner. KISS-Tree: Smart latch-free in-memory indexing on modern architectures. In *DaMoN*, 2012.

[93] M. Kornacker, A. Behm, V. B. T. Bobrovytsky, C. Ching, A. Choi, J. Erickson, M. Grund, D. Hecht, M. Jacobs, I. Joshi, L. Kuff, D. Kumar, A. Leblang, N. Li, I. Pandis, H. Robinson, D. Rorke, S. Rus, J. Russell, D. Tsirogiannis, S. Wanderman-Milne, and M. Yoder. Impala: A modern, open-source SQL engine for Hadoop. In *CIDR*, 2015.

[94] K. Krikellas, S. Viglas, and M. Cintra. Generating code for holistic query evaluation. In *ICDE*, 2010.

[95] T. Lahiri, M. Neimat, and S. Folkman. Oracle TimesTen: An in-memory database for enterprise applications. *IEEE Data Eng. Bull.*, 36(2):6–13, 2013.

[96] H. Lang, V. Leis, M.-C. Albutiu, T. Neumann, and A. Kemper. Massively parallel NUMA-aware hash joins. In *IMDM Workshop*, 2013.

[97] H. Lang, T. Mühlbauer, F. Funke, P. Boncz, T. Neumann, and A. Kemper. Data blocks: Hybrid oltp and olap on compressed storage using both vectorization and compilation. In *SIGMOD*, 2016.

[98] P.-Å. Larson, S. Blanas, C. Diaconu, C. Freedman, J. M. Patel, and M. Zwilling. High-performance concurrency control mechanisms for main-memory databases. *PVLDB*, 5(4), 2011.

[99] P.-Å. Larson, C. Clinciu, C. Fraser, E. N. Hanson, M. Mokhtar, M. Nowakiewicz, V. Papadimos, S. L. Price, S. Rangarajan, R. Rusanu, and M. Saubhasik. Enhancements to SQL Server column stores. In *SIGMOD*, 2013.

[100] P.-Å. Larson, C. Clinciu, E. N. Hanson, A. Oks, S. L. Price, S. Rangarajan, A. Surna, and Q. Zhou. SQL Server column store indexes. In *SIGMOD*, 2011.

[101] P.-Å. Larson, E. N. Hanson, and S. L. Price. Columnar storage in SQL Server 2012. *IEEE Data Eng. Bull.*, 35(1), 2012.

[102] P.-Å. Larson, M. Zwilling, , and K. Farlee. The Hekaton memory-optimized OLTP engine. *IEEE Data Eng. Bull.*, 36(2), 2013.

[103] J. R. Larus and R. Rajwar. *Transactional Memory*. Morgan & Claypool Publishers, 2006.

[104] C. Lattner and V. Adve. LLVM: A compilation framework for lifelong program analysis and transformation. pages 75–88, Mar 2004.

[105] P. L. Lehman and S. B. Yao. Efficient locking for concurrent operations on B-trees. *ACM Trans. Database Syst.*, 6(4):650–670, 1981.

[106] V. Leis, P. Boncz, A. Kemper, and T. Neumann. Morsel-driven parallelism: A NUMA-aware query evaluation framework for the many-core age. In *SIGMOD*, pages 743–754, 2014.

[107] V. Leis, A. Gubichev, A. Mirchev, P. Boncz, A. Kemper, and T. Neumann. How good are query optimizers, really? *PVLDB*, 9(3), 2015.

[108] V. Leis, A. Kemper, and T. Neumann. The adaptive radix tree: ARTful indexing for main-memory databases. In *ICDE*, 2013.

[109] V. Leis, A. Kemper, and T. Neumann. Exploiting hardware transactional memory in main-memory databases. In *ICDE*, pages 580–591, 2014.

[110] V. Leis, A. Kemper, and T. Neumann. Scaling HTM-supported database transactions to many cores. *IEEE Trans. Knowl. Data Eng.*, 28(2):297–310, 2016.

[111] V. Leis, K. Kundhikanjana, A. Kemper, and T. Neumann. Efficient processing of window functions in analytical SQL queries. *PVLDB*, 8(10):1058–1069, 2015.

[112] V. Leis, F. Scheibner, A. Kemper, and T. Neumann. The ART of practical synchronization. In *DaMoN*, 2016.

[113] J. J. Levandoski, P. Larson, and R. Stoica. Identifying hot and cold data in main-memory databases. In *ICDE*, pages 26–37, 2013.

[114] J. J. Levandoski, D. B. Lomet, and S. Sengupta. The Bw-tree: A B-tree for new hardware platforms. In *ICDE*, 2013.

[115] J. J. Levandoski, D. B. Lomet, and S. Sengupta. LLAMA: a cache/storage subsystem for modern hardware. *PVLDB*, 6(10):877–888, 2013.

[116] Q. Li, M. Shao, V. Markl, K. S. Beyer, L. S. Colby, and G. M. Lohman. Adaptively reordering joins during query execution. In *ICDE*, pages 26–35, 2007.

[117] Y. Li, I. Pandis, R. Müller, V. Raman, and G. M. Lohman. NUMA-aware algorithms: the case of data shuffling. In *CIDR*, 2013.

[118] J. Lindström, V. Raatikka, J. Ruuth, P. Soini, and K. Vakkila. IBM solidDB: In-memory database optimized for extreme speed and availability. *IEEE Data Eng. Bull.*, 36(2), 2013.

[119] H. Litz, D. R. Cheriton, A. Firoozshahian, O. Azizi, and J. P. Stevenson. SI-TM: reducing transactional memory abort rates through snapshot isolation. In *ASPLOS*, 2014.

[120] F. Liu and S. Blanas. Forecasting the cost of processing multi-join queries via hashing for main-memory databases. In *SoCC*, pages 153–166, 2015.

[121] G. Lohman. Is query optimization a "solved" problem? `http://wp.sigmod.org/?p=1075`, 2014.

[122] D. B. Lomet, A. Fekete, R. Wang, and P. Ward. Multi-version concurrency via timestamp range conflict management. In *ICDE*, 2012.

[123] L. Ma, J. Arulraj, S. Zhao, A. Pavlo, S. R. Dulloor, M. J. Giardino, J. Parkhurst, J. L. Gardner, K. Doshi, and S. B. Zdonik. Larger-than-memory data management on modern storage hardware for in-memory OLTP database systems. In *DaMoN*, 2016.

[124] L. F. Mackert and G. M. Lohman. R* optimizer validation and performance evaluation for local queries. In *SIGMOD*, pages 84–95, 1986.

[125] R. MacNicol and B. French. Sybase IQ multiplex - designed for analytics. In *VLDB*, pages 1227–1230, 2004.

[126] D. Makreshanski, J. J. Levandoski, and R. Stutsman. To lock, swap, or elide: On the interplay of hardware transactional memory and lock-free indexing. *PVLDB*, 8(11), 2015.

[127] N. Malviya, A. Weisberg, S. Madden, and M. Stonebraker. Rethinking main memory OLTP recovery. In *ICDE*, pages 604–615, 2014.

[128] S. Manegold, P. A. Boncz, and M. L. Kersten. Optimizing main-memory join on modern hardware. *IEEE Trans. Knowl. Data Eng.*, 14(4), 2002.

[129] Y. Mao, E. Kohler, and R. T. Morris. Cache craftiness for fast multicore key-value storage. In *EuroSys*, 2012.

[130] V. Markl, N. Megiddo, M. Kutsch, T. M. Tran, P. J. Haas, and U. Srivastava. Consistently estimating the selectivity of conjuncts of predicates. In *VLDB*, pages 373–384, 2005.

[131] G. Moerkotte and T. Neumann. Dynamic programming strikes back. In *SIGMOD*, pages 539–552, 2008.

[132] G. Moerkotte, T. Neumann, and G. Steidl. Preventing bad plans by bounding the impact of cardinality estimation errors. *PVLDB*, 2(1):982–993, 2009.

[133] C. Mohan, D. Haderle, B. Lindsay, H. Pirahesh, and P. Schwarz. ARIES: a transaction recovery method supporting fine-granularity locking and partial rollbacks using write-ahead logging. *ACM Trans. Database Syst.*, 17(1), 1992.

[134] H. Mühe, A. Kemper, and T. Neumann. Executing long-running transactions in synchronization-free main memory database systems. In *CIDR*, 2013.

[135] I. Müller, P. Sanders, A. Lacurie, W. Lehner, and F. Färber. Cache-efficient aggregation: Hashing is sorting. In *SIGMOD*, pages 1123–1136, 2015.

[136] R. O. Nambiar and M. Poess. The making of TPC-DS. In *VLDB*, pages 1049–1058, 2006.

[137] N. Narula, C. Cutler, E. Kohler, and R. Morris. Phase reconciliation for contended in-memory transactions. In *OSDI*, 2014.

[138] T. Neumann. Query simplification: graceful degradation for join-order optimization. In *SIGMOD*, pages 403–414, 2009.

[139] T. Neumann. Efficiently compiling efficient query plans for modern hardware. *PVLDB*, 4(9), 2011.

[140] T. Neumann and C. A. Galindo-Legaria. Taking the edge off cardinality estimation errors using incremental execution. In *BTW*, pages 73–92, 2013.

[141] T. Neumann and A. Kemper. Unnesting arbitrary queries. In *BTW*, pages 383–402, 2015.

[142] T. Neumann and V. Leis. Compiling database queries into machine code. *IEEE Data Eng. Bull.*, 37(1):3–11, 2014.

[143] T. Neumann, T. Mühlbauer, and A. Kemper. Fast serializable multi-version concurrency control for main-memory database systems. In *SIGMOD*, pages 677–689, 2015.

[144] P. O'Neil, B. O'Neil, and X. Chen. The star schema benchmark (SSB), 2007. `http://www.cs.umb.edu/~poneil/StarSchemaB.PDF`.

[145] I. Oukid, D. Booss, W. Lehner, P. Bumbulis, and T. Willhalm. SOFORT: a hybrid SCM-DRAM storage engine for fast data recovery. In *DaMoN*, 2014.

[146] I. Pandis, R. Johnson, N. Hardavellas, and A. Ailamaki. Data-oriented transaction execution. *PVLDB*, 3(1), 2010.

[147] A. Pavlo, C. Curino, and S. B. Zdonik. Skew-aware automatic database partitioning in shared-nothing, parallel OLTP systems. In *SIGMOD*, 2012.

[148] O. Polychroniou, A. Raghavan, and K. A. Ross. Rethinking SIMD vectorization for in-memory databases. In *SIGMOD*, pages 1493–1508, 2015.

[149] O. Polychroniou and K. A. Ross. High throughput heavy hitter aggregation for modern SIMD processors. In *DaMoN*, 2013.

[150] V. Poosala and Y. E. Ioannidis. Selectivity estimation without the attribute value independence assumption. In *VLDB*, pages 486–495, 1997.

[151] D. Porobic, E. Liarou, P. Tözün, and A. Ailamaki. ATraPos: Adaptive transaction processing on hardware islands. In *ICDE*, 2014.

[152] D. Porobic, I. Pandis, M. Branco, P. Tözün, and A. Ailamaki. OLTP on hardware islands. *PVLDB*, 5(11), 2012.

[153] I. Psaroudakis, T. Scheuer, N. May, and A. Ailamaki. Task scheduling for highly concurrent analytical and transactional main-memory workloads. In *ADMS Workshop*, 2013.

[154] F. Putze, P. Sanders, and J. Singler. MCSTL: the multi-core standard template library. In *PPOPP*, pages 144–145, 2007.

[155] R. Rajwar and M. Dixon. Intel transactional synchronization extensions. `http://intel.com/go/idfsessions`, 2012.

[156] V. Raman, G. Attaluri, R. Barber, N. Chainani, D. Kalmuk, V. KulandaiSamy, J. Leenstra, S. Lightstone, S. Liu, G. M. Lohman, T. Malkemus, R. Mueller, I. Pandis, B. Schiefer, D. Sharpe, R. Sidle, A. Storm, and L. Zhang. DB2 with BLU acceleration: So much more than just a column store. In *VLDB*, 2013.

[157] K. Ren, A. Thomson, and D. J. Abadi. Lightweight locking for main memory database systems. *PVLDB*, 6(2), 2013.

[158] W. Rödiger, T. Mühlbauer, A. Kemper, and T. Neumann. High-speed query processing over high-speed networks. *PVLDB*, 9(4):228–239, 2015.

[159] F. Rusu and A. Dobra. Sketches for size of join estimation. *TODS*, 33(3), 2008.

[160] S. Schuh, J. Dittrich, and X. Chen. An experimental comparison of thirteen relational equi-joins in main memory. In *SIGMOD*, 2016.

[161] P. G. Selinger, M. M. Astrahan, D. D. Chamberlin, R. A. Lorie, and T. G. Price. Access path selection in a relational database management system. In *SIGMOD*, pages 23–34, 1979.

[162] O. Shalev and N. Shavit. Split-ordered lists: Lock-free extensible hash tables. *J. ACM*, 53(3):379–405, 2006.

[163] N. Shavit and D. Touitou. Software transactional memory. In *PODC*, 1995.

[164] M. Steinbrunn, G. Moerkotte, and A. Kemper. Heuristic and randomized optimization for the join ordering problem. *VLDB J.*, 6(3):191–208, 1997.

[165] M. Stillger, G. M. Lohman, V. Markl, and M. Kandil. LEO - DB2's learning optimizer. In *VLDB*, pages 19–28, 2001.

[166] R. Stoica and A. Ailamaki. Enabling efficient OS paging for main-memory OLTP databases. In *DaMoN*, 2013.

[167] M. Stonebraker, D. J. Abadi, A. Batkin, X. Chen, M. Cherniack, M. Ferreira, E. Lau, A. Lin, S. Madden, E. J. O'Neil, P. E. O'Neil, A. Rasin, N. Tran, and S. B. Zdonik. C-store: A column-oriented DBMS. In *VLDB*, pages 553–564, 2005.

[168] M. Stonebraker and A. Weisberg. The VoltDB main memory DBMS. *IEEE Data Eng. Bull.*, 36(2), 2013.

[169] J. Teubner and R. Müller. How soccer players would do stream joins. In *SIGMOD*, 2011.

[170] J. Teubner and L. Woods. *Data Processing on FPGAs*. Synthesis Lectures on Data Management. Morgan & Claypool Publishers, 2013.

[171] A. Thomson, T. Diamond, S. Weng, K. Ren, P. Shao, and D. J. Abadi. Calvin: fast distributed transactions for partitioned database systems. In *SIGMOD*, pages 1–12, 2012.

[172] S. Tu, W. Zheng, E. Kohler, B. Liskov, and S. Madden. Speedy transactions in multicore in-memory databases. In *SOSP*, 2013.

[173] K. Tzoumas, A. Deshpande, and C. S. Jensen. Lightweight graphical models for selectivity estimation without independence assumptions. *PVLDB*, 4(11):852–863, 2011.

[174] F. Waas and A. Pellenkoft. Join order selection - good enough is easy. In *BNCOD*, pages 51–67, 2000.

[175] F. M. Waas, L. Giakoumakis, and S. Zhang. Plan space analysis: an early warning system to detect plan regressions in cost-based optimizers. In *DBTest*, 2011.

[176] A. Wang, M. Gaudet, P. Wu, J. N. Amaral, M. Ohmacht, C. Barton, R. Silvera, and M. M. Michael. Evaluation of Blue Gene/Q hardware support for transactional memories. In *PACT*, 2012.

[177] Z. Wang, H. Qian, J. Li, and H. Chen. Using restricted transactional memory to build a scalable in-memory database. In *EuroSys 2014*, 2014.

[178] G. Weikum and G. Vossen. *Transactional Information Systems: Theory, Algorithms, and the Practice of Concurrency Control and Recovery*. Morgan Kaufmann, 2002.

[179] S. Wolf, H. Mühe, A. Kemper, and T. Neumann. An evaluation of strict timestamp ordering concurrency control for main-memory database systems. In *IMDM*, 2013.

[180] W. Wu, Y. Chi, S. Zhu, J. Tatemura, H. Hacigümüs, and J. F. Naughton. Predicting query execution time: Are optimizer cost models really unusable? In *ICDE*, pages 1081–1092, 2013.

[181] W. Wu, J. F. Naughton, and H. Singh. Sampling-based query re-optimization. In *SIGMOD*, 2016.

[182] J. Yang and J. Widom. Incremental computation and maintenance of temporal aggregates. In *ICDE*, pages 51–60, 2001.

[183] Y. Ye, K. A. Ross, and N. Vesdapunt. Scalable aggregation on multicore processors. In *DaMoN*, 2011.

[184] F. Yu, W. Hou, C. Luo, D. Che, and M. Zhu. CS2: a new database synopsis for query estimation. In *SIGMOD*, pages 469–480, 2013.

[185] X. Yu, G. Bezerra, A. Pavlo, S. Devadas, and M. Stonebraker. Staring into the abyss: An evaluation of concurrency control with one thousand cores. *PVLDB*, 8(3):209–220, 2014.

[186] F. Zemke. What's new in SQL:2011. *SIGMOD Record*, 41(1):67–73, 2012.

[187] M. Zukowski and P. A. Boncz. Vectorwise: Beyond column stores. *IEEE Data Eng. Bull.*, 35(1), 2012.

[188] C. Zuzarte, H. Pirahesh, W. Ma, Q. Cheng, L. Liu, and K. Wong. WinMagic: Subquery elimination using window aggregation. In *SIGMOD*, pages 652–656, 2003.